Principles of energy optimization underlying human walking gait adaptations

by

Surabhi N. Simha

B.E., VTU, 2012

Thesis Submitted in Partial Fulfillment of the
Requirements for the Degree of
Doctor of Philosophy

in the
Department of Biomedical Physiology and Kinesiology
Faculty of Science

SIMON FRASER UNIVERSITY
Fall 2020

Declaration of Committee

Name:	**Surabhi N. Simha**
Degree:	**Doctor of Philosophy**
Thesis title:	**Principles of energy optimization underlying human walking gait adaptations**
Committee:	**Chair:** Sam Doesburg Associate Professor, Biomedical Physiology and Kinesiology
	Max Donelan Supervisor Professor, Biomedical Physiology and Kinesiology
	Dawn Mackey Committee Member Associate Professor, Biomedical Physiology and Kinesiology
	Daniel Marigold Committee Member Associate Professor, Biomedical Physiology and Kinesiology
	Dylan Cooke Examiner Assistant Professor, Biomedical Physiology and Kinesiology
	Young-Hui Chang External Examiner Professor, Biological Sciences Georgia Tech

Ethics Statement

The author, whose name appears on the title page of this work, has obtained, for the research described in this work, either:

a. human research ethics approval from the Simon Fraser University Office of Research Ethics

or

b. advance approval of the animal care protocol from the University Animal Care Committee of Simon Fraser University

or has conducted the research

c. as a co-investigator, collaborator, or research assistant in a research project approved in advance.

A copy of the approval letter has been filed with the Theses Office of the University Library at the time of submission of this thesis or project.

The original application for approval and letter of approval are filed with the relevant offices. Inquiries may be directed to those authorities.

Simon Fraser University Library
Burnaby, British Columbia, Canada

Update Spring 2016

Abstract

Learning to move in novel situations is a complex process. We need to continually learn the changing situations and determine the best way to move. Optimization is a widely accepted framework for this process. However, little is known about algorithms used by the nervous system to perform this optimization. Our lab recently found evidence that people can continuously optimize energy during walking. My goal in this thesis is to identify principles of optimization, particularly energy optimization in walking, that govern our choice of movement in novel situations. I used two novel walking tasks for this purpose. For the first task, I designed, built, and tested a mechatronic system that can quickly, accurately, and precisely apply forces to a user's torso. It changes the relationship between a walking gait and its associated energetic cost—cost landscape—to shift the energy optimal walking gait. Participants shift their gait towards the new optimum in these landscapes. In my second project, I aimed to understand how the nervous system identifies when to initiate optimization. I used my system to create cost landscapes of three different cost gradients. I found that experiencing a steeper cost gradient through natural variability is not sufficient to cue the nervous system to initiate optimization. For my third and fourth projects, I used the task of split-belt walking. I collaborated with another research group to analyse the mechanics and energetics of walking with different step lengths on a split-belt treadmill. I found that people can harness energy from a split-belt treadmill by placing their leading leg further forward on the fast belt, and that there may be an energy optimal gait. In my fourth project, I used computer modelling to identify that there may exist an energy optimal gait due to the trade-off between the cost of swinging the leg and the cost of redirecting the body center of mass when transitioning from step to step. Together, these projects develop a new system and a new approach to understand energy optimization in walking. They uncover principles governing the initiation of this process and our ability to benefit from it.

Keywords: energy optimization; motor learning; mechatronic system; cost gradient; split-belt treadmill; dynamic walking

Acknowledgements

I am extremely grateful to my senior supervisor Dr. Max Donelan for his guidance and encouragement through these years. Max, your contribution towards making me the scientist I am today is unmeasurable. Thank you for giving me the opportunity to work in your lab, believing in me to when I was discouraged, patiently guiding me as I learnt a wide range of new skills, and putting in the effort to provide me with outside opportunities. Your passion for perpetual learning and clear communication will always inspire me. It has been a pleasure and an honour to work with you all these years.

I thank the members of my supervisory committee, Dr. Dan Marigold and Dr. Dawn Mackey for their support and guidance during key stages of my Ph.D. Dan, thank you for pushing me to develop a well-rounded understanding of the concepts in my thesis. Dawn, thank you for encouraging me to broaden the perspective of my thesis topics while keeping them grounded, and for your support particularly during times of stress.

To all my lab mates over the years, you have been a wonderful source of joy, laughter, and intellectual as well as aimless conversations. This Ph.D. would not have been possible without your moral, emotional, and sometimes physical support. Thank you.

A special thank you to all the participants for volunteering their time and energy.

I owe a huge thank you to a number of my friends who are now spread across the globe. You have been the keepers of my sanity through this wild adventure.

Most importantly, none of this would have been possible without the support of my family. Amma and Appa, thank you for your unconditional love in this journey that has taken me so far away from you and no doubt made you anxious. Aṇṇa, thank you for always pushing me to be the best I can be. Raghav, thank you for your unwavering support and always being there when I needed you.

Table of Contents

List of Tables

List of Figures

Glossary

Assistive device	A device that can provide assistance to its user in the form of adding mechanical energy, reducing mechanical energy required to perform a task or reducing metabolic energy required to perform a task.
Control policy	A rule or mapping that specifies what motor command to execute for a given state of the body
Cost function/ objective function	A weighted sum of the various costs associated with a movement. The two terms are used interchangeably throughout the thesis.
Cost landscape	Throughout the thesis, this is used to refer to the relationship between walking with different step frequencies and the costs associated with them. In Chapter 3, it is sometimes used to refer to a more general relationship between different control policies and the costs associated with them.
de novo or skill learning	The process where the nervous system has to learn a new mapping between its actions and the task goal.
Energetic cost	Primarily used to mean the metabolic energetic cost measured as metabolic power in Chapters 2-4. In Chapter 5, it is used to refer to an estimate of metabolic power. It is used interchangeably with metabolic power and metabolic energy.
Error-based learning	The process of learning the appropriate motor commands in a novel situation that involves updating the forward model.
Fast belt	The treadmill belt that is moving faster of the two in a split-belt treadmill.
Fast leg/ limb	The leg that is contacting the fast belt during split-belt treadmill walking.
Forward model	A model used by the nervous system to depict the mapping between motor commands and actions.
Motor adaptation	In the Introduction (Chapter 1), I present the neuroscience definition—a process where the nervous system has to recalibrate its forward model in a novel situation. In the remainder of the thesis, I use it to mean the general process of learning to move in a novel situation and use it interchangeably with “optimization”.
Motor control	The process of planning a movement by the nervous system.

Novel situation	A situation where there is a change to the body, the environment, or the task objective necessitating the nervous system to learn whether a change is required to its movement.
Optimization	The computational process of selecting a movement in a novel situation by minimizing a cost function.
Prediction	Recall of a previously learned control policy for a situation. It is quick but requires prior experience with the situation.
Reinforcement learning	A set of optimization algorithms that are adaptive to changing situations whose properties are incompletely known.
Reward-based learning	The process of learning how to move in novel situations by maximizing a reward function or minimizing a cost function.
Reward-prediction error	The error between the nervous system's prediction of the reward associated with an action and the measured reward received from that action.
Sensorimotor prediction error	The error between the nervous system's prediction of the mapping between motor commands and actions, and the measured actions produced by the motor commands.
Slow belt	The treadmill belt that is moving slower of the two in a split-belt treadmill.
Slow leg/ limb	The leg that is contacting the slow belt during split-belt treadmill walking.
Step-to-step transition cost	The energetic cost involved in the transition from step-to-step due to contacting the ground, in steady-state walking at a constant speed.
Swing cost	The energetic cost involved in swinging the leg during walking.
Use-dependant learning	The process of learning a movement along the task-redundant dimension. This term is only used in the Introduction (Chapter 1).

Published Studies

Research contained in this thesis has been published in the following peer-reviewed journals:

Chapter 2	Simha SN, Wong JD, Selinger JC, Donelan JM. A mechatronic system for studying energy optimization during walking. IEEE Transactions on Neural Systems and Rehabilitation Engineering. 2019 May 17;27(7):1416-25.
Chapter 3	Simha SN, Wong JD, Selinger JC, Abram, SJ, Donelan JM. Increasing the gradient of energetic cost does not initiate adaptation in human walking. (in revision). Journal of Neurophysiology.
Chapter 4	Sánchez N*, Simha SN*, Donelan JM, Finley JM. Taking advantage of external mechanical work to reduce metabolic cost: The mechanics and energetics of split-belt treadmill walking. The Journal of physiology. 2019 Aug;597(15):4053-68. (1st two authors contributed equally to this work).

Chapter 1.

Introduction

Humans are adept at successfully performing movements in a variety of situations. This is quite impressive considering the complexity involved in performing even everyday movements. Let us consider one such task of walking down a partially flooded street. In most cases, we can walk through without even getting our shoes wet. To achieve this, our nervous system needs to integrate the physics of the road and the potholes, the dynamics of the water in the potholes, dynamics of our body, our clothes and shoes, our sensory systems and the noise in their measurements, the algorithms that govern our movement, and the objectives or motivations that govern our behaviour. Given this breadth and complexity, the question of how humans control movement is a research topic spanning multiple scientific disciplines. In this introduction, I will provide a brief consolidated summary of the topic as it applies to this thesis. I will gradually increase focus on the concepts related to the algorithms governing our movement, which is the primary focus of this thesis.

Our current understanding of motor control is derived from the combination of many theories. Our primary machinery for movement is the skeletal muscle (1). It consists of bundles of fascicles which themselves are made up of bundles of muscle fibres (1). A single skeletal muscle fibre consists of many myofibrils, each of which is made up of repeating cylindrical units called sarcomeres (1,2). A sarcomere is the smallest functional unit of a muscle (1,2). It is made of thick and thin filaments that extend from the z-disc. Each of these filaments are made of proteins that are the fundamental contractile machinery of the skeletal muscle (1,2). Huxley's sliding filament theory about how they function from the 1950s is still widely used though further advances have been made to the theory (3). Briefly, the thick filament is made up of myosin molecules while the thin filament consists of proteins called actin, tropomyosin and troponin. The myosins have a globular head that can sit in a cocked position by using energy from ATP and converting it to ADP. The actins have a binding site that is covered by the troponin-tropomyosin complex. However, an action potential delivered by a motor neuron along the surface of the muscle fibre can allow Ca^{2+} ions to enter and bind to the troponin, leading to a

conformational change to the troponin-tropomyosin complex, exposing the binding site on the actin. The cocked myosin head can then bind to this site, releasing the ADP. It can then form a crossbridge that pulls on the thin filaments, causing an overlap between the filaments, shortening the length of the muscle and producing force. The myosin head will have to bind with ATP again to detach and go back to the cocked position. This is the process of active force production by the muscle (1). The motor neuron that delivers the action potential to the muscle fibre has its nucleus in the spinal cord or brain stem (1). A single motor neuron can innervate multiple muscle fibres (1). The motor neuron together with all its muscle fibres is called a motor unit and represents the simplest pathway of the nervous system's control of muscles.

The total force produced by the muscle depends on more than just active force. It depends on the number of cross-bridges which are responsible for the active force production, force produced by a single cross-bridge which in part depends on the length of the muscle, the velocity of the muscle, and the force from the non-contractile elements in the muscle such as the connective filaments, connective tissue and collagen surrounding the muscle fibres (1). It is possible for the nervous system to control certain movements, without continuous control of active force production. For example, walking downhill can be largely explained using the passive dynamics of our body (4). Our muscles can also reject some perturbations from the environment using preflexes—immediate responses from a muscle due to its intrinsic force-length and force-velocity properties (5). Such passive dynamics-based control can be modulated by the nervous system but only by changing the muscle activation for the nominal task being performed, rather than in response to a stimulus (5). Such largely passive control can only sustain a limited set of movements.

The simplest stimulus-based active control is a reflex. Sherrington proposed that a reflex is a stereotyped, involuntary response to a stimulus that activates receptors in the skin or muscles (6). However, for such a reflex, the neural control is contained within the spinal cord (1). More recent understanding of reflexes is that movements are performed through *feedforward reflex pathways*—a mechanism defined as our nervous systems' use of voluntary control to combine and adapt multiple reflexes to perform a movement (1). This means that the activation of the muscle is still set according to the task being performed. However, a sensory input can elicit responses away from the site of the stimulus suggesting that supraspinal control is involved. For example, the reflex response

of one elbow extensor is affected by the task being performed by the other arm. Such reflexes can also be adapted to (7). While this provides useful insight into motor control, it does not sufficiently explain the specificity of control, particularly in response to a changing body and environment.

Current theory of motor control combines feedforward and feedback mechanisms. This means that the nervous system uses a forward model of the environment and the body to predict motor commands that will perform the required movement. It simultaneously senses the environment and its body, comparing its prediction to its measurements and makes corrections to the required motor commands (8). Rather than solve for a set of independent motor commands, the nervous system solves for a control policy for a given task. Here, control policy is a rule or mapping that specifies what motor command to execute for a given state of the body (8–10). The nervous system then executes the motor commands to implement that policy. Figure 1.1 presents a simple schematic of this process. In this thesis, I aim to understand how the nervous system chooses a preferred control policy.

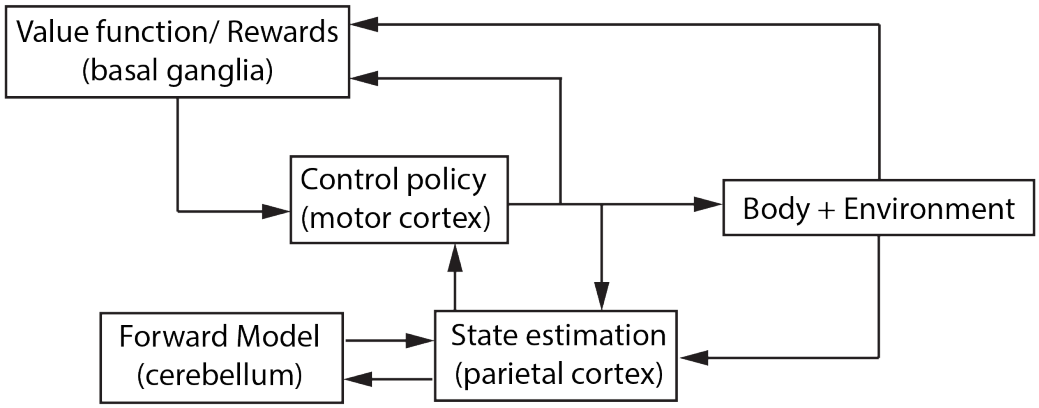

Figure 1.1: Simple schematic representation of motor control

1.1. Motor control in novel situations

As we experience different situations, our nervous system uses different processes to select its preferred control policy. In a familiar situation, our nervous system has learnt its preferred control policy. This allows it to quickly implement the policy through prediction (11). In an unfamiliar situation, the nervous system must learn about the new situation and

select its preferred control policy for that situation. In some unfamiliar situations, the nervous system has to learn a new mapping between its actions and task goal and then identify the control policy it wants to use, known as *de novo* learning (9). An example is a situation where the keys on our keyboard are switched such that pressing “y” now types “n”. Some other unfamiliar situations may only change the relationship between motor commands and the expected actions, and thus require the nervous system to recalibrate its forward model—a process referred to as motor adaptation (9). For example, pressing “y” still types “y” but its location on the keyboard has changed. In other unfamiliar situations, there is no change to the control policy or the forward model and the nervous system needs to learn that its original control policy is still appropriate for the new situation. This might be the case if the keyboard is now replaced with a mechanical keyboard where we just need to press harder. These examples were chosen to provide a clear distinction between the tasks. However, in many tasks such a distinction may not be immediately apparent. An example is if the nervous system suddenly encounters a system that applies unpredictable forces to the torso. The classification mentioned here arises from neuroscience. In the next section, I discuss computational methods where these tasks are described through a single framework. Neither of these sections are meant to be an exhaustive review of the fields, but only meant to provide a foundation to understand the interdisciplinary projects in this thesis. The focus of the thesis is on how the nervous system solves for a control policy in unfamiliar situations.

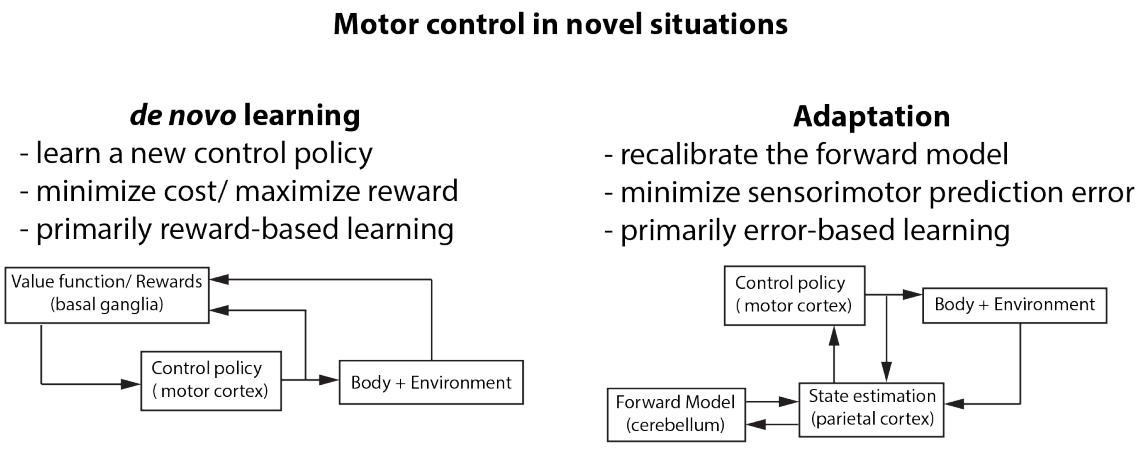

Figure 1.2: Schematic representation of motor control in novel situations

Three processes broadly explain how the nervous system selects its movement in novel situations: error-based learning, use-dependant learning, and reward-based

learning (12). According to error-based learning, the nervous system learns the appropriate motor commands to a novel situation by updating its forward model to reflect the changes due to the novel situation. The sensorimotor system senses the motor command and outcome, and compares that to its prediction to evaluate a sensorimotor prediction error (Figure 1.2). This way it knows when a target is missed and by how much and can adapt its forward model accordingly. This form of learning states that the nervous system has already developed a control policy that it finds appropriate for the task. This is the form of learning that has traditionally been studied in laboratory settings. Such experiments typically include making reaching movements to a target while wearing prism goggles that shift the visual field, while receiving visually rotated feedback on a screen, or while force-fields are applied to perturb the arm dynamics (13–16). Importantly, for this form a learning, participants receive some form of sensory feedback about the movement of limb that is being adapted.

A second form of learning is called use-dependent learning. A general use of this term refers to the changes in movement learnt simply through repetition irrespective of the goal of the task (12). Diedrichsen et al. developed a more specific usage (17). They refer to a process where a movement is biased by a previous movement but not along the task-relevant dimension. They suggest that when a perturbation does not hinder the performance of a task, it may be beneficial to learn to move along the direction of the perturbation. This form of learning has typically been studied by modifying tasks that require the minimization of a sensorimotor error, such as reaching to a target and thus also states that the nervous system already has a preferred control policy for the task. In such tasks, error-based and use-based learning can occur in parallel. For example, when participants' reach was constrained towards the right, they applied a force against that constraint. However, when the constraint was removed, after the effect of the error-based learning, participants showed a preference to move towards the right which was task-redundant direction during the constrained task.

Reward-based learning is based on the concept that the nervous system tries to maximize some reward without a prediction about how to move. In such tasks, the nervous system either does not know how to move in order to develop a sensorimotor prediction error, or does not receive or does not use the sensorimotor prediction error. Instead, the nervous system uses a signal about whether a certain movement was successful or not. Therefore, it does not know how exactly to alter its movement to obtain more reward and

may have to explore multiple options before arriving at one that maximizes its reward. This is useful for improving movements beyond achieving a specific goal. This process is typically used to understand learning a new skill where the nervous system has not even solved for a control policy, and hence cannot simply minimize a sensorimotor prediction error to achieve the goal of the task. Recent experiments have modified the original arm reaching paradigms such that the participants only receive feedback of the final results—success or failure—rather than feedback of their limb movements. Some such studies pitted error-based learning and reward-based learning within the same task and found that both processes can occur independently in the same task and when they conflict, error-based learning may take preference (16,18,19). In this thesis, I probe reward-based learning in novel situations.

1.2. Computational methods for motor control in novel situations

Computational methods serve as detailed and cohesive formulations of the processes of motor control in novel situations. A widely accepted framework for such computational methods is optimization—the nervous system selects a preferred movement that optimizes a certain cost function (20–22). Optimal control, derived from the field of control theory, has been quantitatively used in motor control at least since the early 1960s (23). The computational methods of optimal control have steadily improved to capture more aspects of observed motor behaviour. These improvements have been in the form of algorithmic changes to incorporate more realistic aspects of the body and the environment, and in the identification of appropriate cost functions. Section 1.3 provides a brief overview of the cost functions. A landmark improvement for optimal control methods was the development of the Optimal Feedback Control algorithm in early 2000. It has proved to be a unifying theory for how the nervous system optimally combines sensory inputs with forward models in the presence of noise and changing dynamics to determine an optimal control policy (20,24). This framework can combine the various forms of learning described earlier into a single cohesive optimization process.

Motor adaptation is described as a minimization of sensorimotor prediction error through error-based learning of the new forward model. This presupposes that the original

control policy is still relevant in the new situation. The optimal control framework proposes that in the process of learning a new control policy in any new situation, the nervous system learns a new forward model and uses that to determine the control policy that minimizes a cost, or maximizes a reward as proposed by reward-based learning. However, the computational complexity of such an algorithm is extremely huge, causing it to be more generally accepted for motor control in a stationary situation than in novel situations (20,25,26). This complexity primarily arises from the need to develop an accurate forward model and use that to solve for an optimal policy—the algorithms are model-based (Figure 1.3). More recently, simpler optimal control algorithms that don't require a comprehensive forward model, and whose cost functions can capture some of the dynamics related properties of the system, such as effort, stability and metabolic cost, have been able to accurately predict motor behaviour observed during learning (15,27). Incorporating optimal control methods into a framework that is adaptive to changing situations is an ongoing research problem.

Reinforcement learning has provided a framework of computational methods that can describe behaviour when situations are continuously changing. Reinforcement learning is an optimal control method that is applied to a situation and task whose properties are incompletely known and may be changing. The distinguishing feature of reinforcement learning algorithms that allows this is that the algorithms solve for the optimal control policy by exploring the costs associated with different control policies (28). These algorithms are model-free (Figure 1.3). Through trial-and-error, they learn a value function—the total reward that can be obtained if a given control policy is implemented from the current state—and find the control policy with the optimal value. Reward-based learning is often used interchangeably with this computational method of learning since learning from only a success or failure feedback is model-free. However, there is also a class of reinforcement learning algorithms that are model based. Here, the value function is computed by developing a model of the system and the environment (29). Through these algorithms, the optimal control models described in the previous paragraph also naturally fit into the reinforcement learning framework. The results from the projects in this thesis do not necessitate a reinforcement learning algorithm. However, the development of hypotheses and design of projects have been based on the framework of model-free reinforcement learning.

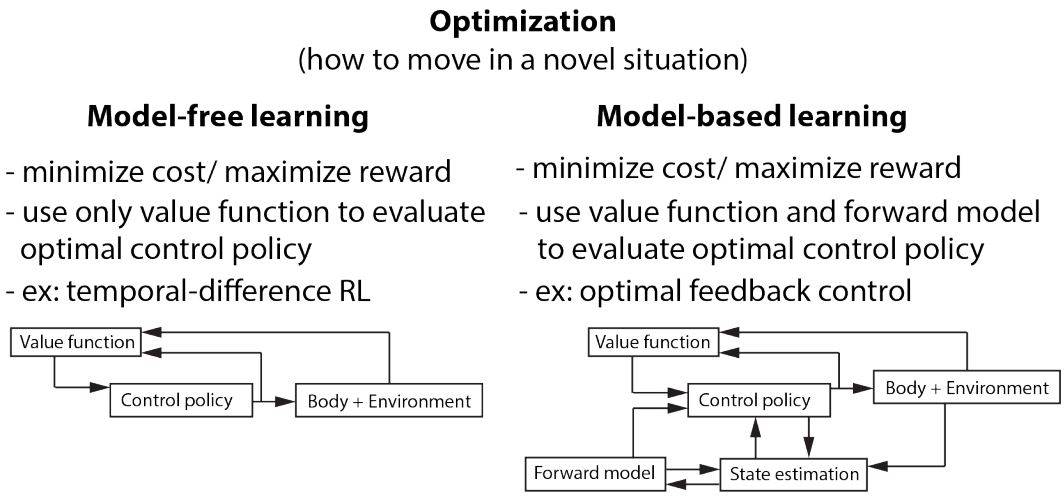

Figure 1.3: Schematic representation of optimization in motor control in novel situations

1.3. Neural implementation of computational methods

Mechanisms in the human body are essential to validate computational methods as representations of human motor control. But understanding how the nervous system determines how to move in a novel situation through computational methods and through neural mechanisms requires contrasting knowledge and skillset. The projects in this thesis were not developed to probe the neural mechanisms, and do not directly depend on the pathways of a particular neural mechanism. Therefore, I only present a brief overview of relevant mechanisms that informed the relevance of the computational framework chosen for the projects in this thesis. Knowledge about neural mechanisms has developed through invasive recordings from animals, the study of motor behaviour in patients and more recently, with the development of brain imaging techniques, the study of motor behaviours in healthy humans. Such findings suggest that the control policy may reside in the motor cortex (10). I will use the neuroscience-developed classification of learning processes here since they better delineate the roles of different neural structures.

It is widely accepted that the cerebellum is responsible for the sensory prediction error that is essential for model-based learning. The evidence for this has been gathered through studies on monkeys with cerebellar lesions, patients with cerebellar degeneration, and healthy participants (9). The evidence also spans multiple tasks including arm

reaching in with visuomotor rotation, arm reaching with force fields, and locomotion (30–32). In patients with cerebellar degeneration it has been observed that they are unable to accurately predict the required motor commands when the dynamics of a task are altered—the patient could not adjust their grip force to account for a ball being dropped in a basket they were holding. More recently, brain imagining studies with healthy adults found a correlation between cerebellar activation and experiencing a sensory prediction error (33). Specifically, it is thought that the cerebellum is involved in the formation of a forward model as well as in learning through performance feedback in a task. This has been evidenced through the spiking of cerebellar Purkinje cells of monkeys both at the beginning of a reaching task, as well as at the end of the movement (34). It is thought that the cerebellum is more sensitive to large and abrupt perturbations and is involved in an implicit process (12,34,35). While evidence for the relationship between the cerebellum and forward model in robust, there isn't a clear theory for the neural circuitry used for implementing the computations, particularly for using the forward model to solve for an optimal control policy.

The basal ganglia is the brain region primarily implicated in reward-based learning. Reward-based learning had its early roots in psychology. Thus, much of the neurophysiology is from the study of decision making in the presence of rewards. A particular algorithm of interest to psychology and neuroscience is temporal-difference reinforcement learning where learning occurs by comparing temporally successive estimates of reward. In psychology, it is used to explain the process of learning through reward-prediction. Pavlov's conditioning and Law of Effect tell us that any action or stimulus accompanied with a pleasant consequence is likely to be repeated (36). This forms a prediction between action and reward. In the subsequent execution of the action, rewards that are better than predicted lead to a positive reward-prediction error and to improvement of action, while rewards that are worse lead to a negative reward-prediction error and thus stopping of the action. Rewards that lead to zero reward-prediction error continue the action but put an end to learning (37). Therefore, even though this form of learning does not necessitate a goal-directed sensorimotor prediction error similar to error-based learning, it is driven by on an error. The reward-prediction error may be coded in the phasic activity of dopamine-producing neurons in mammals, delivering this signal throughout the brain (38). This was observed by recording the dopamine neurons from the brain of monkeys as they learnt to perform different actions to obtain rewards (37). The

axons of most dopamine neurons contact the axons in the basal ganglia. The primary input to the basal ganglia is the striatum and the output from the striatum connects with the cortex and other motor areas (37,38). It is proposed that this network allows the basal ganglia to influence movement and motor control in novel situations.

Direct evidence of the role of basal ganglia in the control of movement in novel situations is expanding. Early studies of the basal ganglia were only related to learning a new skill. In a task of throwing when the visual field was reversed, a task thought to be primarily driven by reward-based learning, patients with damage to the basal ganglia were unable to learn the task (39). More recent measurements from the caudate nucleus, which is located in the striatum, suggest that it may be active during the early stages of error-based learning tasks (34). Some functional MRI studies also implicate the basal ganglia in regulating kinematic properties such as movement velocity, amplitude and force duration (34). However, it is observed that patients with damage to the striatum can still learn to reduce the error in an error-based learning task (9). A unifying view is based on the observations that the output from the basal ganglia is inhibitory. This means that the basal ganglia primarily controls movement by choosing which movements are to be allowed. During tasks that require correcting of sensorimotor prediction error, regions of the striatum have been found to be deactivated. This is consistent with the hypothesis that error-based learning and reward-based learning work together, and with the findings that in the presence of errors, error-based learning may take preference.

1.4. Cost functions for motor control in novel situations

The cost function plays a major role in optimization but is not universally predetermined. The cost function can theoretically include an infinite number of terms. These may be energy, stability, time, accuracy, pain and many more. Some of these terms, particularly explicit costs such as pain and time can also be modelled as constraints, limiting the cost function to few terms. Importantly, we cannot directly observe the cost function used by our nervous systems. This uncertainty about the nervous system's cost function, combined with the generality of optimization allows us to explain most motor actions by selecting the appropriate cost function. However, such an endeavour provides minimal insight into the nervous system's motor control processes.

Therefore, it is important to form a hypothesis of the nervous system's cost function *a priori (10)*. Such hypotheses of cost functions are inherently influenced by the task being studied. Traditionally, motor adaptation has been studied in tasks of reaching to a target in the presence of visuomotor rotation or force fields. In such tasks, it's been hypothesized that the cost function is a weighted sum of error and effort (15). Here, error is associated with kinematics where moving away from the baseline trajectory is perceived as a sensorimotor prediction error. Effort is a term representing the system dynamics and can be quantified in multiple ways such as mechanical energy, muscle activity, or metabolic energetic cost. The effort term is generalizable to different learning algorithms, while a kinematic error necessitates error-based learning. I will focus my review to terms in the cost function that can serve as rewards.

Rewards can be broadly classified into primary and non-primary (37). Primary rewards relate to evolutionary fitness and reproduction. These are food or activities necessary to produce an offspring. All other rewards are non-primary rewards. In animal studies, food is often used as a reward and the learning can be framed as maximizing the cost function of food. Primary rewards work less well in human studies. Here, typical rewards include money or points for successfully completing a task. A cost function may be a combination of both these reward terms. In computational methods used to model these human studies, rewards refer to a broader set of terms that may be intrinsic to the task. One example is when the algorithm attempts to minimize the uncertainty in the forward model (40,41). Here the reward is the reduction of something unexpected. Other rewards include savings in joint torque, reduction of pain, reduction in time spent on a task, and increase in metabolic energy/ reduction in metabolic energy expenditure. Some of these, such as an increase in metabolic energy, act as a primary reward while others, such as reducing pain serve as a non-primary reward. I aim to identify general principles of motor adaptation by studying the optimization of a cost function where metabolic energetic cost is the significant contributor.

I have four reasons for selecting metabolic energetic cost as the significant term in the cost function. First, minimizing energy expenditure is a universal objective from an evolutionary perspective (42). Second, preferences in a variety of movements such as walking and running gaits, frequency of bench stepping, bicycle seat height while riding, and arm trajectories in reaching movements have been observed to be at or near the optimum of the measured energetic curve for humans (42–44). It is important to note here

that this is not to mean that energetic cost is the primary contributor to the objective function for all tasks. Rather, the significant role energetic cost plays in varied motor tasks allows us to use it as a tool in probing motor adaptation. To this end, the third reason in support of energetic cost as the primary term in the cost function is that principles learnt through studying energy optimization can translate to the optimization of other cost functions as well, such as the role of increased variability leading to improvements in motor adaptations and skill learning (45,46). Finally, savings in metabolic energetic cost can serve as a primary physiological reward to be used in the neural computations of reward-prediction error.

While there is plenty of evidence for the prevalence of metabolic energetic cost in the cost function, how it affects movement in novel situations is still poorly understood. One reason for this is that the time scales of metabolic energy optimization are unclear. That natural preferences support energy optimality could mean that developmental time scales are necessary for energy optimization. In support of shorter timescales, recent experiments have shown that adaptations in arm reaching and walking tasks correlate with reductions in metabolic power (44,47). A recent study showed that preferred reaching movements in new situations can also be modelled using a cost function that combines metabolic energy and rewards from stimuli (48). However, most computational methods use reward terms that represent effort or mechanical work rather than metabolic energy. Thus, there is limited knowledge about algorithms of metabolic energetic cost minimization when learning motor control in novel situations.

Algorithms involved in minimizing metabolic energetic cost can also inform improvements to quality of life. In the pursuit of fundamental mechanisms, it is important to address the generalizability of hypotheses. However, many tasks can benefit particularly from the reduction in energetic costs associated with them, even if the inherent cost function associated with those tasks may not prioritize energetic cost. For example, irrespective of whether energetic cost is the primary contributor to the cost function for walking in older adults, there is an obvious benefit to making the task energetically cheaper for the individuals. Understanding the algorithms used by the nervous system to obtain savings in metabolic energetic costs can help us develop techniques to achieve this in tasks where it is beneficial.

1.5. Implementation of energy minimization

There is some evidence that the human nervous system is equipped to implement energy optimization. The first step for this process would be to sense metabolic energetic cost. There are three candidate options for this. The blood gas chemoreceptors sensitive to oxygen and carbon dioxide are hypothesized to regulate ventilation (49). An increase in ventilation correlates with an increase in energetic cost since the body needs to use oxygen to generate energy to meet the increased energy demands (50). These receptors are present in the medulla oblongata and carotid bodies (51,52). They could help the nervous system sense a quantity representative of whole-body energy expenditure, similar to the indirect calorimetry systems we use in our experiments. Our lab tested the role of these sensors in energy optimization by attempting to trick the body into adapting to a gait that increased the oxygen sensed by these sensors (53). However, participants did not adapt suggesting that the body may have some other means to sense metabolic energetic cost. Another candidate mechanism for sensing metabolic energetic cost is through group III and group IV afferents from muscles. These are known to increase ventilation when stimulated and decrease ventilation when chemically suppressed (54,55). Their role has not been directly tested in the process of energy optimization and it is an interesting open question. Finally, it is possible that the nervous system senses energetic cost through some proxies of muscle mechanical work. This would require a computation involving muscle force, length and velocity. Mechanisms for sensing these have been established through muscle spindles and Golgi tendon organs (56). These are proprioceptive receptors and suppressing feedback from them has been found to change aspects of gait and recent studies have found some evidence of their role in energy optimization of gait (57,57).

The sensed metabolic energetic cost needs a mechanism to affect energy optimization. I hypothesize that metabolic energetic cost acts a primary physiological reward in the reward-prediction error mechanism. A common and primary reward that is used in experiments is food. But what makes food a primary reward is the consequences of digesting the food. The typical experiments with food as reward show learning times faster than the time it takes to digest food. However, this is because the animal has already learnt that some aspect of the food such as taste predicts reward. When rats were given neutral flavour food with varying glucose load, they learnt flavour preferences proportional

to the glucose load (58). Thus, the actual primary reward is the end product of the metabolism of food. Metabolic energy is one of those end products. Even if metabolic energy is not directly the primary reward, all consequences of digesting food can directly serve as proxies for metabolic energy. This reward still needs to be sensed by the brain to elicit firing of dopamine neurons in the striatum. Our nervous systems do not have any known reward receptors that directly sense reward (37). Rather the nervous system is known to be able to use signals from multiple chemical and mechanical receptors as reward signals (37). The exact chemical pathway used to transmit these signals is still unknown.

1.6. Energy minimization in human walking

Preferences in human walking are strongly predicted by metabolic energetic cost minimization. Humans typically prefer to walk in ways that are close to the measured energetic cost minimum (59). Studies in experimental and non-experimental settings have observed that the choice of walking speed, step frequency, step length, step width, toe-clearance, and starting and stopping, all coincide with the energetic minimum or are quite close to it (60–68). There are also walking tasks such as walking downhill or walking barefoot where preferences do not coincide with the metabolic energy minimum (69,70). However, these preferences do not fall far away from the metabolic energy minimum. This suggests that metabolic energetic cost is a significant contributor to the cost function of human walking but may be outweighed in certain situations.

The study of motor adaptation in walking has traditionally focused on minimizing the sensorimotor prediction error. The study of motor adaptation gathered momentum in locomotion only after the field had adopted arm reaching as a candidate task and identified the process of error-based learning. Early adaptation tasks in walking included walking in the presence of force fields or resistances applied to the legs, similar to the force-fields applied in arm reaching experiments, and identified features of sensorimotor prediction error in walking (71,72). A second walking task, unlike that used in arm reaching, is split-belt treadmill walking. This has also been used in understanding how the nervous system minimizes sensorimotor prediction error and has been the source of many insights into the role of the cerebellum in this process (73,74). However, just as in arm reaching,

minimization of sensorimotor prediction error is unlikely to be the only contributor to motor adaptation.

Recent work from our lab has provided direct evidence of metabolic energetic cost minimization in novel walking situations. Selinger and Abram, in separate experiments, manipulated the energetic costs associated with participants' walking step frequency and step width respectively (75,76). These manipulations shifted the energy optimum away from the original optimum. In these situations, participants now preferred a walking step frequency or step width that minimized the new measured energetic cost curve. The process of adaptation provides evidence that our nervous system uses a local search strategy in arriving at the energy optimal gait. This can be computationally modelled using a simple reinforcement learning algorithm (45). My projects in this thesis develop on these findings.

1.7. Two walking tasks

I use two different walking tasks to understand the energy optimization process. In both tasks, I measure walking gait to infer the control policy and measure metabolic energetic cost to represent the cost function.

The first task is walking on a treadmill while a mechatronic system applies controlled fore-aft forces to the hip. I built this system to further probe the results from Selinger et al. that was performed using a knee exoskeleton (75). Selinger manipulated the energetics of treadmill walking to observe participants adapt to the new energy optimum. However, this exoskeleton system was limited in its ability to probe the motor adaptation process further. It was only able to penalize its users—increase the energetic costs of gaits relative to natural. It was also limited in the range of penalties it could provide (13% to 41%) and the maximum cost gradient (0.93%) it could provide. In contrast, fore-aft forces to the hip can change the energetic cost of walking from -50% to more than +250%. Despite the application of forces, such a task feels safe and natural. Studies have found that forces to the torso can psychologically and biomechanically simulate walking on slopes and even climbing stairs (77,78). The energetics of walking with torso forces is also proportional to the energetics of walking on slopes (79). However, unlike slopes,

forces can be changed quickly and accurately while targeting the energetic consequences of small portions of gait. Note that the comparison between walking on inclines and walking with forces applied to the torso presented here is only to explain that the latter task does not feel unsafe or strange for the participants. The two tasks are not identical and differ in the work required at different stages of the gait cycle (80). However, these differences do not affect the hypotheses or the results presented in this thesis using the mechatronic system. I use this system to probe the algorithms underlying energy optimization during walking, particularly what features of a novel situation cue the nervous system to adapt.

The second task presented in this thesis is walking on a split-belt treadmill. A split-belt treadmill is a treadmill with two belts that can individually move at different speeds. A user typically walks with one foot on each belt. This is a useful adaptation paradigm and historically has been used to understand error-based learning—how the nervous system minimizes sensorimotor prediction error of step length when each foot moves at a different speed (74). In such adaptations, the stance time remains asymmetric even after adaptation. In fact, the temporal and spatial adaptation processes are thought to be distinct but not always mutually exclusive during split-belt walking (81). Therefore, it is unclear what error signal is actually being minimized as the sensorimotor prediction error. Recent studies have observed that metabolic energetic cost and mechanical work reduce with adaptation to split-belt treadmill walking, and these reductions may be possible due to the unique nature of walking on two belts of different speeds (82–85). In the projects in this thesis, I build on these results and probe the hypothesis that the observed adaptations to split-belt treadmill walking can be explained through a more unifying framework of energy optimization. I present direct evidence that the split-belt treadmill can be characterized as an assistive device than can provide energy to its users, making energy a significant factor in the task. I use experiments to measure mechanical work and metabolic energetic cost of walking on a split-belt treadmill and different step length asymmetries. I also use computer modelling to establish how different contributors to the energetic cost of walking affect walking on a split-belt treadmill.

Both these systems have a broader application as systems that can assist walking. The systems can provide energy that the user can learn to use. While the fore-aft force control system is designed for this purpose, the ability of the split-belt treadmill to provide energy was only recently hypothesized (85). I directly tested the hypothesis in the third project of this thesis. Both these tasks are used in rehabilitation and gait training. Here,

split-belt walking is an established fixture while walking with torso forces is new but promising (74,80,86,87). I use the fore-aft force control system for only one project in this thesis, but it can be programmed to be used in multiple ways relevant to public needs. For example, it can be programmed to provide a constant assistive force during walking to be used as an exercise device for people with gait impairments. Similarly, the identification of energy minimization in split-belt walking paves the way for identifying learning mechanisms in a system that is already well-integrated into patient treatments.

1.8. Aims

Learning to move in novel situations is a complex process. Our nervous systems can do this by solving for a control policy that minimizes a cost function in the novel situation. One of the processes that is used to solve for a control policy is reward-based learning which states that the nervous system selects the control policy that maximizes a reward. Reductions in metabolic energetic cost expenditure is a primary physiological reward of movements. While there is a lot of evidence for preferred movements being energy optimal, the role of energetic cost in the process of learning movements in response to novel situations and the algorithms involved in the process are unknown. My objective in this thesis is to probe the role and process of energy optimization in identifying an optimal control policy in novel situations. Our lab recently identified that adaptations to novel walking situations can occur through energy optimization. Given this finding and the significant contribution of metabolic energetic cost to walking in familiar situations, I use adaptation of walking in two novel situations as candidate tasks for understanding energy optimization.

My objective while working on this thesis was also to advance my skills as a scientist to enable me to continue the pursuit of principles that govern human movement. This is reflected in the thesis as it journeys through mechatronics, computational neuroscience, mechanics and energetics, and rigid-body dynamics.

Aim 1: Design, build and test a mechatronic system to study energy optimization in humans. To study the process of optimization, I need a system that can reshape the energetic cost landscape such that the person's originally preferred gait is

now sub-optimal. This allows me to observe the gait behavior executed by the nervous system in the process of finding the new optimal gait in any new landscape. I designed a system to reshape the landscape using fore-aft forces applied near the user's center of mass as a function of their walking step frequency. I built it to apply quick, accurate, and precise forces at each new measured walking step. I validated its effectiveness for studying energy optimization by introducing participants to a cost landscape, created with this system, in which participants have been known to re-optimize their gait within a few minutes.

Aim 2: Determine whether a steeper cost gradient causes the nervous system to initiate energy optimization in novel situations. When our nervous system encounters a novel situation, it has to learn whether the existing preferred control policy is optimal or not before it searches for a new policy. Without this knowledge, our nervous system may prefer to, perhaps erroneously, exploit the previous preferred control policy. This is reflected in the observation that our nervous systems do not always adapt to novel tasks. However, changing some aspects of the same task can allow the nervous system to initiate adaptation. The algorithm involved in this initiation is still unknown. In my second study, I used my fore-aft force control system to test whether a feature of a novel task, specifically the cost gradient, can allow the nervous system to initiate adaptation. I introduce participants to cost landscapes with increasing cost gradients and measure adaptation of their walking step frequency.

Aim 3: Determine the biomechanics and energetics of split-belt walking. When walking on a split-belt treadmill, participants typically adapt their step lengths to be symmetric. This means that the distance measured between the heels of the two feet—step length—is equal for two consecutive steps. This is traditionally explained as a process of minimizing a sensorimotor prediction error since, when walking over ground, people typically prefer equal step lengths for all steps. In this project, I collaborate with a research group at University of Southern California to determine the biomechanics and energetics of different step length choices during split belt walking. We hypothesized that the step lengths participants adapt to are also step lengths with a lower energetic cost suggesting that the adaptation can also be explained as a process of reducing energetic cost.

Aim 4: Develop a computer model to determine the energetic contributors to the energy optimal gait in split-belt walking. Measurements of metabolic energetic cost

from participants reveals that there is an energy optimal step length asymmetry when walking on a split-belt treadmill. Step length asymmetry is a measure of the relationship between two consecutive step lengths. However, it is unknown what factors contribute to this relationship between step length asymmetry and energetic cost or why there should be a minimum. In over ground walking, computer models have identified that the cost of step-to-step transition and the cost to swing the leg are the two primary contributors to energetic cost that trade-off to give rise to the preferred walking gait. In this project I develop a dynamic walking computer model to test whether the same trade-off leads to the observed energy optimal step length asymmetry in split-belt walking.

Together, these projects develop a new system and a new approach for studying motor adaptation through walking. The results uncover fundamental principles of these adaptation processes.

Chapter 2.

A mechatronic system for studying energy optimization during walking

2.1. Abstract

A general principle of human movement is that our nervous system is able to learn optimal coordination strategies. However, how our nervous system performs this optimization is not well understood. Here we design, build, and test a mechatronic system to probe the algorithms underlying optimization of energetic cost in walking. The system applies controlled fore-aft forces to a hip-belt worn by a user, decreasing their energetic cost by pulling forward or increasing it by pulling backward. The system controls the forces, and thus energetic cost, as a function of how the user is moving. In testing, we found that the system can quickly, accurately, and precisely apply target forces within a walking step. We next controlled the forces as a function of the user's step frequency and found that we could predictably reshape their energetic cost landscape. Finally, we tested whether users adapted their walking in response to the new cost landscapes created by our system and found that users shifted their step frequency towards the new energetic minima. Our system design appears to be effective for reshaping energetic cost landscapes in human walking to study how the nervous system optimizes movement.

2.2. Introduction

Optimization is perhaps our most general principle of coordination. That is, people prefer to move in ways that minimize a cost function (20,88). A cost function is a weighted sum of one or more variables related to the movement, with the particular variables and their weights depending upon the task (20,22,48,89–94). For example, the cost function in reaching to a target is often modelled as a weighted sum of error and effort (15,48). One way to study optimization is to determine if the predicted cost minimum correlates with people's preferences. Using reaching tasks as an example again, minimizing the sum of the variance about the target and squared muscle activations can explain people's preferred arm trajectories (15). While preferences suggest that the nervous system is concerned with optimizing coordination, preferences alone don't provide insight into how it is accomplished. To study the nervous system's optimization algorithms, it is useful to manipulate the nervous system's cost function and determine whether, and how, people respond. This is best accomplished in tasks where the cost function is well established, easy to manipulate, and directly measurable.

Walking is a well-suited task to study the nervous system's optimization mechanisms. It has been well established that people typically prefer to walk in ways that minimize metabolic energetic cost (42,60,63,64,95–97). For example, at every given speed, people choose to walk at the step frequency that minimizes their energy use (96,97). In addition to the many studies demonstrating preferences for energy minimal gaits in familiar conditions, recent research from our lab by Selinger *et al.* found direct evidence that the nervous system can continuously adapt these preferences to optimize energy during walking (75). Selinger *et al.* used a knee exoskeleton to manipulate a user's cost landscape by penalizing certain step frequencies, shifting the energy minimum away from the originally preferred step frequency. We use cost landscape to refer to the relationship between a gait parameter and its resulting metabolic energetic cost. Using such purposeful manipulation, Selinger *et al.* demonstrated that the nervous system could continuously optimize movements to converge on the new energy minimal gait within minutes (75). Thus, energy optimization in walking is a useful model system because the nervous system's cost function is unambiguous, we can measure the cost directly, we can directly manipulate the values returned by the cost function to study how the nervous

system solves it, and the time course of optimization can be rapid enough that we can study it in a single experimental session.

This prior exoskeleton system allowed us to observe continuous optimization, but it was limited in its ability to probe the underlying mechanisms. The exoskeletons could only penalize users, and not reward them by decreasing their cost below their normal values. The range of penalties were limited to between 13% and 41% of the user's original cost minimum, achieving a maximum gradient of 0.93% change in energetic cost for every 1% change in step frequency. In contrast, an ideal system would be able to precisely and rapidly prescribe cost landscapes of any shape. Such control over the shape of the cost landscape would allow both steeper and shallower cost gradients to study how the nervous system detects cost savings through its movement variability (16,46,98), the creation of complex cost landscapes to study the nervous system's optimization algorithms (20,25), and the lowering of energetic cost to study whether the nervous system differentially values energetic penalties and rewards (99,100). Applying new costs rapidly is also important because the nervous system's association of a particular coordination pattern with its resulting energetic cost may depend upon the delay between the movement and its energetic consequence (101,102). A quick system can always be slowed down to study the effects of delayed costs, but an inherently slow system cannot be sped up.

Here we present a new mechatronic system designed to probe optimization mechanisms during walking. Based on data-driven simulations, the system uses controlled horizontal fore-aft forces applied near the center of mass of the user to change energetic cost landscapes. This system can generate a wide range of cost gradients because energetic costs during walking depend strongly on horizontal forces (103). It can also provide both energetic penalties with backward forces and energetic rewards with forward forces. It uses a series elastic actuator to apply these controlled forces precisely and rapidly (104). In the following sections, we first develop the high-level design using simulations that leverage literature data and then describe the construction of the system. Next, we evaluate system performance including a) how well it controls forces, b) how well the measured energetic costs match the predictions generated during design, and c) how users adapt their walking in response to new cost landscapes created by our system.

2.3. System Design

We designed a system to manipulate the energetic cost of human walking. We achieve this by applying controlled horizontal fore-aft forces to the user as a function of one or more measured gait parameters. In this paper, we use a single parameter, step frequency, for ease of comparison with prior work (75,96,103). For an individual walking at a constant speed, there is an energetic cost associated with each step frequency, with the minimal cost occurring at their preferred step frequency. We term this their originally preferred step frequency. Our system applies a backward or forward pulling force at each measured step frequency. Thus, the final energetic cost experienced by the user is the sum of the energetic cost associated with that step frequency and the energetic penalty (or reward) from the applied force. This new association between step frequency and energetic cost is the new cost landscape. In this manner, we can shift the energetic optimum higher or lower than the originally preferred step frequency. We then measure users' preferred step frequency in the new cost landscape to determine their new preferred step frequency.

As a first test of our design, we simulated the system's effect on a user's energetic cost. We used literature data of the energetic cost associated with various walking step frequencies when no force is applied, where step frequency is measured as percent of the individual's preferred step frequency (96). We also used literature data for the energetic cost of walking at the preferred step frequency while a range of forces are applied, where the forces are measured as percent body weight of the individual (103). We then combined these two data sets to obtain the energetic cost of walking at various step frequencies over a range of applied horizontal forces. Constraining the range of step frequencies to ±15% of preferred, and the range of horizontal forces to ±15% of body weight, we estimated that our system could vary a user's energetic cost of walking from -45% to +230% relative to their original energetic minimum.

Based on these initial simulations, we built a mechatronic system to apply rapid, accurate, and precise forces as a function of the user's measured step frequency (Figure 2.1). In this system, users walk on a single-belt treadmill (Trackmaster TMX425C, Full Vision Inc., Kansas, USA) while wearing a hip-belt (Osprey Isoform4 CM) that places them in a closed loop with the actuator. The hip-belt is tailored with extended belt loops in the front and back to which we attach long inextensible nylon cables. The long lengths (~409

cm in front and ~197 cm in back) help ensure that the forces on the user remain nearly purely in the fore-aft direction despite the within-stride vertical and medio-lateral movements of the center of mass during walking. These cables pass through nylon pulleys with bearings (McMaster-Carr Nylon Pulley 3434T16) on either end and meet the actuator located behind the user (Figure 2.1). We use light weight pulleys with low friction bearings to ensure low reflected inertia and minimal loss of forces during transmission. We use a series elastic actuator designed by Yobotics to produce the required force [29]. It consists of a 70 Watt brushless DC motor (BN23-23PM-03LH, Moog Inc.) that rotates a custom molded lead ball screw to maintain a set of four compression springs (McMaster-Carr Compression Spring 9434K147; spring stiffness = 33 lbs./in) at the required compression as determined by the commanded force. We measure the actual compression of the springs using a linear optical encoder (LIN-120-32, US Digital, Vancouver, WA, USA) and maintain their position with a proportional-integral controller implemented with a motor driver (Accelnet panel ACP-090-36, Copley Controls) that commands the motor using a 15 kHz center-weighted pulse-width-modulated signal. The required spring compression is commanded to the motor driver from a real-time controller (ds1103, dSPACE GmbH, Paderborn, Germany).

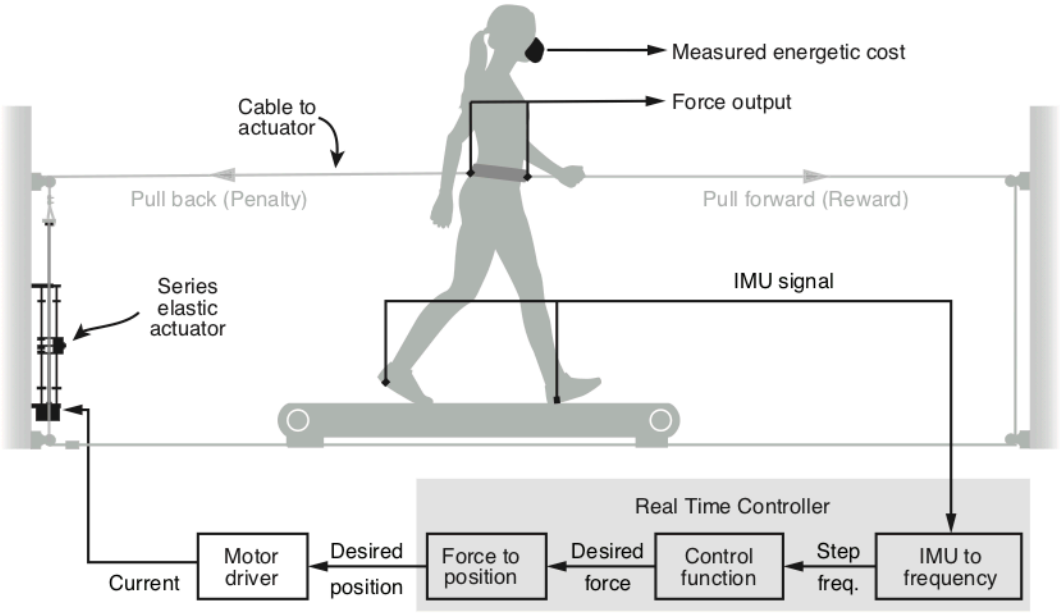

Figure 2.1: Mechatronic system
An actuator pulls backwards or forwards on a walking user via long tensioned cables attached to a hip belt. The cables are routed through pulleys, so that they attach on either side of the same linear actuator. Backward forces provide an energetic penalty, raising the cost of walking relative to normal. Moderate forward forces provide an energetic reward, lowering energetic cost. Force transducers between the cables and belt measure the forces applied to the user. Step frequency

is measured from IMUs attached to the feet. Output forces from the motor are controlled using real-time custom designed control hardware and motor driver. Metabolic energetic cost is measured using indirect gas calorimetry.

This real-time controller measures step frequency, performs online calculations, and sends the resulting force commands to the motor driver. It is built in Simulink (Mathworks, NA, USA), and once compiled, runs at 1 kHz on the controller hardware. The controller receives analog signals from inertial measurement units (IMU) placed near the heel of each foot and estimates the step frequency by identifying foot ground contact events using characteristic zero crossings in angular velocity. To reduce error, it filters the analog signals using a 10 Hz, 2nd order low-pass Butterworth filter and requires that consecutive zero-crossings arise from alternate feet. The implementation of this condition requires the controller to divide this value by two to obtain step frequency. It passes this step frequency through a control function that determines the force to be commanded depending on whether we want to reward or penalize the measured step frequency and by how much. We then use a pre-determined calibration function to estimate the spring compression required to produce the commanded force. The calibration function was obtained by measuring force output for a range of commanded spring compressions. Finally, the controller commands the estimated spring compression to the motor driver. We designed the controller to accept inputs from a MATLAB 2013b (Mathworks, NA, USA) script for parameters such as the user's mass. We use dSPACE ControlDesk 5.2 (dSPACE GmbH, Paderborn, Germany) to monitor and record the data.

We also use the dSPACE board to monitor and record the forces and the signals required to calculate energetic cost measures. We calculate the actual net force applied to the user as the sum of forces measured by the two load cells (LCM201, Omega Engineering) attached to the cables at the front and back of the user's hip-belt. The forces are transmitted as analog signals to the dSPACE board where they are filtered using a 30 Hz, 2nd order low-pass Butterworth filter. To calculate energetic cost, the dSPACE board records from oxygen, carbon dioxide, and flow sensors, mounted on the mask worn by the user (Vmax Encore Metabolic Cart, Viasys, Pennsylvania, USA).

2.4. System Performance

We evaluated system performance at four levels. First, we considered open loop control of constant forces when there is no user present in the system. Second, we tested open loop control of constant forces while a user walked in the system. Third, we closed the force control loop using our controller and evaluated the control of forces when the commanded force changed with each walking step. Finally, we measured the effect of the system on the user's energetic cost and gait adaptation. All walking trials were at a constant speed of 1.25 m-s^{-1}. All protocols with human users were approved by the Simon Fraser University's Office of Research Ethics, and all users gave their written, informed consent before participation.

2.4.1. Open-loop force control

We first evaluated open-loop force control performance to determine whether our system could change between target forces within a walking step. We measured this responsiveness as rise time—time taken for the measured force to reach 90% of the way towards a new commanded value from an original commanded value. To accomplish this, we replaced the hip-belt with a wooden plank attached rigidly to the treadmill frame. We measured the force applied on the plank when we manually commanded step changes in force between 0N and either -49 N or +49 N. We repeated each step change 20 times, and each step lasted 4 seconds. We choose these force levels to match 10% of the body weight of our primary system tester, who weighs 490 N (body mass=50 kg, acceleration due to gravity=9.81 m-s^{-2}). By design, the magnitude of these step changes is conservatively large—when under closed-loop control, users would normally not make a large step-to-step adjustment in step frequency, and thus would not experience a step-to-step change in force as large as we tested here. We found an average rise time of 85 ms. Even assuming a high walking step frequency where each step takes only 400 ms, this easily allows for force changes within a single walking step (105) (Figure 2.2).

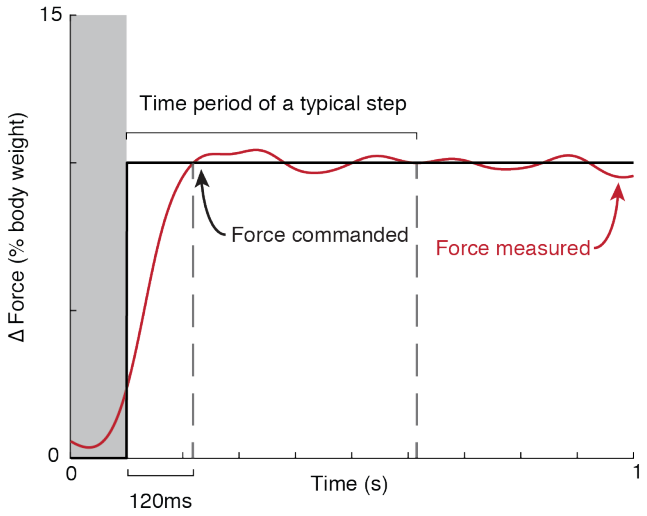

Figure 2.2: Open loop force control - responsiveness
Time taken for the measured force (red) to reach a new commanded value from an original commanded value (black). Data shown here were averaged over 20 step changes. Each step was a change of 10% body weight—the original commanded value was always 0 N while the final value was ±10% body weight (body mass=50kg; acceleration due to gravity=9.81 m-s^{-2}).

We next evaluated the system's accuracy and precision in applying the commanded force to a walking user. We quantified accuracy as the steady state error between the commanded force and the measured force and precision as the steady state variability in force about the steady state force. We measured the force applied to our system tester as they walked at their self-selected step frequency for two six-minute trials. During this time, we manually commanded step changes in force between 0N and ±10% body weight (body mass=50 kg, acceleration due to gravity=9.81 m-s^{-2}). Importantly, the force commands were in open-loop—they did not depend upon the user's step frequency. Each condition lasted one minute, and each non-zero force was preceded by the zero force condition. We allowed 35 seconds for the self-selected step frequency to approach steady state (106,107) and performed our analyses on the remaining 25 seconds. We first averaged the force over each step, obtaining a single force value per step, and then averaged this value over the 25 seconds. We determined steady state error as the difference between this averaged force and the commanded force for that condition. We found that our system can match a commanded force with an average steady state error of 0.13% body weight (Figure 2.3). The average steady state variability for this user was 0.39% body weight when calculated between steps (root-mean-squared error). The force variability within a step was considerably higher at 2.64% body weight. We were not concerned about the magnitude of this within-step variability since our controller is

designed to manipulate the energetic cost only at each new step since it applies force as a function of step frequency. Similarly, the exoskeleton of Selinger *et al.* (75) had considerable within step variability in the torque it applied to the knee. Because the applied horizontal forces affect energetic cost, any inaccuracies or imprecision in applied forces will result in inaccuracies and imprecision in the cost landscapes created by our system. Based on our modelling during system design and the identified force control performance described here, we predict steady state energetic cost errors of ~1.3% and steady state energetic cost variability of ~3.8%, relative to the average minimum energetic cost of regular walking (96). One consequence of this step-to-step energetic cost variability is that it is necessary to average over several walking steps to accurately estimate the steady state energetic cost generated by the controlled forces. This is not a major practical concern for the experimenter as the significantly greater variability in breath-to-breath measures of energetic cost (108) normally requires averaging energetic cost over 2-3 minutes, or about 200-300 steps.

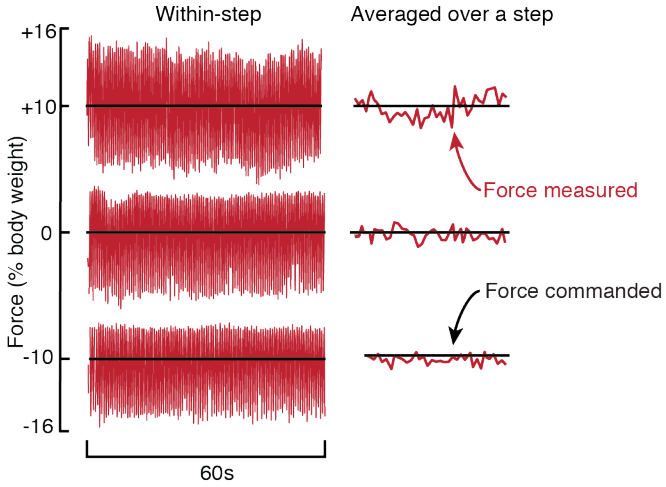

Figure 2.3: Open loop force control - accuracy and precision
The measured force (red) has a steady-state-error of 0.13% body weight when averaged over a step. The RMS error is 2.64% body weight within a step and 0.39% body weight when the force is averaged over a step. Data were collected from one user (body mass=50 kg; acceleration due to gravity=9.81 m-s^{-2}) walking at 1.25 m-s^{-1} while attached to our system, with a constant force being commanded (black).

2.4.2. Closed-loop force control

At the third level of evaluation, we applied the forces to a walking user as a function of their step frequency. We only evaluated precision at this level because there was no steady state force—the commanded force depended on the user's execution of step frequency. We measured the net force applied to one user as they matched an audio metronome that played seven frequencies spanning ±15% of their originally preferred step frequency. Each step frequency condition lasted one minute, and the measured net force was first averaged over a step, and then over the last 25 seconds of that condition. We repeated this with two control functions where a control function defines the relationship between measured step frequency (sf) and commanded force (F):

$$F = f(sf) \tag{2.1}$$

Both control functions were linear with zero offset, but one had a slope (k) of +1 thereby penalizing low step frequencies, while the other was -1 penalizing high step frequencies:

$$F = k \cdot sf, \;\; k = +1, -1 \tag{2.2}$$

We averaged the steady state variability, calculated as root-mean-squared error, across all 14 trials and found it to be 0.59% body weight (user's body mass=50 kg, acceleration due to gravity=9.81 m-s^{-2}) (Figure 2.4). This results in a predicted steady state energetic cost variability of ~5.7%, which, as described in the previous paragraph, is not of practical concern for the experimenter when estimating steady state energetic cost.

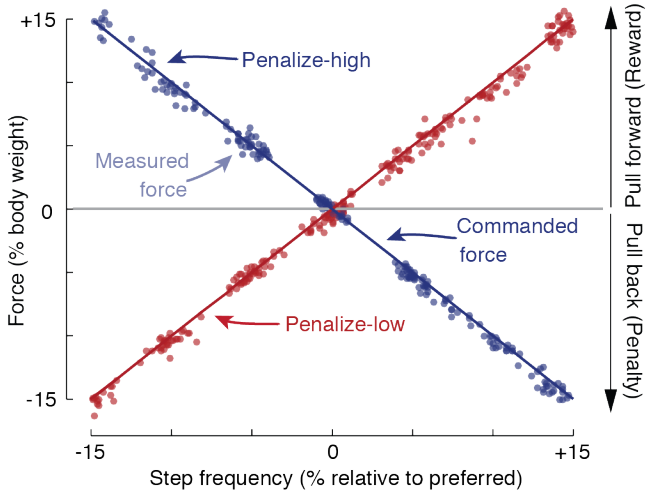

Figure 2.4: Closed loop force control
Measured force averaged over each step (dots) as a function of step frequency while walking at 1.25 m-s^{-1} for a single trial by a single user. The user matched an audio metronome played at seven different step frequencies ranging from -15% to +15%. Red and blue lines illustrate that we used these forces to create two different cost landscapes—one that penalized low step frequencies (red), and the other that penalized high step frequencies (blue).

2.4.3. Effect on energetic cost

In the fourth level of evaluation, we created a new energetic cost landscape with our system and compared it to our predictions. Specifically, we measured how the metabolic energetic cost changed for one user as they walked in the system with a controller that commanded a force as a function of their step frequency. We tested the same two control functions described above. We designed them to create very steep cost landscapes that shifted the cost landscape minimum in different directions. First, we measured the user's resting energetic cost during a 5-minute standing trial. Next, the user walked on the treadmill without the hip-belt, and unattached to the cables, for 12 minutes. We averaged the step frequency over the last three minutes to determine their originally preferred step frequency. Then, for each control function, the user walked at seven step frequencies spanning ±15% of their originally preferred step frequency. We enforced the step frequencies using a metronome and presented them in random order. To determine energetic cost, we measured the volume of oxygen consumed and volume of carbon dioxide produced using a respiratory gas analysis system (Vmax Encore Metabolic Cart, Viasys, Pennsylvania, USA). We divided these volumes by the measurement period to determine the rate of oxygen consumption ($\dot{V}_{O_2}$) and carbon dioxide production ($\dot{V}_{CO_2}$). We applied the standard Brockway equation (109) to obtain the gross metabolic power:

$$P_{met,gross} = \left(16.48 \frac{W\ s}{ml\ O_2} \dot{V}_{O_2}\right) + \left(4.48 \frac{W\ s}{ml\ CO_2} \dot{V}_{CO_2}\right) \quad (2.3)$$

We define metabolic energetic cost as the energy used per unit time normalized for the person's body mass (W/kg). This user's body mass was 66 kg. Each trial lasted five minutes of which we allowed the first three minutes for the respiratory gases to reach steady state (110) and performed our analyses on the remaining two-minute measurement period. To compare with the user's original cost of walking on a treadmill, we also measured their energetic cost at the same step frequencies while they walked on the treadmill without wearing the hip-belt or being attached to the cables. We subtracted the user's resting energetic cost for each condition and present here the net energetic cost. In accordance with our predictions, we could manipulate this users' energetic cost of walking by as much as -49% to +230% of their original minimum (Figure 2.5). This is more than a 5-fold increase in the magnitude of applied penalty when compared to our exoskeletons, and unlike with our exoskeletons, our current system can provide an energetic reward by lowering cost.

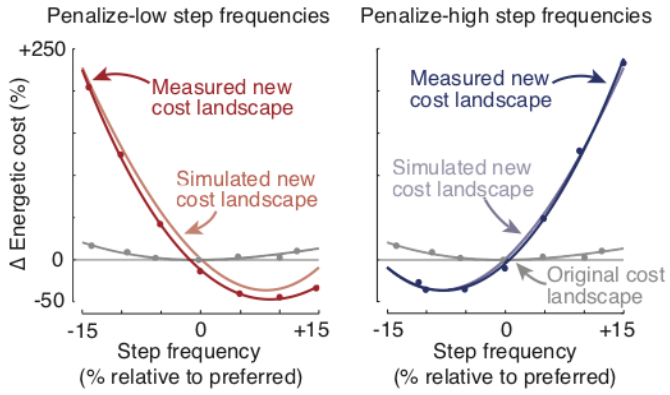

Figure 2.5: Simulated vs measured energetic costs
Metabolic cost measures (dots) for a single trial by a single user walking at 1.25 m-s^{-1}, when force changed as a function of step frequency as shown in Figure 2.4. Grey curves illustrate the original cost landscape of the user while the red and blue curves illustrate cost landscapes that penalized low and high step frequencies respectively. Light colored curves illustrate our predicted results from simulations, and dark colored curves illustrate quadratic fits to measured data.

2.4.4. Adaptation to new cost landscapes

Next, we evaluated the ability of the nervous system to adapt gait towards the minima of new cost landscapes created by our system. Since different people's nervous system can adapt differently, we used group analysis rather than single-subject analysis for the remaining tests. To do so, we closely matched the cost landscapes and protocol

used in our prior exoskeleton experiment, as that design was sufficient to generate continuous energy optimization during walking (75). We used the following control function designed to penalize high step frequencies and shift the new cost landscape minimum to step frequencies lower than originally preferred:

$$F = \begin{cases} -0.07 \cdot sf - 1.49, & sf \leq -5 \\ -0.19 \cdot sf - 1.98, & sf > -5 \end{cases} \quad (2.4)$$

However, while prior studies parameterized the change in step frequency as percent deviation from the originally preferred step frequency, here we used step-to-step variability in step frequency, measured in standard deviations (SD). This allows us to understand the shift in preferred step frequency relative to the probability of it occurring by random chance. A 1SD shift was nevertheless comparable to a 1% shift as we found that the average standard deviation of our participants was 1.04%±0.12% (N=20). One concern is whether the application of these forces might cause people to change their preferred walking step frequency independent of the control. We suspect that this is not the case for two reasons. First, our system is biomechanically similar to walking on inclines (e.g. (77)) and the literature shows no clear relationship between preferred walking step frequency and incline (e.g. (111)). Second, we performed a pilot study of the effect of applied horizontal forces on preferred step frequency using 13 participants and found no relationship (data not presented here).

Each participant completed three protocols on the same day (N=8; female=3; male=5; mass=67±8 kg; height=172±6 cm). The purpose of the first protocol was to quantify each participant's originally preferred step frequency, as well as the variability about the preferred step frequency (Figure 2.6A). To accomplish this, each participant walked on the treadmill without the hip-belt for 12 minutes. To parameterize step frequency in future trials, we calculated the average and standard deviation of step frequency during the last three minutes.

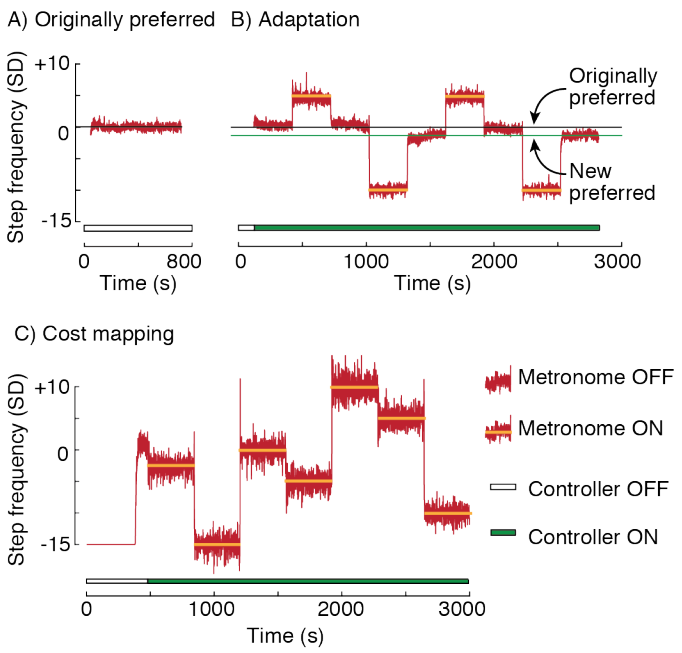

Figure 2.6: Experimental protocol
A) and **B)** represent average measures from 8 participants while **C)** is from a single representative participant since the order of the metronome frequencies was different for each participant. **A**) Average originally preferred step frequency in the original landscape. **B)** Participants' average step frequency time series during the protocol when we tested for gait adaptation. When the controller came on (green bar at the bottom) participants walked in a new cost landscape (Figure 2.7) created by our system. Following the first five minutes of self-selected step frequency, they matched an audio metronome (orange bar) that either held them at a high step frequency (higher cost) or low step frequency (lower cost) relative to their originally preferred step frequency (black line) in the new cost landscape. **C)** Step frequency time series from a single representative participant during the third protocol when we measured their new cost landscape. Participants matched seven audio frequencies (orange bar) when walking in the new cost landscape (Figure 2.7) while we measured their energetic cost.

The purpose of the second protocol was to determine the step frequency that participants preferred in the new cost landscape (Figure 2.6B). To accomplish this, participants wore the hip-belt and walked continuously for 47 minutes while attached to our system. In the first 30 seconds, no force was applied, allowing the treadmill to reach the prescribed speed, and the participants to approach their originally preferred step frequency. Over the following 60 seconds, the force was slowly ramped up to match the force that participants experience at their originally preferred step frequency in the new cost landscape. This ensured that participants were not perturbed by a sudden force when we engaged the controller. The force was then held constant for 30 seconds, following which we engaged the controller, placing participants in the new cost landscape. Participants then alternated between periods of walking with a self-selected step frequency and walking to an audio metronome played at a prescribed frequency, with each

period lasting five minutes. The metronome frequency alternated between +5SD and -10SD, to allow the participant to experience both higher and lower energetic costs relative to the cost of walking at their originally preferred step frequency in the new cost landscape. In our instructions to the participants we said, “when you hear the metronome please try to match it but otherwise you may walk however you like”. We determined participants’ new preferred step frequency in this new cost landscape as the average self-selected step frequency over the final three minutes of this protocol.

The purpose of the third protocol was to quantify the new cost landscape experienced by each participant (Figure 2.6C). This was necessary since our hypothesis of observing adaptation towards the new energy optimum is conditional upon the new cost landscape having an energy optimum different from the original cost landscape. We first measured the energetic cost of standing still for six minutes for each participant. Next, participants walked in the system while under the same control function with the same force ramp up as described earlier. Participants matched seven step frequencies (-15SD, -10SD, -5SD, -2.5SD, 0SD, +5SD, and +10SD) produced by an audio metronome and played in random order. We measured each condition for six minutes. This was a minute longer than what we did with the previous control function (Eqn. 3) because we designed this cost landscape to be shallower. An extra minute of measurement provided us with more breath-by-breath samples of the energetic cost associated with each measured step frequency, and thus greater confidence in our cost estimates for each condition for each user. We subtracted resting energetic cost from each walking condition to obtain net energetic cost. Importantly, this was always the last trial that each participant performed, to ensure that it did not influence their gait adaptation.

Before analyzing our results, we tried to ensure that we had collected data from sufficient number of participants to effectively test for adaptation. We were primarily concerned with two issues. The first issue was that participants vary in the amount they shift their preferred step frequency in response to new energetic cost landscapes—the larger the variability, the greater the number of participants required to confidently detect a significant shift. To estimate the required number, we first needed to estimate the between-participant variability in self-selected step frequencies in new cost landscapes. To accomplish this, we conducted a pilot study with seven participants in a new cost landscape and found that the variability between participants in their self-selected step frequencies was 1.6SD. Using a power analysis for a one-tailed t-test, we determined that

eight participants were required to detect a reduction of 2SD in their new preferred step frequency relative to their originally preferred step frequency (β > 0.90, α < 0.05).

The second issue was that individuals have different energetic responses to the same applied forces resulting in cost landscapes that vary between individuals. This variability, when combined with a control function designed to create small changes to the original cost landscape, results in some new cost landscapes that do not shift the new minimum cost to lower step frequencies. And we can only test the effectiveness of our system in causing adaptation to lower step frequencies when the new cost landscapes have a new energetic minimum at a lower step frequency. We operationalized this constraint by requiring that an individual's new cost landscape meet three criteria—the cost at the new minimum, -2.5SD, and -10SD should all be more than 3SD lower than the cost measured at the originally preferred step frequency. We calculate this 3SD value from the variability in breath-to-breath energetic cost measured during the last three minutes of walking at 0SD. The first condition ensures that the new minimum provides a cost saving to the nervous system; the second ensures that there is a cost gradient at the originally preferred step frequency to direct the nervous system towards the new minimum; the third ensures that the nervous system experiences a cost saving during the metronome-enforced experience period. We performed a preliminary analysis of the cost landscapes of our first eight participants and estimated that we would need to collect from a total of 20 participants to have eight that met all three criteria. After collecting from 20 participants, we screened them to determine that they did not hit the end ranges of our actuator, consistently matched the commanded step frequencies when we measured their cost landscape and had cost landscapes that met our defined criteria. Eight participants met these conditions. Importantly, we screened for these conditions prior to testing for gait adaptation in order to not bias our results towards a positive finding. Our subsequent analysis is of these eight participants. During the manuscript revision process, we were asked by reviewers to consider the behavior of all 20 participants. We found the same general patterns.

Finally, we determined the step frequency that minimized energetic cost in the new cost landscape, and whether our participants adapted towards this new minimum. To determine the step frequency that minimized cost, we used a linear mixed effects model to fit a quadratic relationship between step frequency and energetic cost to our measurements from all eight participants (112). We chose this method, over fitting each

participant's costs individually, because breath by breath measures of energetic cost are quite variable, and this variability can dominate the differences in actual energetic cost between different step frequencies, causing noise to dominate when fitting individual cost landscapes. This method yields a value for confidence in the location of this minimum. We used Monte Carlo simulations to determine the 95% confidence interval in this location. We resampled with replacement from the residuals of the linear mixed effects model and added it back to the average fit from the model. Each resampling yielded one simulated energetic cost for one step frequency for one simulated participant. We obtained 56 (8 participants by 7 step frequencies) such values to simulate one experiment and used a mixed effects model to fit these simulated values. We simulated 1000 such experiments and determined the location of the minimum in each case. We found that the average energetic minimum at -5.7 SD would have reduced the cost of walking by 6.1%, and the 95% CI of the location of the minimum spanned from -6.8 SD to -4.8SD (Figure 2.7). To compare, in the study by Selinger *et al.* with the exoskeletons, we observed energy optimization in new cost landscapes where the energetic minimum reduced the cost by 8.1% ± 7.0% (mean±SD) (75). Using a one-tailed paired Student's t-test, we found that in our new cost landscape, participants shifted their preferred step frequency away from their originally preferred step frequency and towards the energetic minimum by an average of -1.27 SD ($p=0.005$) (Figure 2.6B). This reduced their average energetic cost by 3.4%. We found similar patterns when we performed the same analyses including all 20 participants—a significant shift of the preferred step frequency towards the energetic minimum. The 20 participants shifted by an average of -0.69 SD ($p=0.025$) which reduced their average cost by 0.5%. We suspect the more modest shift in step frequency and cost, and larger p-value, is due to some of the participants having smaller changes in their cost landscape in response to our system's manipulation, as well as not consistently matching the commanded step frequency when we measured their cost landscape, and hitting the end ranges of our actuator.

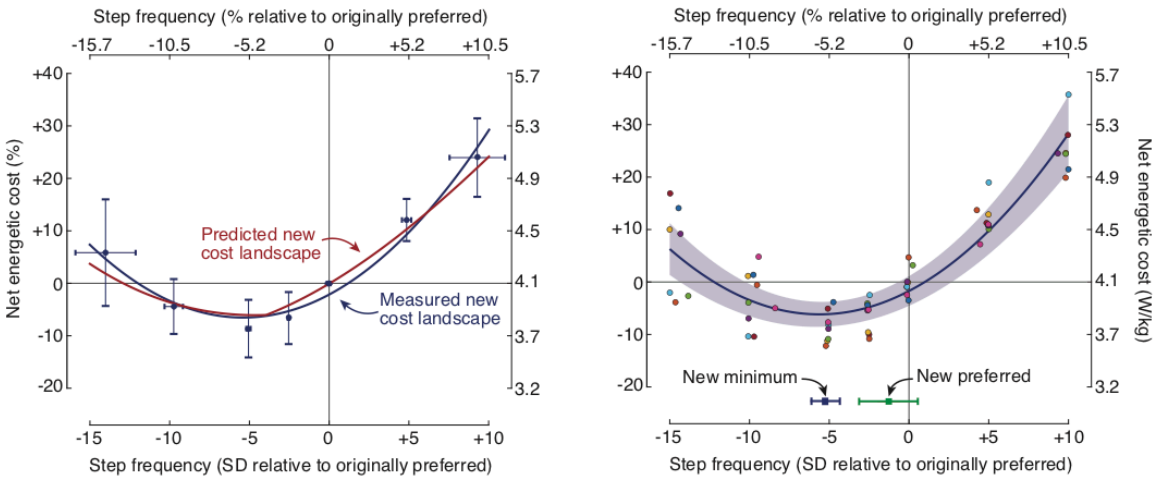

Figure 2.7: New cost landscape
The new cost landscape shifts the energy optimal step frequency lower than participants' originally preferred step frequency (0 SD). On left, we averaged the participants' measured step frequency and energetic cost for each commanded step frequency condition (blue dots with error bar indicating one standard deviation). The blue curve represents a quadratic fit to these measured data, while the red line represents the cost landscape predicted by the control function in Eqn. 4. On right, each dot represents the steady-state energetic cost measured from a participant at the step frequency that they executed. Each color corresponds to one participant. The blue curve illustrates a 2nd order linear mixed effects model of these data. The shaded region illustrates the 95%CI of the model, while the blue square at the bottom denotes the minimum predicted by the model, and the 95% CI of this minimum obtained using the Monte Carlo simulations. The green square denotes the average and 95% CI of participants' new preferred step frequency in the new cost landscape. This reduced their energetic cost by 3.4% relative to the cost at 0 SD. Left-hand y-axis values are normalized to the average energetic cost of 4.07 W/kg measured at 0 SD.

2.5. Discussion

Our system meets our performance requirements for studying energy optimization during walking. It can apply a large range of forces within the duration of a typical walking step. These forces are applied accurately and precisely even when the commanded force changes as a function of the user's walking step frequency. These features together allow us to manipulate the energetic costs associated with every walking step. The system can apply forces that both reward and penalize the energetic cost of walking, relative to the user's original cost landscape. We can also predict the average energetic cost landscape that the system creates for users for a given control function. The new cost landscapes created by our system caused users to adapt their walking gait towards the new energetic minimum, reducing their energetic cost by 3.4%. Interestingly, most users did not fully

converge on the new optimum, which would have reduced their energetic cost by an additional 2.7% on average.

We considered two explanations for this incomplete energy optimization. One explanation is that the nervous system is optimizing a weighted function of the originally preferred and executed step frequency, and the most recently executed step frequency (113). However, our adaptation protocol required participants to walk at both high and low frequencies for the same duration, and participants only adapted to lower step frequencies, towards the new energetic minimum. A second candidate explanation for the incomplete energy optimization is that the optimization process is slow, particularly in our system. One factor that can slow optimization is measurement noise—the greater the variability in energetic cost, the greater the challenge for the nervous system to detect its gradient and assess the direction of the energetic minimum. This effect is especially pronounced near the minimum where the gradient is typically shallow, yet the noise is unchanged. The force variability in our system contributes to a noisy energetic cost gradient. For one user, we measured a between-step force variability of ~0.6% body weight resulting in a steady state energetic cost variability of ~6%. To confidently detect the gradient in the presence of this variability, the nervous system may need to average cost over longer periods of time, much like we do in our experimental methods, thus slowing down optimization. Indeed, learning tasks such as walking on a split-belt treadmill, crawling on hands and knees, and ergometer rowing can continue across many days of exposure (43,82,114,115).

Our system may be modified to reduce this force variability. We studied this in pilot experiments by first using closed-loop control of the forces applied to the torso, as measured with the force transducers, rather than the original design of maintaining a constant spring compression. We used proportional-integral-derivative control to drive the error between measured force and the commanded within-step force to zero. This appeared to successfully reduce the within and between step force variability, but we found that the controller gains were highly user-sensitive and required tuning specifically for each user. The tuning process required users to walk for ~10 minutes some of which time was spent feeling perturbed. This had several undesirable consequences including that users felt less safe in our system, that the nervous system had to discriminate between many different controllers in learning how to adapt, and that users were no longer naïve to the presence of a relationship between step frequency and the applied system

forces. It is possible that these limitations may be overcome, but we decided to continue with the original approach at the possible expense of incomplete optimization. An alternative to closed-loop force control is to add compliance in series with the forward and backward pulling cables. We piloted this with three users and found them to adapt between 1SD and 3SD towards the new minimum, similar to the magnitude of adaptation we found in our original group of participants. While we suspect that the speed and completeness of optimization may increase with reduced force variability, we do not think it is necessary to eliminate it entirely. This is because not only was it present in the study by Selinger *et al.* where we did observe what appeared to be complete energy optimization, but such variability is also characteristic of everyday walking.

A second candidate explanation for incomplete optimization in our system is that it may be manipulating contributors to the nervous system's cost function other than simply energetic cost. Our system applies physical forces to a user that change as a function of how they walk. It seems possible, if not likely, that our system changes the stability of walking along with energetic cost. We noted in the introduction that the nervous system's cost function can be the weighted sum of one or more variables, with the particular variables and their weights depending upon the task. If stability normally contributes to the nervous system's cost function during walking, or if the nervous system increases the contribution of stability to the cost function when walking in our system, the minimum of this cost function may not necessarily coincide with the minimum of our new energetic cost landscape—it may even be located at the step frequencies to which our participants adapted. Consistent with the possible contribution of stability to the cost function, pilot testing found that in steeper cost landscapes, the step to step changes in forces are perceptible and make walking uncomfortable. This means that while we can create cost landscapes of a wide range of gradients, and quickly apply these cost changes within a walking step, we may be required to trade-off between these two factors. We explored this in pilot experiments by designing a steep cost landscape but averaging step frequency over multiple steps before inputting into the control function that calculates the required force command. Since steep cost landscapes require large force changes between steps, the averaging reduces the effect these force changes have on stability by applying them over multiple steps. This may be an advantage to the nervous system for optimization as there are larger steady-state differences in energetic cost between steady-state step frequencies. Or, it may instead be a disadvantage as the nervous system may find it more

difficult to associate variability in step frequency with the resulting changes in energetic cost. Thus, for the larger experiment we presented here, we chose to average step frequency only over a single stride and keep the cost landscape relatively shallow. We did design and pilot a cost landscape three times steeper than the one used here where the step frequencies were more heavily filtered through a three step mean filter. We tested two users and found that they were not noticeably uncomfortable with the force changes and shifted their step frequency by ~2SD towards the new minimum. This could be studied more systematically and is worth future research.

Were we to build our system again, there are several things that we would change. First, we would consider using a different actuator. As described above, the series elastic actuator provided sufficient control of forces. But it was expensive, often required maintenance, and it had limited travel—participants were restricted in the distance they could travel on the treadmill. Due to this last limitation, we had to disqualify several pilot subjects who hit the limits while walking. We would replace the series-elastic actuator with a rotary motor, which would provide the system with unlimited travel. In our new design, the motor is housed off-board allowing one to use large, high-powered motors with high performance control of applied forces (116). We suspect that this would allow us better control of the forces within and between steps. Second, we found that it was important to ensure a high degree of user comfort in the system. Towards this end, we would now prefer to use a wider and longer treadmill. This would help the user feel more comfortable when walking with potentially perturbing forces applied to them.

Our system, in its present form, can manipulate the energetic costs of walking in real-time. We focused on studying the performance of our device in healthy users who experienced shallow and simple cost landscapes that only penalized gait. Our system can also reduce the energetic cost of walking by as much as 50%, allowing future studies to determine if the nervous system treats energetic rewards and penalties differently. The ability to create cost landscapes of various shapes will help study the nervous system's optimization algorithms, including if they are speeded up by steeper cost gradients. Finally, reshaping cost landscapes may allow the nervous system's internal drive for reducing energetic cost to aid gait rehabilitation in patients recovering from injuries and disorders (87).

Chapter 3.

Increasing the gradient of energetic cost does not initiate adaptation in human walking

3.1. Abstract

When in a new situation, the nervous system may benefit from adapting its control policy. In determining whether or not to initiate this adaptation, the nervous system may rely on some features of the new situation. Here we tested whether one such feature is salient cost savings. We changed cost saliency by manipulating the gradient of participants' energetic cost landscape during walking. We hypothesized that steeper gradients would cause participants to spontaneously adapt their step frequency to lower costs. To manipulate the gradient, a mechatronic system applied controlled fore-aft forces to the waist of participants as a function of their step frequency as they walked on a treadmill. These forces increased the energetic cost of walking at high step frequencies and reduced it at low step frequencies. We successfully created three cost landscapes of increasing gradients, where the natural variability in participants' step frequency provided cost changes of 3.6% (shallow), 7.2% (intermediate) and 10.2% (steep). Participants did not spontaneously initiate adaptation in response to any of the gradients. Using metronome-guided walking—a previously established protocol for eliciting initiation of adaptation—participants next experienced a step frequency with a lower cost. Participants then adapted by -1.41±0.81 ($p=0.007$) normalized units away from their originally preferred step frequency obtaining cost savings of 4.80±3.12%. That participants would adapt under some conditions, but not in response to steeper cost gradients, suggests that the nervous system does not solely rely on the gradient of energetic cost to initiate adaptation in novel situations.

3.2. Introduction

We routinely perform movements in a variety of situations. This includes handling of different-sized objects, walking on uneven terrain, or running with fatiguing muscles. Some of these situations are familiar, and for these situations, our nervous system may have already learned an optimal, or near-optimal, control policy (12,18,24). In the task of walking on a treadmill, for example, people can rapidly select the step frequency that minimizes energetic cost for each new walking speed (106,107). But in novel situations, the nervous system hasn't had the experience to determine whether an existing policy remains optimal, or if a new policy would be better (12,24). To determine this, the nervous system must adapt the existing policy and experience the outcome (12,26). This adaptation is beneficial only when there is a new optimal solution, the presence of which the nervous system does not know in advance. If the old policy remains the optimal policy, then the act of adapting to new policies is itself sub-optimal—the nervous system would benefit most by exploiting its existing control policy (38). In this paper, we aim to identify a feature of novel situations that cues the human nervous system to initiate adaptation of its control policy.

Our nervous systems do not always initiate adaptation in novel situations. In reaching experiments, people typically initiate adaptation when presented with a force-field that creates a novel relationship between cost and control policy (12,14). However, when this is followed by another force-field that creates a different novel relationship, the nervous system reverts to erroneously exploiting its original control policy (12,117). Similar interference to adaptation is also observed in studies that create novel situations using visuomotor rotations or reversals (9). In walking tasks, exoskeletons designed to improve walking economy can underperform partly because people are unable to adapt their gait to take full advantage of the benefits that the exoskeleton can offer (118–120). In split-belt walking, people do not adapt their step lengths back to baseline when the speeds of the two belts are changed gradually (121). However, in all of these tasks, the nervous system can and does adapt when certain modifications are made to the novel situations (9,24,74,75,120). This suggests that the nervous system relies on particular features of the novel situations to determine if and when to initiate adaptation.

One potential feature used by the nervous system to initiate adaptation is salient cost savings. Here we use *cost savings* to refer to an improvement in the nervous system's

objective function. This may be decreased energetic cost, increased stability, increased accuracy, or some combination of these and other contributors to the objective function. *Saliency* refers to how clear it is to the nervous system that cost savings can be gained, and how it should adapt its control policy to gain the savings. As illustrated in Figure 3.1, saliency depends on at least three factors. First, execution variability about the nominal policy—due to either imperfect execution, purposeful exploration, or guidance by an external input—allows the nervous system to experience a greater range of cost savings if they exist (Figure 3.1B). Second, measurement noise decreases the ability of the nervous system to discern the presence of cost savings (Figure 3.1C). Third, for any given execution variability and measurement noise, an increase in the gradient of the cost landscape increases the ability of the nervous system to discern a cost savings (Figure 3.1D). If cost savings are not salient—be it due to any combination of shallow cost gradient, high measurement noise, or low execution variability—the nervous system may choose to exploit its current control policy because whether it should adapt, and if so how it should adapt, is simply not clear.

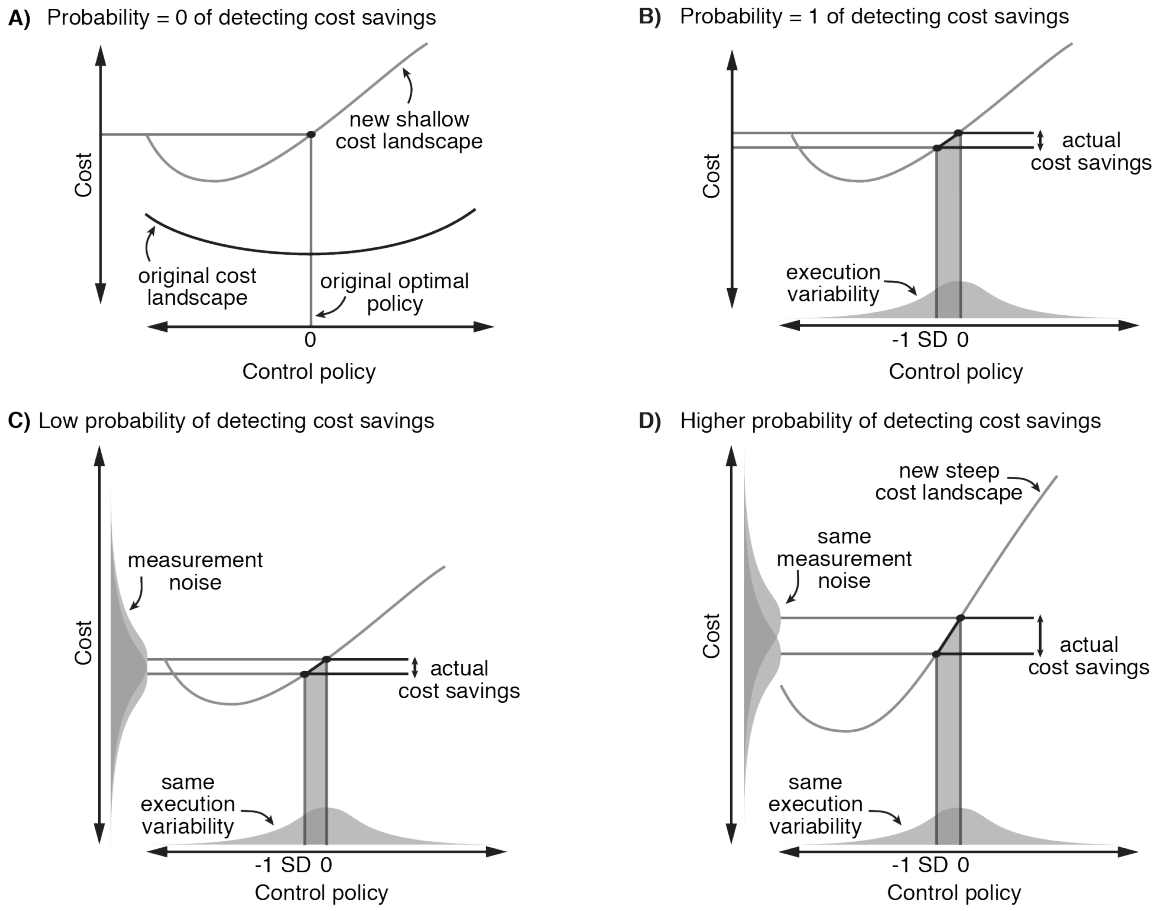

Figure 3.1: Conceptual representation of how the nervous system might detect cost savings from a cost landscape

A) The nervous system is introduced to a novel situation where the relationship between the control policy and cost has changed (black to grey curve) such that the original optimal policy is no longer optimal. With exact execution and measurement, the nervous system cannot detect any cost savings in the new landscape. **B)** Execution variability—illustrated by the horizontally aligned Gaussian distribution—allows the nervous system to exactly experience the lower costs relative to the original policy, making the energetic cost savings salient **C)** The presence of measurement noise—illustrated by the two vertically-aligned Gaussian distributions centered on the means of the two cost measurements—can reduce saliency by reducing the probability that the nervous system can detect a cost savings. In this example, the cost measurement means are close, and the cost measurement noise distributions are wide resulting in a low probability that the nervous system will detect a cost savings for the given execution variability. **D)** An increased gradient can increase the probability of detecting cost savings and thus increase the saliency of a cost landscape for the same execution variability and measurement noise.

Recent studies in walking support the premise that the nervous system relies on salient cost savings to initiate adaptation. One of the primary real-time objectives of the nervous system during walking is to minimize energetic cost (45,75,76,122). In one of our recent studies, we used robotic exoskeletons to reshape the energetic cost landscape of treadmill walking. Here *cost landscape* refers to the relationship between step frequency

and metabolic energetic cost. We reshaped the cost landscape to shift the optimal step frequency to step frequencies lower than normally preferred. Upon their first experience with the new cost landscape, only some participants spontaneously initiated adaptation to the new optimal step frequency. These *spontaneous initiators* had greater step frequency variability than the *non-spontaneous initiators* who persisted walking at the previous optimal step frequency. This suggests that the naturally higher variability increased the saliency of the cost savings to the nervous system which led to the initiation of adaptation. We were also able to prompt the non-spontaneous initiators to initiate adaptation by providing them with experience with step frequencies that resulted in a lower energetic cost. One interpretation of this result is that the experience increased the saliency of the energetic cost savings for the nervous system causing it to initiate further exploration. Counter to these findings, we did not find that increased gait variability was sufficient to initiate adaptation in a subsequent study on over ground walking (119). When compared to our treadmill studies, changes in cost in this over ground study were due not only to changes in step frequency, but also speed and terrain. We suspect that the nervous system did not initiate adaptation within the duration of this over ground experiment because the added dimensionality increased the complexity of the credit assignment problem making it difficult for the nervous system to determine which energetic changes could be attributed to its control, and which were due to the differences in terrain.

In the present study, we aimed to test whether the saliency of energetic cost savings is a feature that the nervous system uses to initiate adaptation in human walking. To accomplish this, rather than manipulate measurement noise or movement variability, we changed saliency by manipulating the gradient of the energetic cost landscape. We manipulated the gradient using a mechatronic system that applied controlled fore-aft forces to the waist of participants as they walked on a treadmill. These applied forces were a function of participants' step frequency and acted to increase energetic cost at high step frequencies and reduce it at low step frequencies. By making the forces a function of only step frequency and keeping the walking speed constant, we aimed to only affect the gradient of the step frequency cost landscape, indirectly signaling to the nervous system how it should adapt its control policy to obtain cost savings. We increased the gradient of the cost landscape about participants' originally preferred step frequency by increasing the magnitude of force change that the system provided for a given change in step

frequency. We hypothesized that increasing the gradient of the cost landscape will cause participants to spontaneously initiate adaptation of their step frequency.

3.3. Methods

3.3.1. Experimental Design

We manipulated cost landscapes using our recently developed mechatronic system (Figure 3.2A). We describe this system in detail in our earlier paper (122). Briefly, it manipulates a participant's original cost landscape by applying fore-aft forces to their waist while they walk on a treadmill. The controller specifies the forces as a function of the participant's step frequency. Backward forces increase the energetic cost associated with the executed step frequency, relative to normal, while moderate forward forces decrease the energetic cost (103). The system uses inertial measurement units placed on participants' feet to detect ground contact events, and this signal is processed by a real-time controller to determine the participants' executed *step frequency*, defined as the inverse of the time elapsed between left and right foot ground contact events. We provide the controller with a *control function* that defines the relationship it has to maintain between the measured step frequency and the applied force. Based on this control function and the measured step frequency, the controller commands the required force for each new step to an actuator via a motor driver. The force applied by the actuator is transmitted to the participants through long tensioned cables that are attached to a hip belt, and we monitor that force using force transducers in-line with the front and back cables.

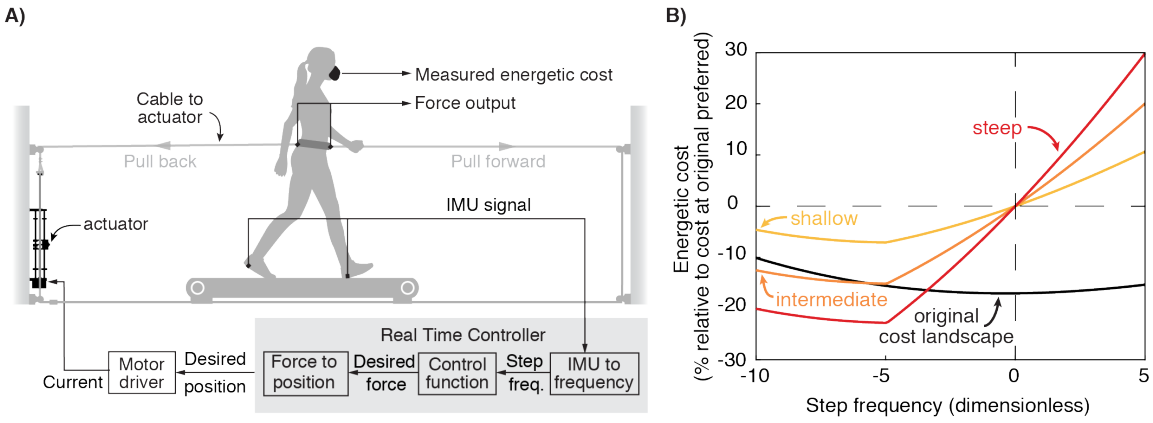

Figure 3.2: Mechatronic system and cost landscapes used in the experiment
A) Participants walked in a mechatronic system that applied controlled fore-aft forces as a function of their walking step frequency. Backward forces provided an energetic penalty, raising the cost of

walking relative to normal. Moderate forward forces provided an energetic reward, lowering energetic cost. **B)** Using simulations, we predicted that participants would experience cost landscapes with gradients of 1.4 (shallow), 2.8 (intermediate), and 4.2 (steep) percentage change in cost per unit change in step frequency, about their originally preferred step frequency (0).

We tested participants' behavior in cost landscapes of three different gradients (Fig 3.2B). Using data from literature, we can predict for an average participant the energetic cost associated with each step frequency when walking without any external force (96), as well as the energetic cost of walking when a range of fore-aft forces are applied but at a fixed step frequency (103). We combined these relationships and used them to design three control functions—*shallow, intermediate,* and *steep*—that created cost landscapes of three different gradients.

$$F_{shallow} = \begin{cases} -0.07 \cdot sf - 1.36, & sf \leq -5 \\ -0.19 \cdot sf - 1.98, & sf > -5 \end{cases} \quad (3.1)$$

$$F_{intermediate} = \begin{cases} -0.07 \cdot sf - 0.40, & sf \leq -5 \\ -0.39 \cdot sf - 1.98, & sf > -5 \end{cases} \quad (3.2)$$

$$F_{steep} = \begin{cases} -0.07 \cdot sf + 0.56, & sf \leq -5 \\ -0.58 \cdot sf - 1.98, & sf > -5 \end{cases} \quad (3.3)$$

Here, sf is a normalized step frequency and is dimensionless. To perform this normalization, we first measured the average step frequency originally preferred by each participant during a baseline trial (c.f. Experimental Protocol), as well as the standard deviation in step frequency about this average preferred step frequency. We then calculated the normalized step frequency for each step in the subsequent trials by subtracting the average originally preferred step frequency from each step's measured step frequency and then dividing by the standard deviation about the originally preferred step frequency. This normalization controls for the differences between participants in their step frequency variability, which is normally one of the contributors to the saliency of cost savings. It also forces measured step frequencies that are equal to the originally preferred step frequency to evaluate to 0. We normalized the forces applied to a participant by their body weight. In equations 1-3, the intercepts, slopes, and the forces all have units of percent body weight (sf is dimensionless). We designed these control functions to generate new cost landscapes with cost gradients of 1.4, 2.8, and 4.2 about the originally preferred step frequency. These gradients have units of percent change in energetic cost for a unit change in normalized step frequency. For example, were a participant walking

in the intermediate gradient condition to choose a step frequency 1 normalized unit lower than their originally preferred step frequency, the participant will experience a 2.8% reduction in energetic cost relative to what they experienced at the originally preferred step frequency. For comparison, the cost landscape used in Selinger's study roughly corresponds to the shallowest gradient we use here (45,75). To experience a cost gradient as steep as our steepest, one would have to walk at a step frequency roughly 7.5% higher than their preferred step frequency in their original cost landscape (96). Finally, we designed all the new cost landscapes to have the same cost at the originally preferred step frequency. This helped ensure that when we changed the cost landscape, participants only experienced the gradient change, without experiencing any change in the average steady-state cost. Since different nervous systems can respond differently to our control functions, each participant may not experience exactly the cost landscape that we aimed to create. However, our prior results show that, on average, we are able to accurately create our designed cost landscapes (122).

3.3.2. Experimental Protocol

We collected data from 11 participants (5 females, 6 males; mean±SD; Age: 24±3 years; Height: 167±11 cm; Mass: 68±11 kg). All participants were healthy and had no known history of cardiopulmonary or gait impairments. The study protocol was approved by the Simon Fraser University Research Ethics Board and all participants gave written informed consent before participation. To determine the sample size necessary to evaluate our hypothesis, we first performed pilot experiments and estimated that we can expect a group standard deviation of 1.01 steps per minute. We then performed a power analysis for a one-tailed Students' t-test to detect an average change of 1 normalized unit in step frequency ($\alpha = 0.05$, $1-\beta = 0.90$).

Each participant completed four periods of walking on the same day (Figure 3.3). Prior to the beginning of these four experimental periods, all participants spent ~10 minutes habituating to walking on our treadmill at a speed of 1.25 $m \cdot s^{-1}$. During this habituation, we instructed them to walk with both short and long steps. They were not attached to the mechatronic system. This was followed by the first period of the experiment where participants walked for 9 minutes while attached to the mechatronic system. We used data from this period to quantify the characteristics of their baseline walking step

frequency. During this time, the system controlled for a target applied force of 0 N (Figure 3.3A). We calculated the average and standard deviation of their step frequency from the 6th to 9th minute to parameterize the step frequency in future trials. We refer to this average as the *originally preferred step frequency* and the standard deviation as *original step frequency variability*.

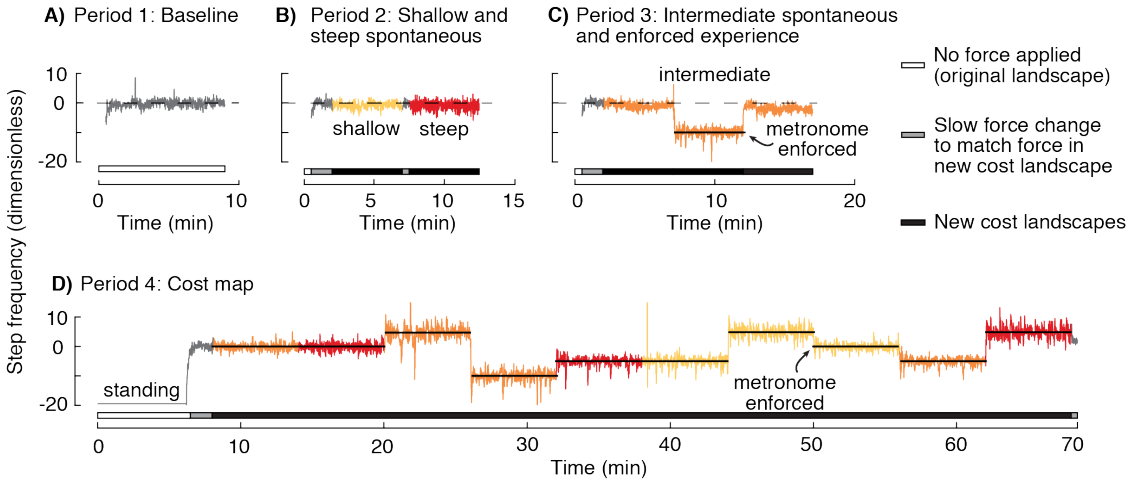

Figure 3.3: Experimental protocol
Step frequency measured from a representative participant during the different walking periods. Each participant completed four periods of walking in a single day. **A)** First, they walked for 9 minutes as the system controlled for a force of 0 N to be applied to their waist. We used this baseline period to estimate their average original preferred step frequency and original step frequency variability**. B)** Then participants walked for 5 minutes each in the shallow and steep gradients to test for spontaneous adaptation. **C)** In the third period, participants walked in an intermediate gradient. We used this condition to test for both spontaneous adaptation to an intermediate gradient and adaptation after enforced experience with a low cost. **D)** Finally, we measured the actual gradients experienced by participants in each the cost landscapes.

In the second period, we tested whether participants would spontaneously initiate adaptation in the shallow and steep gradients (Figure 3.3B). They experienced 0 N for the first 30 s to allow them to reach a steady-state step frequency (107). We programmed the system to ramp up the force over the next minute (minute 0.5 to 1.5) to the force that would be applied at the participants' originally preferred step frequency in the new cost landscapes. This ensured that participants were not perturbed by a sudden change in force when the cost landscape changed. This force was held constant for 30 s (minute 1.5 to 2; *shallow pre-spontaneous*). The controller then engaged the control function for the shallow gradient, and participants walked at a self-selected step frequency for 5 minutes (minute 2 to 7; *shallow spontaneous*). Then the controller switched to the steep gradient. Once again, we ensured that participants were not perturbed during the cost landscape

transition by using a limit on the rate at which the force could change for 30 s (minute 7 to 7.5). Participants then self-selected their step frequency for five minutes (minute 7.5 to 12.5; *steep spontaneous*). To avoid fatigue, we then provided a break of 5-10 minutes before beginning the third period. For each participant, we averaged their self-selected step frequency over the last 30 s of walking in each gradient to determine their *spontaneous adaptation* in that gradient (*shallow spontaneous*: minute 6.5 to 7; *steep spontaneous*: minute 12 to 12.5).

We used the third period to test for adaptation in an intermediate gradient (Figure 3.3C). The first part of this period served as a sort of Goldilocks test in the event that the shallow and steep gradients were both perceived as extreme by the nervous system (123). Similar to the second period, the force was ramped up in the first two minutes to prevent perturbing forces. The controller then engaged the control function for the intermediate gradient, and participants self-selected their step frequency for 5 minutes (minute 2 to 7; *intermediate spontaneous*). One possible outcome of our experiment was that participants would not spontaneously adapt in any of the gradients. With this outcome, we would not be able to distinguish between the possibility that participants will adapt but not spontaneously, and the possibility that participants won't adapt at all in our system with our experimental paradigm. Therefore, the next part of this experimental period was to verify whether adaptation was possible at all. Prior work has shown that experiencing a lower cost in a new cost landscape is sufficient to cause the nervous system to initiate adaptation (45). Using this principle, we next required participants to match their step frequency to an audio metronome that played a frequency -10 normalized units away from their originally preferred step frequency. According to our designed cost landscape, we expected this step frequency to provide a cost savings of 12.5% relative to the cost at 0. After five minutes of matching the metronome (minute 7 to 12; *intermediate metronome guided*), the metronome was turned off and participants self-selected their step frequency for another five minutes (minute 12 to 17; *intermediate post-experience*). Once again, we averaged each participant's step frequency during the last 30 s of each condition to determine their preferred step frequency in that condition (*intermediate spontaneous*: minute 6.5 to 7; *intermediate post-experience:* minute 16.5 to 17).

The purpose of the fourth period was to measure the actual energetic cost experienced by the participants in each of the new cost landscapes (*cost mapping*; Figure 3.3D). During this period, participants were also instrumented with a respiratory gas

analysis system (Vmax Encore Metabolic Cart, Viasys, Pennsylvania, USA). They spent the first six minutes standing still while we measured their resting metabolic rate (minute 0 to 6). They then started walking while the mechatronic system maintained a force of 0 N to allow them to reach a steady-state gait (minute 6 to 7). Following this, participants walked at specific walking conditions chosen to allow us to estimate the gradient about the originally preferred step frequency in each of the cost landscapes, and also to estimate if the *experience low* period indeed allowed participants to experience a lower cost. Participants walked in 10 conditions total: step frequencies of 0, -5, and +5 in shallow, intermediate and steep gradients, and -10 in only the intermediate gradient. We enforced this by instructing participants to match an audio metronome that played these frequencies. We programmed the controller to present these conditions in a random order to each participant, to prevent any order effects on these metabolic energy measures. To determine energetic cost, we measured the total volume of oxygen consumed and volume of carbon dioxide produced in the last three minutes of each condition, and divided them by the duration over which they were measured, to obtain the steady state average rates of oxygen consumption ($\dot{V}_{O_2}$) and carbon dioxide production ($\dot{V}_{CO_2}$). We then estimated the metabolic rate using the following equation (109,124,125):

$$P_{met,gross} = \left(16.48 \frac{W\ s}{ml\ O_2} \dot{V}_{O_2}\right) + \left(4.48 \frac{W\ s}{ml\ CO_2}\ \dot{V}_{CO_2}\right) \tag{3.4}$$

We subtracted resting metabolic power for each participant and present net energetic cost as the energy used per unit time normalized for the person's body mass. It has the units $W \cdot kg^{-1}$.

3.3.3. Data Analysis

We first determined the average gradients and metronome-guided cost that participants experienced in each cost landscape. We used MATLAB's fitlm command to find the best linear fit through the energetic costs at -5, 0, +5 normalized step frequencies for each participant, in each cost landscape. We define the cost landscape gradient for each participant as the slope of this fit. We also used a one-tailed paired Students' t-test to determine whether the cost at a step frequency of –10, where we held participants during the *intermediate metronome guided* condition, is lower than the cost at a step frequency of 0 in the intermediate gradient.

We evaluated whether participants spontaneously initiated adaptation in response to steeper gradients. We first compared the preferred step frequency in the shallow gradient with the originally preferred step frequency using a one-tailed Student's t-test. We found that these values were indeed different, but we did not attribute this shift in preferred step frequency to an adaptation in response to a new cost gradient (c.f. Results). To determine if there was any additional changes in preferred step frequency in the steeper gradients, we then compared the average step frequencies during the spontaneous adaptation periods in the intermediate and steep gradient to the same period in the shallow gradient.

We also determined whether participants initiated adaptation after enforced experience with a low cost. We used a one-tailed paired Students t-test to determine whether participants' preferred step frequency after the *intermediate metronome guided* condition was significantly lower than the average step frequency 30 s prior to the experience with low cost. The step frequency in this 30s prior to the experience corresponds to the spontaneous adaptation in the intermediate gradient, allowing us to determine whether the metronome guided experience generated adaptation that did not occur spontaneously.

In the conditions where we observed adaptation, we characterized the rate of adaptation. We did so because a preferred step frequency can arise from fast predictive processes that can occur over a few seconds or optimization processes that can occur over tens or hundreds of seconds (107). As described in the introduction, we are interested in the slow process since it is indicative of the nervous system learning to adapt its policy to a novel situation. We modelled each participant's adaptation of step frequency over time as a two-process exponential. We first averaged the step frequency during the last 30 s prior to the beginning of the condition of interest, and the step frequency during the last 30 s of the condition. If these two averages were different, we normalized the step frequency data during that condition such that the average step frequency of the 30 s prior to the condition evaluated to 0, and the average of the last 30 s evaluated to 1. We then used least squares regression implemented through MATLAB's fitnlm function to model these data as the sum of two exponentials (107). We used the time constants from this model to estimate the duration of the optimization process.

3.4. Results

We were successful in creating cost landscapes of different gradients. We found that participants on average experienced a shallow gradient of 0.07±0.03 $W \cdot kg^{-1}$ (mean±SD), an intermediate gradient of 0.14±0.03 $W \cdot kg^{-1}$, and a steep gradient of 0.20±0.04 $W \cdot kg^{-1}$ (Figure 3.4). This is calculated as the change in energetic cost per normalized unit of step frequency. We use 1 standard deviation of participants' preferred step frequency in their original cost landscape, to normalize the measured step frequency. This means that participants experience the reported gradient through a variability of 0.5 standard deviations higher and lower than their originally preferred step frequency. Thus, 1 standard deviation higher and lower than their originally preferred step frequency, which accounts for 68% of their steps, would have allowed participants to experience a change in energetic cost of 3.6%, 7.2%, and 10.2% in the shallow, intermediate, and steep gradients, respectively. We also found that when participants in the intermediate gradient were held -10 normalized step frequencies lower than their originally preferred step frequency, they experienced an average cost savings of 8.1%±9.1% relative to the cost at the originally preferred step frequency ($p=0.006$).

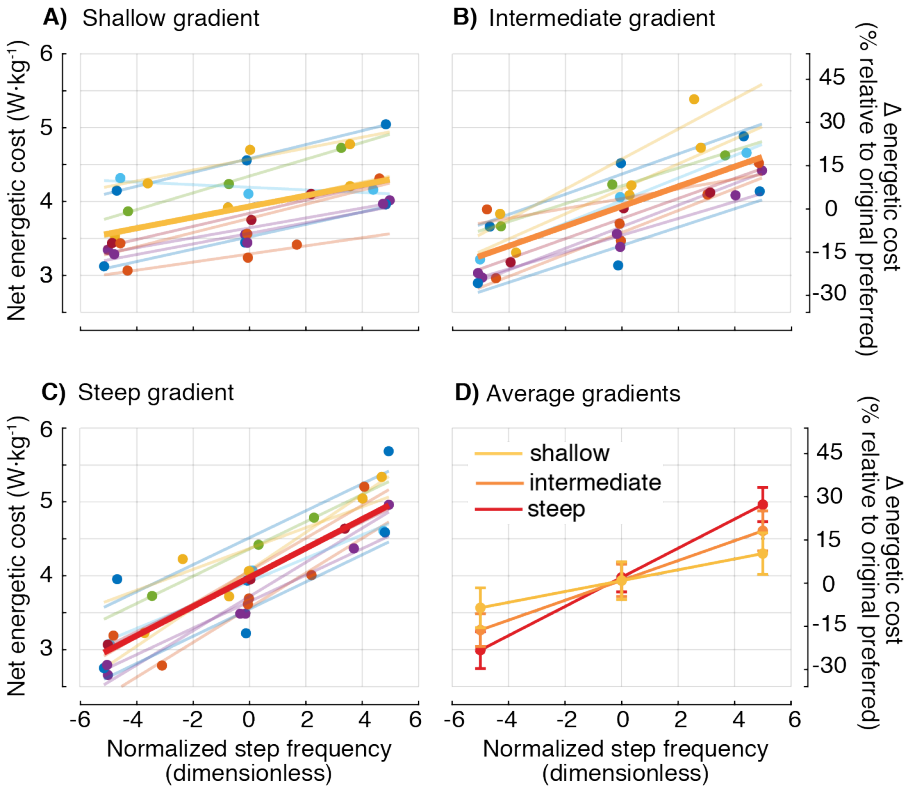

Figure 3.4: Cost landscapes measured from participants
A) Shallow **B)** intermediate and **C)** steep gradients. Each filled circle represents one measurement from one participant. Thin, lighter lines are linear fits to each participant's cost measurements. Data points and best-fit lines from a given participant is presented in a single colour. Thick lines are the average of these linear fits. **D)** On average the gradients are increasing from shallow to steep. The filled circles represent the average cost measures at the commanded step frequencies, and the error bars represent the 95% CI of the same.

Participants did not spontaneously initiate adaptation in response to steeper cost gradients. In the second period, participants first experienced the shallow cost landscape, and then the steep cost landscape. They walked freely at their self-selected step frequency for 5 min in both cost landscapes. The average step frequency from the last 30 seconds of the shallow period was lower than the original preferred step frequency (-0.69±0.82 vs. 0; p = 0.01). However, this step frequency was indistinguishable from the average step frequency preferred by participants during the 30 s prior to the beginning of the shallow gradient (Figure 3.5: Shallow pre-spontaneous vs Shallow spontaneous; -0.69±0.82 vs. -1.02±0.64; p = 0.33). Therefore, we do not interpret this to be an initiation of adaptation towards the optimal policy. When the system switched from the shallow landscape to the steep landscape, participants still did not initiate adaptation, and preferred a step frequency (Figure 3.5: Steep spontaneous; -0.76±0.99) that was indistinguishable from that preferred in the shallow cost landscape (Figure 3.5: Shallow

spontaneous; -0.69±0.82; p = 0.40). Our goldilocks test with the intermediate gradient also resulted in preferred step frequencies that were indistinguishable from that preferred in the shallow landscape (Figure 3.5: Shallow spontaneous vs Intermediate spontaneous; -0.69±0.82 vs. -0.74±0.82; p = 0.43).

Participants did, however, initiate adaptation after enforced experience with a lower cost. We allowed participants to self-select their step frequency after matching a metronome that held them at a step frequency that had a cost lower than the cost at 0 in the intermediate cost landscape. On average, participants adapted by -1.41±0.81 towards the new cost minimum (Figure 3.5: Intermediate post-experience). This adaptation was to step frequencies significantly lower than that spontaneously preferred in the intermediate gradient (p=0.007). It led to an average cost savings of 4.80±3.12% relative to the cost at 0. We found that the time course of the change in step frequency of most participants was captured well with a two-process exponential model (RMSE=0.16±0.08; R-squared=0.36±0.21). The time constant of the fast process was 4.4±2.5 s while that of the slow process was 190.2±209 s. We interpret the presence of this slow process as evidence that the nervous system indeed initiated adaptation in response to the enforced experience with a lower cost gait.

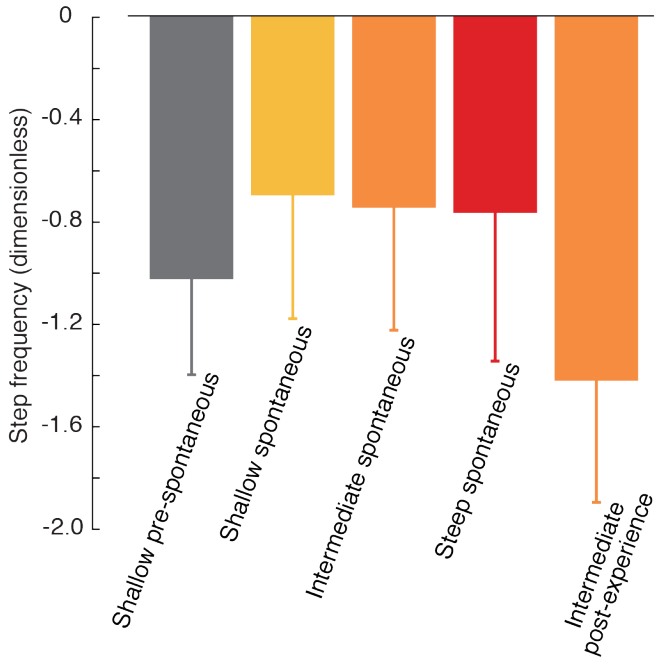

Figure 3.5: Average adaptation in each cost landscape
Average spontaneous adaptation in the shallow gradient was indistinguishable from participants' preferred step frequency just prior to the beginning of the shallow cost landscape (shallow pre-

spontaneous vs shallow spontaneous). The spontaneous adaptation in all gradients were also indistinguishable from each other after five minutes of walking (shallow, intermediate, steep spontaneous). However, after experience with a lower cost in the intermediate gradient, participants preferred to walk at a significantly lower step frequency (intermediate post-experience).

3.5. Discussion

Contrary to our hypothesis, steeper gradients did not lead to spontaneous initiation of adaptation. This null finding is not because our methods were unsuccessful in creating gradients of increasing steepness. We used our cost mapping trials to verify that the participants did indeed experience three different gradients—the intermediate and steep gradients were about 2-fold and 3-fold the shallow gradient, respectively. The lack of initiation also does not appear to be a consequence of the rapid exposure to multiple gradient conditions preventing the nervous system from attempting any adaptation. We verified this by leveraging results from previous studies that found that adaptation can be initiated by guiding the nervous system to experience a cost lower than the cost at the originally preferred step frequency (45). We did the same here and found that participants could indeed initiate adaptation in the intermediate landscape after such experience, despite the intermediate landscape being the third landscape experienced by participants. When considered together, these results suggest that either the nervous system does not use salient cost savings to initiate adaptation, or that the cost savings were not salient to the nervous system in our experiment.

For savings to be salient, the nervous system needs to both detect that cost savings can be gained and determine how it should adapt its control policy to gain the savings. Depending upon how the nervous system senses energetic cost, it may be challenging for the nervous system to detect cost savings from the cost landscape gradient. For example, one possible candidate sensory system for estimating energetic cost involves the ergoreceptors that are sensitive to the slow build-up, or slow reduction, of muscle metabolic by-products (54,126,127). This build-up creates a sensory response that is an integration of the effect of many steps, rather than one that closely follows the step-to-step changes in energetic cost. It will be more difficult for the nervous system to detect a gradient in cost landscape from the step-to-step variability in energetic cost when using this mechanism because integration has the effect of decreasing the sensed

gradient, perhaps even to zero if the build-up is particularly slow. This, or a similar integrative sensing mechanism, may be why metronome-guided experience is effective at initiating adaptation—the metronome holds participants at a lower cost for many steps allowing time for integration. However, some participants in some conditions are able to use the step-to-step variability in energetic cost to spontaneously initiate adaptation (45). This suggests that if a slow sensing system does indeed play a role in estimating energetic cost, it is not the only contributing system.

Another possibility for the lack of initiation of adaptation is that the gradients allowed participants' nervous systems to sense the presence of cost savings but not how to adapt their control policy to obtain those savings. That is, the nervous system has difficulty with credit assignment in our experiment (128). We manipulated the cost gradient associated with only one gait parameter—step frequency—to allow the nervous system to detect an increase in cost savings and detect the gait parameter to adapt to obtain those savings. But when walking in our system, we suspect that it is not clear to most participants that the backward force depends on any aspect of their gait, including their step frequency. It appears to be challenging for the nervous system to identify salient cost savings using the structure of natural variability in gait to determine the gradient of a cost landscape—a finding consistent with our earlier experiment studying adaptation in over ground walking (119). Metronome-guided experience of step frequencies with lower cost may provide the nervous system with an explicit association between the cost savings and the changes to control policy that provide those cost savings. Similarly, reaching experiments have found that presenting participants with multiple different force-fields interferes with learning, but that such interference can be overcome with certain contextual cues such as follow through movements or cues that associate a change in the optimal control policy with another change such as spatial location of movement (129,130). Differences in contextual clues might explain why it was easier for the nervous system to identify that there was a relationship between step frequency and the changes to knee torque for some participants in our previous experiment than with step frequency and torso forces in the present experiment (45). This interpretation is consistent with recent study in visuomotor adaptation that found that implicit and explicit learning work together to improve adaptation (131).

While we designed our custom-built equipment and our protocol to meet the requirement for energetic cost saliency, our experiment nevertheless had limitations.

Towards this requirement, the maximum cost savings that participants experienced from their variability in step frequency, relative to the cost at their originally preferred step frequency, was 5.1% in the steep gradient. In contrast, participants experienced cost savings of 8.2% during their metronome-guided lower cost experience in the intermediate gradient. This suggests that even the steep gradient may not have allowed participants to experience a large enough cost savings. However, we suspect this is not the case because in our previous study with the shallow gradient, participants initiated adaptation after experiencing cost savings of only 3.5% through similar metronome-guided walking (122). This earlier cost savings was smaller than that experienced by our current participants in the steep gradient condition suggesting that the currently experienced cost savings, at least in the steep gradient condition, were sufficiently large for the nervous system to detect.

A second limitation is that our experimental design resulted in participants preferring step frequencies slightly lower than the original preferred step frequencies in all gradient conditions (Figure 3.5). We do not interpret these shifts as evidence of the initiation of energetic cost optimization in response to new cost landscapes. Our rationale is that participants were already walking at a shifted step frequency during the 30 s prior to the beginning of each new cost landscape (shallow: -1.02±0.64, intermediate: -0.25±0.63, steep: -0.62±0.54). Why is step frequency shifted lower than the baseline measures both before and during the experience with the new cost landscapes? One possible explanation is that we may not have provided a long enough baseline period for participants to settle into their preferred step frequency. However, others have found that two minutes of walking is sufficient for stride frequency to reach steady state—we provided 9 minutes (132,133). A second possible explanation for the presence of these shifts may be the net backward force that participants experienced both immediately before and during the cost landscape, but not during the baseline phase when the net force was zero. Our system slowly ramped up the backward force to that which participants would experience in the new cost landscapes at their originally preferred step frequency. The force was then held constant for 30 s before the controller switched to the new cost landscapes, and our step frequency estimate prior to the beginning of the new cost landscape is from this constant-force period. However, concerned about the possible role of net backward force on step frequency, we performed pilot experiments prior to our reported experiments and found no relationship. In support of our pilot results, a recent

study also found that backward forces do not have an effect on stride period (80). Furthermore, walking uphill, which is biomechanically similar to experiencing a net backward force, also results in step frequencies that are not significantly different from walking on level (111). Further research will be required to understand why we observed this consistent shift in step frequency.

After metronome-guided experience, our participants did not converge on the energy minimal step frequency. To determine the location of the cost minimum, and the magnitude of cost savings obtainable at the minimum, we fit a quadratic relationship to the costs measured in the intermediate gradient condition during cost mapping. From this relationship, we estimate that, on average, participants could have obtained a cost savings of 10.8% if they had shifted their step frequency -6.1 normalized units away from their originally preferred step frequency. Yet we found that participants only adapted their step frequency by -1.4±0.8 to obtain a cost savings of only 4.83±3.61%. This might suggest to some that energetic cost savings do not play a role in the adaptation of step frequency in the cost landscapes we used. We suspect that this is not the case since participants did adapt after experience with a lower energetic cost. A candidate explanation is that the nervous system seeks to minimize an objective function that is a combination of energetic cost, stability, accuracy and other contributors (76). The minimum of this combined cost function may coincide with the final preferred step frequency and not with the energetic cost minimum.

In conclusion, the nervous system does not solely rely on the gradient of energetic cost to initiate adaptation in novel situations. As we and others have previously found, explicit experience with more optimal movements can assist with the initiation of adaptation. A better understanding of the interplay between implicit and explicit experience for the nervous system to initiate adaptation when the saliency of cost savings is not apparent may help improve rehabilitation for those recovering from injuries, help coaches speed up training with new techniques, or aid scientists looking to study adaptation in complex novel environments.

Chapter 4.

Taking advantage of external mechanical work to reduce metabolic cost: the mechanics and energetics of split-belt treadmill walking

4.1. Abstract

In everyday tasks such as walking and running, we often exploit the work performed by external sources to reduce effort. For example, when walking downhill we allow the acceleration due to gravity to compensate for the loss of velocity incurred from the leading leg's contact with the ground. Recent research has focused on designing assistive devices capable of performing mechanical work to reduce the work performed by muscles and improve walking function. The success of these devices relies on the user learning to take advantage of this external assistance. Although adaptation is central to this process, the study of adaptation is often done using approaches that seem to have little in common with the use of external assistance. We show in 16 young, healthy participants that a common approach for studying adaptation, split-belt treadmill walking, can be understood from a perspective in which people learn to take advantage of mechanical work performed by the treadmill. Initially, during split-belt walking, people step further forward on the slow belt than the fast belt which we measure as a negative step length asymmetry, but this asymmetry is reduced with practice. We demonstrate that reductions in asymmetry allow people to extract positive work from the treadmill, reduce the positive work performed by the legs, and reduce metabolic cost. We also show that walking with positive step length asymmetries, defined by longer steps on the fast belt, minimizes metabolic cost, and people choose this pattern after guided experience of a wide range of asymmetries. Our results suggest that split-belt adaptation can be interpreted as a process by which people learn to take advantage of mechanical work performed by an external device to improve economy.

4.2. Introduction

The neuromotor system can learn to take advantage of external energetic assistance to produce and sustain motion. In everyday tasks such as walking and running, we often exploit the passive dynamics that arise from the interaction between the body and gravity to reduce the need for muscle force (4,134). External assistance of our motion is restricted to gravity in common tasks such as in downhill walking (70). In more skilled tasks such as wave surfing, we learn to harvest the assistance of waves and in wind surfing we learn to harvest the assistance of the wind. The ability of the neuromotor system to harness energy is critical if we are to take advantage of assistance from devices like powered prostheses and exoskeletons. Specifically, exoskeletons for the lower limbs are often designed to reduce muscular work, reduce effort, and increase endurance during walking (135–137). These devices commonly use powered actuators (118,138–144), designed to reduce metabolic cost by performing mechanical work that would otherwise need to be generated by muscles. However, the degree to which these assistive devices reduce metabolic cost depends not only on the amount of work performed by the device, but also on the individual's ability to exploit adaptive learning processes to take advantage of the external assistance (120).

Although learning is key to maximizing the benefits from external assistance, the study of locomotor learning is often done in contexts that do not seem to have much in common with the study of assistive devices. For example, much of the work on adaptive locomotor learning uses a split-belt treadmill paradigm where individuals walk on a treadmill with two belts that move at different speeds (145–147). Upon initial exposure to walking with the belts moving at different speeds, the distance between the feet at leading limb heel-strike—referred to here and in the split-belt literature as step length—becomes asymmetric. The step at foot strike on the slow belt becomes longer than the step length at foot-strike on the fast belt, because the fast belt pulls the leg into a more extended position. This asymmetry in step lengths is gradually reduced over the course of 10 to 15 minutes (145) and is accompanied by a reduction in positive mechanical work performed by the legs (83) and a reduction in metabolic cost (82). By convention, positive mechanical work refers to the work performed by a muscle while shortening—when the force applied by the muscle and displacement of the object that the force is acting on are in the same direction. The gradual reduction in step length asymmetry occurs in parallel with an

increase in step time asymmetry (82), while stance times remains asymmetric throughout the entire split-belt walking period (145). A potential explanation for these observations is that individuals may adapt their gait during split-belt walking to minimize metabolic cost (75,82).

Here we use principles from mechanics and experimental evidence to illustrate that, like exoskeletons, split-belt treadmills can provide assistance during walking. As we detail in the Theory and Predictions section, gaining assistance in the form of net mechanical work on the person from the treadmill is unique to the split-belt treadmill and is not possible on a normal “tied-belt” treadmill, or when walking over ground. Walking at a constant speed in any of these situations requires that the person generates braking and propulsive impulses that are balanced throughout the gait cycle. On a split belt treadmill, however, people can choose how to distribute braking and propulsion between the two belts to take advantage of the difference in belt speeds. If the forces and work generated by the legs are redistributed properly, the work performed by the treadmill on the person could be used to reduce the positive work required by the person’s muscles and ultimately reduce metabolic cost.

Split-belt treadmills provide a unique approach to study how to gain advantage of external assistance, as individuals could reduce the energetic cost of walking by stepping further forward on to the fast belt relative to the slow belt (85,148). As we describe in Theory and Predictions, this pattern would generate a larger braking force on the fast belt, which would be balanced by more propulsive force applied to the slow belt. Because of the difference in belt speeds, this results in net negative work performed by the person on the belts, and net positive work performed by the belts on the person. It is not guaranteed that the person benefits from this positive treadmill work—they may dissipate it by performing additional negative work. But it is also possible that they allow the positive work from the belts to assist walking by increasing their mechanical energy, reducing the positive mechanical work required from their muscles, and reducing their metabolic cost. This can only occur if individuals learn to take advantage of the treadmill work by reducing positive muscle work. Selgrade et al. showed that in the traditionally observed adaptation to step length symmetry is characterized by an exploitation of positive work from the treadmill (85). Here, we show that it is this change of coordination—of placing the leading leg further forward on the fast belt relative to the slow belt—that allows individuals to take

advantage of the resulting positive work performed by the treadmill and reduce metabolic cost.

4.2.1. Theory and Predictions

Here we consider three walking conditions: overground walking, walking on side-by-side treadmills with belts “tied” to move at the same speed, and walking on side-by-side treadmills with belts “split” to move at different speeds. In overground walking, the ground is level and the person walks at a constant average speed relative to the ground. In the two treadmill cases, the treadmills are level and the person keeps the same average position on the treadmills equating to zero average speed relative to the stationary ground. Here, the reference frame is fixed to the ground, yet the arguments hold for other reference frames, as long as they are not accelerating and as long as one does not switch between reference frames. In the treadmill conditions, we consider three systems: the person, the left belt, and the right belt. The left and right belts move at the same speed in the tied-belt condition, and at different speeds in the split-belt condition. In the overground walking condition, the ground has zero speed resulting in only two systems: the person and the ground. In all of the above walking conditions, the following two constraints must be fulfilled.

C1. The sum of the external forces acting on the person must be zero on average. Otherwise, there would be net acceleration or net vertical displacement violating the requirements of steady-state speed and level walking.

C2. The net mechanical work on the person must be zero on average. Otherwise, there would be a net gain in kinetic or potential energy, again violating the steady-state speed and level walking requirements. Importantly, these two constraints taken together do not mean that external forces (e.g. treadmill forces) cannot perform net mechanical work on the person. Indeed, they could perform net negative or net positive work while still summing to zero net system acceleration as long as forces internal to the person system (e.g. muscle forces) perform the opposite amount of work.

These constraints affect the three walking conditions in different ways. For overground walking, they mean that the work performed by the person must be zero on

average. This is because the ground cannot perform work on the person—relative to the ground-fixed reference frame, there is no displacement at the ground point of force application and thus the person must perform no net work (C2). Performing no net work can be accomplished by performing zero work, but more likely it is accomplished with equal amounts of positive and negative work. We consider the person as a point mass body with legs that are massless pistons that generate forces on the ground (or treadmill belts as in Figure 4.1A & B) and equal but opposite forces on the point mass. In this model, all the work performed by the person is performed by the legs. In overground walking, the legs can perform both positive and negative work as long as they sum to zero.

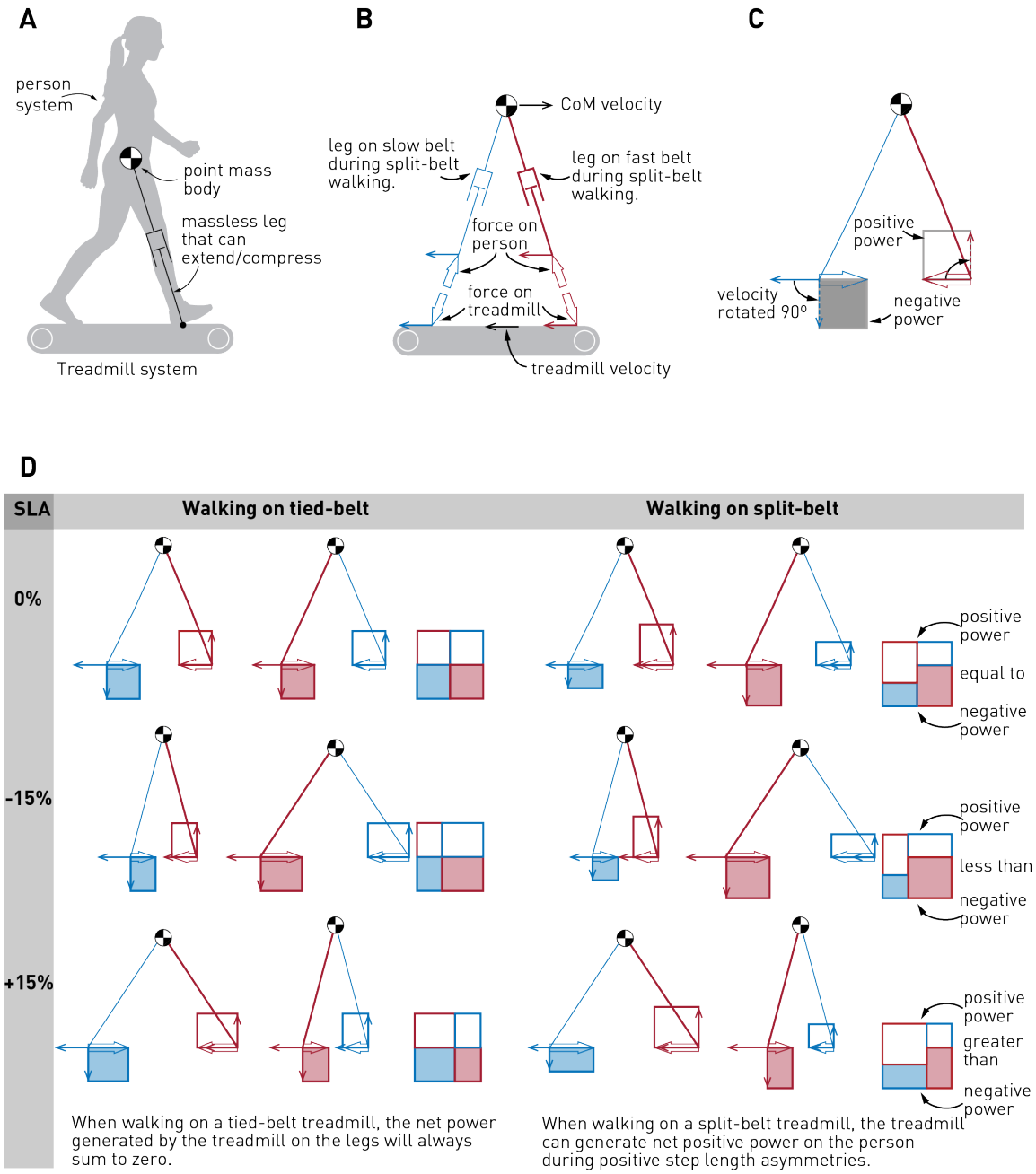

Figure 4.1: Conceptual representation of calculating mechanical work done during split-belt walking

A. We model the person as a point mass body with massless legs that can extend or compress. **B.** Free-body diagram of the person and treadmill systems. Blue represents the leg on the slow belt and red represents the leg on the fast belt when the belt velocities are split. Large open arrows represent forces, line arrows represent velocities. **C.** Power generated by the treadmill on the legs. We use the individual limbs method to calculate the power generated by the treadmill on each leg during a stride (not shown). Dashed arrows represent velocities rotated by 90 degrees to facilitate visualization of the power generated by the treadmill. The positive power generated by the treadmill on the legs is visualized with open rectangles above the point of force application, and negative power with closed rectangles below the point of force application. **D.** Power generated by the

treadmill on the legs. During tied belt walking, the positive power generated by the treadmill on the legs is always equal to the negative power generated within a stride, at all step length asymmetries (SLA). This is true even though the total power generated during the long step is greater than that generated during the short step, at asymmetric step lengths. We can observe this through the rectangles shown to the right of each condition, where the sum of the top open rectangles always equals the sum of the bottom closed rectangles. However, when walking on split-belt treadmill, we see that at positive step length asymmetries (bottom row), the treadmill generates net positive power on the legs during the long step that is greater than the net negative power it generates during the short step. This leads to a net positive power on the person over the stride.

The constraints explained above also require the person to perform zero net work during tied-belt treadmill walking. Unlike overground walking, the person performs work on the belts during treadmill walking when considered from a ground-fixed reference frame. At heel contact, for example, the force exerted by the leading leg opposes the belt velocity at the point of contact (Figure 4.1B). Since the velocity at the point of force application only has a fore-aft component, the power generated by the treadmill on the leg is the dot product of the horizontal fore-aft force from the treadmill and the treadmill velocity. It is positive when the force and velocity are in the same direction, and negative when the two are opposite. At heel contact, this force will perform negative work on the belt. The belt does not slow down because its motor simultaneously does an equal amount of positive work on the belt. The reaction force of the belt on the person is equal and opposite to the force of the person on the belt (Figure 4.1B), but the velocity of the point of force application is the same—when a person does negative work on a belt, the belt does an equal amount of positive work on the person (Figure 4.1C).

When the belts are moving at the same speed, as is the case for the tied-belt condition, the positive and negative work done by the person on the belts, and that done by the belts on the person, both must sum to zero. This is because of the constraint that the external forces must sum to be zero on average (C1). Since the belt speeds are equal, balancing forces also means balancing the work done by the person on the belts, and by the belts on the person. Thus, a person walking on tied belts cannot benefit from net work performed by the belts on the person—it will always sum to zero (Figure 4.1D).

In split-belt walking, the belts can do net work on the person, and the work done by the person does not need to sum to zero. The external forces acting on the person must still average zero (C1), and the net work on the person must also average zero (C2). This zero net work may be accomplished with net positive or negative work by the person and net negative or positive work by the treadmills (Figure 4.1D). For example, the

person's leg on the fast belt might provide net propulsive force on the fast belt resulting in net positive fast leg work, and then the person's slow leg might provide an equal amount of net braking force on the slow belt to bring the average horizontal force to zero. However, because of the differences in belt speeds, this braking force would require the slow leg to perform less net negative work on the slow belt than the net positive work that the fast leg had to perform on the fast belt for the same magnitude horizontal force. Together, the person's legs would perform net positive work on the belts, and consequently, the belts would perform net negative work on the person. Alternatively, if the fast leg was responsible for more of the braking, and the slow leg for more of the propulsion, the person would perform net negative work and the person would gain net positive work from the treadmill belts. This hypothesis is supported by observations by Selgrade et al. that the center of mass has a net backward displacement during the fast step over the course of split-belt walking where participants adapt to step length symmetry by placing the leading leg further forward on the fast belt (85).

Based on these predictions and observations, a split-belt treadmill can be viewed as an assistive device—similar to an exoskeleton—where the person has to learn how to coordinate their legs to maximize the assistance from the motors and reduce the positive work generated. Positive muscle mechanical work is metabolically expensive relative to negative muscle mechanical work requiring roughly five times the ATP per Joule (149,150). To decrease the relatively expensive positive mechanical work, a person should decrease the propulsive forces generated by the fast leg on the fast belt by lifting off the fast belt with less hip extension, and instead rely on the slow leg to perform more propulsion for less positive work by lifting off at a larger hip extension angle and contacting at a smaller angle during heel strike. This effect will shorten the distance between the feet at slow-leg heel-strike (slow step length: SL_{Slow}) and lengthen the distance between the feet at fast-leg heel-strike (fast step length SL_{Fast}). If we consider step length asymmetry as a measure of the difference between the fast step length and the slow step length, this change in coordination will shift asymmetry to more positive values.

To summarize, we predict that as an individual adopts a more positive step length asymmetry, the split-belt treadmill will perform more positive work on the person, reducing the positive work required by their muscles. Because of the relative expense of positive work, we also predict a reduction in the metabolic cost of walking as step length asymmetry becomes more positive, consistent with the findings from previous adaptation

experiments (82). However, we do not attempt to predict the metabolically optimal step length asymmetry as positive muscle mechanical work is only one contributor to metabolic cost, and it is not clear how other contributors, such as the cost of step timing (151), the cost to swing the legs (152), or the cost of maintaining an upright posture (44), change with step length asymmetry.

4.3. Materials and Methods

4.3.1. Experimental Protocol

Sixteen healthy participants (7 female, 9 male, age 27 +/- 3.5 years) completed our study. All experimental procedures were approved by the University of Southern California Institutional Review Board and each participant provided written informed consent before testing began. All aspects of the study conformed to the principles described in the Declaration of Helsinki.

We used a biofeedback-based protocol to map the relationship between mechanical work, metabolic cost, and step length asymmetry during split-belt walking (Figure 4.2B). Participants first walked on an instrumented split-belt treadmill (Fully Instrumented Treadmill, Bertec Corporation, OH) with both belts at 1.0 m/s while we measured their baseline step lengths and metabolic cost. In the next trial, we introduced the visual feedback and participants walked with both belts at 1.0 m/s, while matching their step lengths to the visual targets (see below). For the next seven trials, we set the belt speeds to a 3:1 ratio, with the left belt at 1.5 m/s and the right belt at 0.5 m/s. Participants performed the split-belt trials with visual feedback providing target step length asymmetries of 0.00, +/- 0.05, +/- 0.10 and +/-0.15 (see below). These asymmetries were relative to each participant's baseline and we presented these trials in random order. To determine whether mechanical work or energetic cost increased at extreme positive asymmetries, two participants performed two additional trials at asymmetries of +0.20 and +0.25. Each of these trials was six minutes in duration.

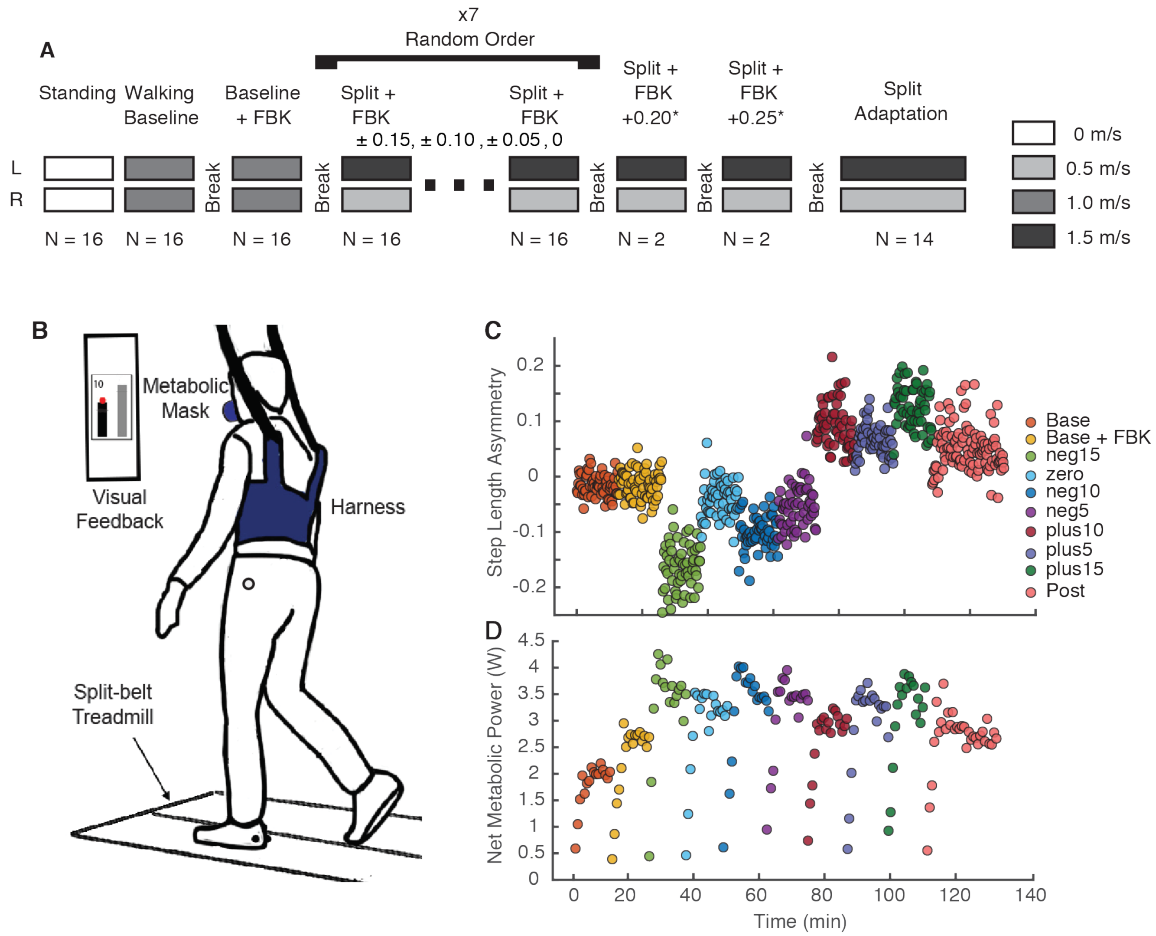

Figure 4.2: Experimental protocol and setup
A) Detailed experimental protocol. We randomized the order of the split-belt trials during which feedback of step lengths was provided to obtain seven different levels of asymmetry. Two participants performed two additional trials for levels of 0.20 and 0.25 step length asymmetry. All participants performed the split-belt adaptation trial last. The adaptation trial was performed freely for 10 minutes, with no feedback of step length and no instructions; all other trials lasted six minutes with four-minute breaks in between. **B)** Experimental setup. Reflective markers were placed bilaterally on the lateral malleoli to measure step lengths in real time. Two additional markers were placed on left and right greater trochanters to measure hip width for the visual feedback. An overhead harness was used to prevent falls without providing body weight support. No handrail was provided. Metabolic cost was measured using expired gas analyses. **C)** Raw values of step length asymmetry for all walking trials for a representative participant. Average step length asymmetry was binned every 10s to illustrate performance in the time domain. **D)** Raw net metabolic power values measured for each walking trial for the participant in panel C. All values were baseline corrected to standing baseline. Data were averaged every three breaths for metabolic cost to reduce the number of data points for visualization purposes. The last three steady state minutes of the metabolic cost data in each trial were used for analyses.

After the visual feedback trials, participants completed a 10-minute split-belt adaptation trial with no visual feedback of their step lengths and no explicit instructions of the step lengths they should maintain. The purpose of the final trial was to test whether

participants would converge towards the metabolically or mechanically optimal level of asymmetry observed during the previous split-belt trials. During all walking trials, participants wore a harness designed to prevent falls while providing no body weight support. Participants did not hold on to handrails during any portion of the trials. After each walking trial, participants sat down and rested for at least four minutes, and we visually inspected measured metabolic cost to ensure that it had returned to resting levels before beginning the next trial.

For all feedback conditions, participants relied on a monitor located at eye-level in front of the treadmill to target the desired step length targets. We measured the position of ankle markers placed bilaterally on the lateral malleoli at 100 Hz using an 11 camera Qualisys Oqus camera system (QTM, Sweden) and the visual display was controlled by custom software written in Vizard (Worldviz, Santa Barbara, CA). A fourth-order low-pass digital Butterworth filter smoothed marker data using a cut-off frequency of 10 Hz. We defined peak fore-aft position of the filtered ankle marker trajectories as heel-strike, and step length as the distance between right and left ankle markers at this instance. The monitor displayed the ankle position for the intervals where the ground reaction forces were less than 20N (153), which corresponded to swing phase. At foot-strike, defined as the point when the ground reaction force exceeded 20N, the ankle marker disappeared from the visual feedback. We instructed participants to step such that the location of the ankle marker at heel-strike would match the top a vertical bar in the visual display (Figure 4.2B). Participants targeted the left bar for the left leg and the right bar for the right leg. We constrained the sum of the step lengths to be equal to the baseline stride length (Equation 1), therefore participants adjusted the individual step lengths while maintaining stride length equal to that measured during the baseline trial. Note that the baseline speed was 1.0 m/s, which is the average of the individual belt speeds during the split-belt condition:

$$SL_{fast} + SL_{slow} = Stride_{baseline} \quad (4.1)$$

We constrained the desired stride length so that the desired step lengths would be fixed for a given level of step length asymmetry. To reinforce performance, the display provided participants with a score for each step at heel-strike, according to the following equation, rounded to the nearest integer:

$$Score = 10 - 20 * abs\left(1 - \frac{StepLength}{TargetStepLength}\right) \quad (4.2)$$

Participants only received a score if their step lengths were within eight standard deviations from the target. For example, for a representative participant, the average step length measured on the baseline trial was 560mm, thus, the achieved step length must be within 14 mm of the target to obtain a score of 10 on each side. For this same participant, the standard deviation was 17mm. If the step length was off-target by more than 136 mm, the participant did not receive a score. We verbally encouraged participants to obtain the maximum score of 10 points for all steps. Participants were successful at maintaining scores of above 8 points for each stride and maintaining each leg on its corresponding belt.

The target step lengths were selected to correspond to different levels of step length asymmetry which, per convention (82,148), was defined as follows:

$$Step\ Length\ Asymmetry = \frac{SL_{fast} - SL_{slow}}{SL_{fast} + SL_{slow}} \quad (4.3)$$

Here SL_{fast} is the step length at the instant the leading leg heel-strikes on the fast belt, and SL_{slow} is the step length at the instant the leading leg heel-strikes on the slow belt. Negative values correspond to longer steps with the slow (right) leg and positive values correspond to longer steps with the fast (left) leg. We used the last 100 strides of each trial to obtain the average step length asymmetry. Participants' baseline step length asymmetry ranged from -0.039 to 0.032, with a mean and standard deviation of 0.007 and 0.018.

There may be more direct methods to change leg coordination to gain positive work from the treadmill than manipulating step length asymmetry. We choose to use step length asymmetry for two reasons. First, prior research has shown that during split-belt walking, people increase fast step lengths by stepping further forward on the fast belt and decrease slow step length by lifting the trailing fast leg sooner, both during adaptation and when increasingly more positive asymmetries are enforced with visual feedback (145,148,154,155). Second, the literature on adapting to split-belts is primarily focused on considering adaptation as a process that minimizes step length asymmetry error (155,156) and keeping our manipulation in terms of step length asymmetry helps make clear that

there are alternative explanations for why the neuromotor system may adapt to reduce negative step length asymmetries. We anticipate that stepping further forward on the fast belt will lead to more braking force by the fast leg around heel-strike, and thus more positive work on the person by the belt. We also anticipate that short steps with the slow leg will be associated with reduced propulsive force generated by the fast leg around toe-off, and thus less positive work generated by that leg. In addition, longer steps with the fast belt will also lead the slow leg to lift off at a greater hip angle, generating increased propulsion.

4.3.2. Analysis

We assessed metabolic cost by determining the rates of oxygen consumption (V_{O2}) and carbon dioxide production (V_{CO2}) using a TrueOne® 2400 system (Parvomedics, UT). The metabolic cart recorded data on a breath-by-breath basis and subsequently, we re-sampled these data at a frequency of 0.1 Hz and averaged for smoothing in 10s bins. Since it takes approximately three minutes for oxygen consumption and carbon dioxide production by the body to reach steady-state in a task, we first identified the time point closest to the third minute of the trial (75) . We then measured the total V_{O2} consumed and the V_{CO2} produced from that time point onwards until the end of the trial, where the cost was at a steady state and when participants had already achieved a steady performance of the task. We then estimated the energy consumed during the last three minutes using the standard Brockway equation (109) as follows:

$$E_{met,gross} = \left(16.48 \frac{J}{ml\ O_2} V_{O_2} \cdot 1000\right) + \left(4.48 \frac{J}{ml\ CO_2}\ V_{CO_2} \cdot 1000\right) \qquad (4.4)$$

From here, we dived $E_{met,gross}$ by the exact duration (T) over which it was calculated to obtain an estimate of the gross metabolic rate $P_{met,gross}$ measured in Watts. Finally, we subtracted each participants' standing metabolic rate from each walking trial. Thus, all metabolic rate values presented here are net metabolic rate. The addition of visual feedback during the second baseline trial increased metabolic rate by 11 +/- 11% compared to the cost of walking without feedback ($p<0.001$) despite there being no changes in step length asymmetry ($p=0.359$). We expect this added cost to remain constant for all trials that required visual feedback.

We estimated the mechanical work performed by the legs using an extension of the individual limbs method (83,157). This method approximates the legs as massless pistons and the entire body as a point mass acting at the center of mass (Figure 4.1A). We use a reference frame attached to the stationary ground—the belt speeds and center of mass velocity are relative to this reference frame. We measured individual leg ground reaction forces from the instrumented treadmill at 1,000 Hz and filtered this signal with 20 Hz cut-off low-pass zero-lag digital Butterworth filter. We segmented the ground reaction forces into strides using a vertical ground reaction force threshold of 32N (83) to identify the beginning and end of each stride and performed the following analysis on a stride-by-stride basis.

We calculated the medio-lateral, fore-aft and vertical center of mass velocities by first calculating the center of mass accelerations as the sum of the forces acting on the body normalized for body mass (83,157). We estimated body mass as the average vertical force during the final 100 strides of the trial, divided by the acceleration due to gravity (9.81 m/s^2). We calculated center of mass velocities from the time integral of the center of mass accelerations. We determined the integration constants by requiring the average center of mass velocity over a stride to be zero in each direction because net movement in any direction must on average be small on a treadmill.

The total mechanical power generated by each leg is composed of power generated by the leg on the body and the power generated by the leg on the treadmill's belts. We define the mechanical power generated on the body by a leg as the dot product of the ground reaction force from that leg and the center of mass velocity. Similarly, we define the mechanical power generated by a leg on a belt as the dot product of the force generated by the leg on the belt, which is equal and opposite to the ground reaction force measured by the treadmill, and the velocity of the corresponding belt. The medio-lateral and vertical components of belt velocity are zero, and the fore-aft component is either -0.5 m/s (slow belt), -1.5 m/s (fast belt), or -1.0 m/s (tied belts). For each leg, we then calculated the instantaneous sum of the two powers to obtain the total instantaneous mechanical power generated by that leg (Figure 4.1B). We calculate the instantaneous power generated by the slow and fast belts on the body as the dot product of the ground reaction force measured from that belt with that belt's velocity.

To determine the total positive and negative work performed by a leg or a belt, we calculated the time integral of the positive or negative portion of its instantaneous power over the stride cycle (110). The net work performed by a leg or a belt is the time integral of the full instantaneous power over the stride cycle. We express all measures of work as work rates by dividing each measure by stride duration. As with step length asymmetry, measures of work rate for each trial are the average values over the last 100 strides.

We converted the metabolic rate and mechanical work rate to dimensionless units to reduce variability between subjects. We divided each individual's values by $ml^{0.5}g^{1.5}$ here m is their body mass, *l* is their leg length and *g* is gravity (9.81 m/s^2). Thus, using the average body mass (75.4 kg) and average leg length (0.88 m) of our participants, all reported dimensionless values can be approximately redimensionalized to the average values in Watts by multiplying by 2.17×10^3.

4.3.3. Statistical Analyses

A participant's mechanical work and metabolic cost depend not only on the conditions that we control but also on differences between individuals. Our purpose here is to test predictions about the former—we do not, for example, seek to explain the differences in metabolic cost between individuals for a given condition. Consequently, we used mixed-effect regression models that allowed individualized intercepts but shared a fixed dependence on the independent variables of interest These models captured the relationship between 1) measure of foot placement and step length asymmetry, 2) measures of mechanical work and step length asymmetry, 3) measures of mechanical work performed by the legs and the mechanical work performed by the treadmill, 4) metabolic power and mechanical work performed by the treadmill, and 5) metabolic power and step length asymmetry. Although the target levels of step length asymmetry were set at discrete values (0.00, +/-0.05, +/-0.10, +/-0.15), the actual step length asymmetry used in our regression models was a continuous variable since each participant's actual performance differed from the target asymmetry. All models included a random intercept for each participant to account for unknown, subject-specific effects. We used a modified version of the marginal R^2 for linear mixed effect models (158) to compute the variance explained by the fixed components of our linear models. We computed R^2 as the ratio of the variance computed from the fixed effects and the sum of the variance from both the fixed effects and residuals from the regression model. We used this approach in lieu of

the conditional R^2, which accounts for the variance explained by both the fixed and random effects, because we were only interested in quantifying the explanatory value of the fixed effects. To make our figures consistent with our statistical analysis approach, we removed the individualized intercepts from each participant's data before generating each scatterplot. Lastly, we determined if participants plateaued at a step length asymmetry that differed from baseline during the adaptation period using a paired-samples t-test. We conducted all statistical analyses in Matlab R2017a (Mathworks, Natick, MA) and set statistical significance level to $p < 0.05$.

4.4. Results

4.4.1. Modulation of Foot Position to Achieve Target Step Length Asymmetry

Participants modified the position of both the leading limb and the trailing limb at initial contact of the leading limb as they varied step length asymmetry throughout the experiment (Figure 4.3). As step length asymmetry became more positive, participants increased the length of their steps when stepping on the fast belt and decreased the length of their steps when stepping on the slow belt. To take longer steps on the fast belt, participants placed their leading foot farther forward on the fast belt (β = 243.4, 95% CI [212.2, 274.6], p=2.22e-29) and extended their trailing foot farther behind the body on the slow belt (β = -356.1, 95% CI [-385.1, -327.1], p=4.43e-46). To take shorter steps on the slow belt, participants placed the leading leg closer to the body (β = -348.5, 95% CI [-385.3, -311.6], p=5.00e-36) but only made minor reductions in trailing limb extension on the fast belt (β = 85.4, 95% CI [56.5, 114.3], p=5.17e-8).

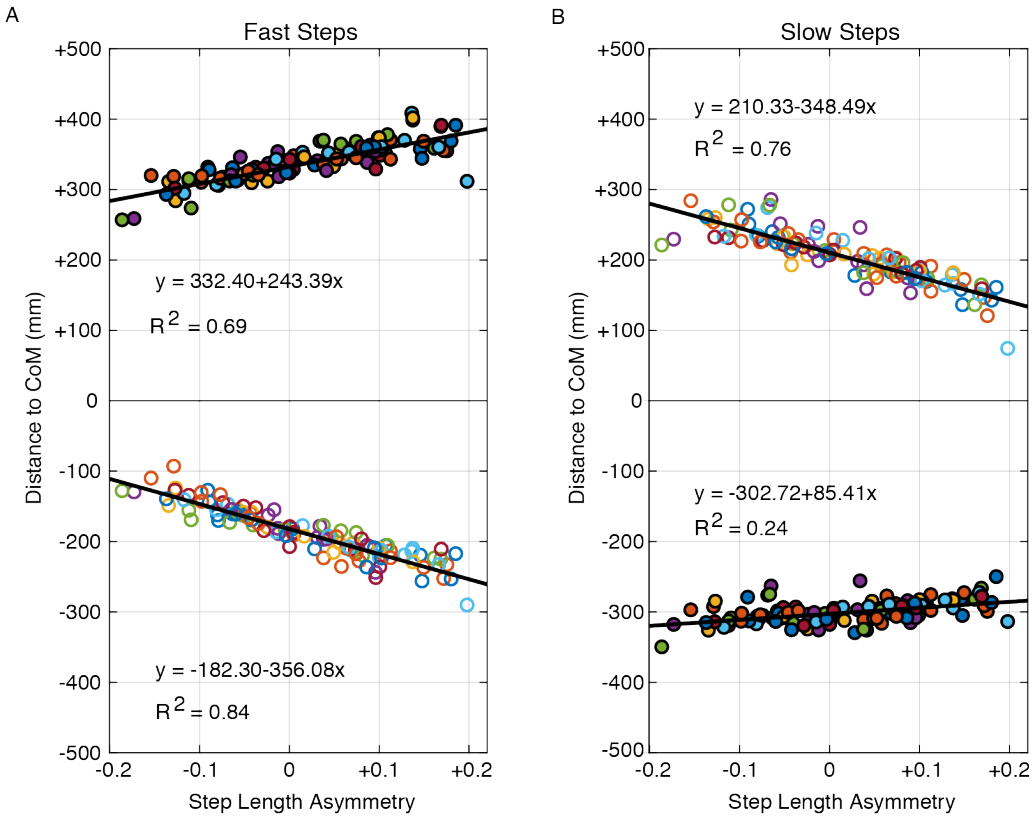

Figure 4.3: Distance from the leading and trailing foot to the center of mass at heel strike

The x-axes show the achieved step length asymmetry for all participants. Positive values indicate that the foot is anterior to the center of mass while negative values indicate that the foot is posterior to the center of mass. Closed and open points correspond to the fast and slow limb, respectively. The distance between the leading and trailing feet at heel strike constitutes the step length. **A)** Fast step lengths. To increase the fast step length as asymmetry increased from negative to positive, participants increased both leading foot distance to the center of mass and trailing foot distance to the center of mass. **B)** Slow step lengths. To decrease the slow step length as asymmetry increased from negative to positive, participants primarily decreased the distance from the leading foot to the center of mass while maintaining a relatively consistent trailing foot position.

4.4.2. Mechanical Work Performed by the Legs and the Treadmill Varies with Step Length Asymmetry

Consistent with our hypothesis, participants transitioned from performing net positive work with the legs at negative step length asymmetries to performing net negative work at positive asymmetries. This change in work performed by the limbs can be appreciated by understanding how the mechanical power generated by each limb changes across levels of asymmetry. The fast leg transitioned from generating a large amount of positive power during push-off at -15% asymmetry to performing a large amount of negative work during weight acceptance at an asymmetry of +15% (Figure 4.4A). In

contrast, there were negligible changes in mechanical power in the slow leg across levels of asymmetry (Figure 4.4B). Overall, the amount of positive work performed by the legs decreased by ~13% between -15% and +15% step length asymmetry (Figure 4.5A, β = -0.009, 95% CI [-0.013, -0.006], p=3.52e-7). In contrast, the amount of negative work performed by the legs increased by ~33% over the full range of step length asymmetries (Figure 4.5B, β = -0.019, 95% CI [-0.0220, -0.0151], p=7.59e-19). As a result of these combined changes, the legs ultimately performed more negative work than positive work at positive asymmetries (Figure 4.5C, β = -0.028, 95% CI [-0.029, -0.027], p=1.66e-67).

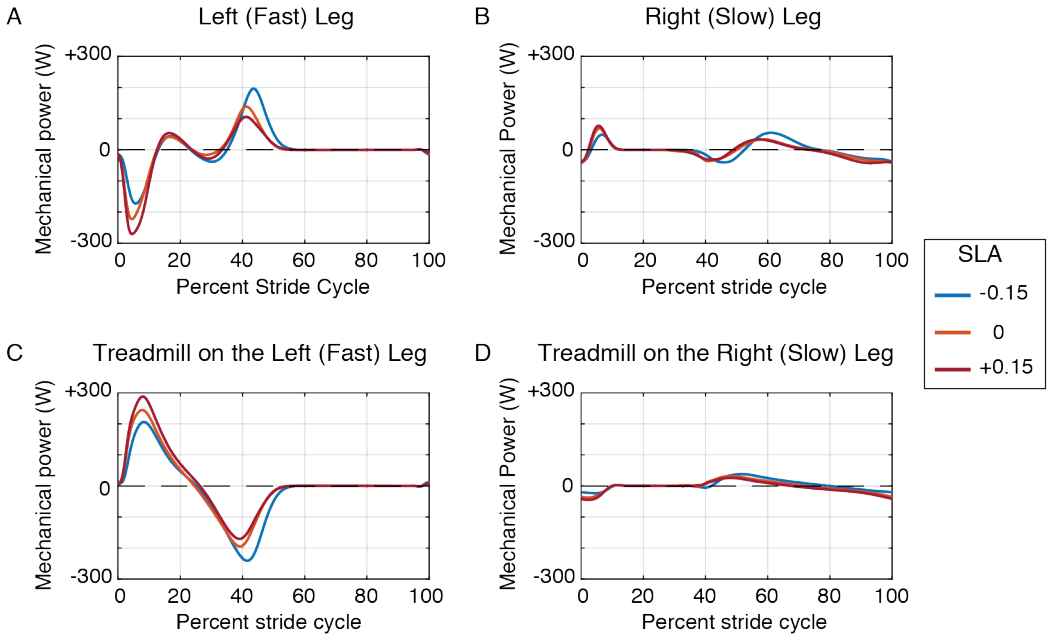

Figure 4.4: Mechanical power generated by the legs
Mechanical power generated by the **A)** fast leg, **B)** slow leg, **C)** fast belt, and **D)** slow belt throughout the stride cycle. The power generated by the treadmill belts represents the rate of mechanical work performed by each belt on the body. During the early portion of the stride cycle (~0-15%), the leading, fast leg generated a large peak negative peak in power while the trailing, slow leg generated a relatively smaller positive peak. This relationship reversed during the later portion of the stride cycle (~40-70% of the gait cycle) such that the fast leg generated a burst of positive power while the slow leg generated a smaller burst of negative power. Each trace is an average of all participants (n = 16). The stride cycle begins and ends at foot-strike of the fast limb. Blue, yellow, and red traces correspond to split-belt walking at step length asymmetries of -15%, 0%, and +15%, respectively.

We predicted that the treadmill would act as an assistive device at positive step length asymmetries by performing net positive work on the body, and our observations were consistent with this prediction (Figure 4.4C). As asymmetry became more positive, there was a ~28% increase in the amount of positive work performed by the belts on the body (Figure 4.5D, β =0.016, 95% CI [0.014, 0.018], p=1.64e-29) and a ~15% decrease

in the amount of negative work performed by the belts on the body (Figure 4.5E, β =0.011, 95% CI [0.010, 0.013], p=1.58e-23). Together, these changes resulted in a shift from the treadmill performing mostly negative work on the body and extracting energy from the person at negative asymmetries to performing mostly positive work on the body and adding energy to the person at positive asymmetries (Figure 4.5F, β =0.028, 95% CI [0.026, 0.029], p=4.76e-67).

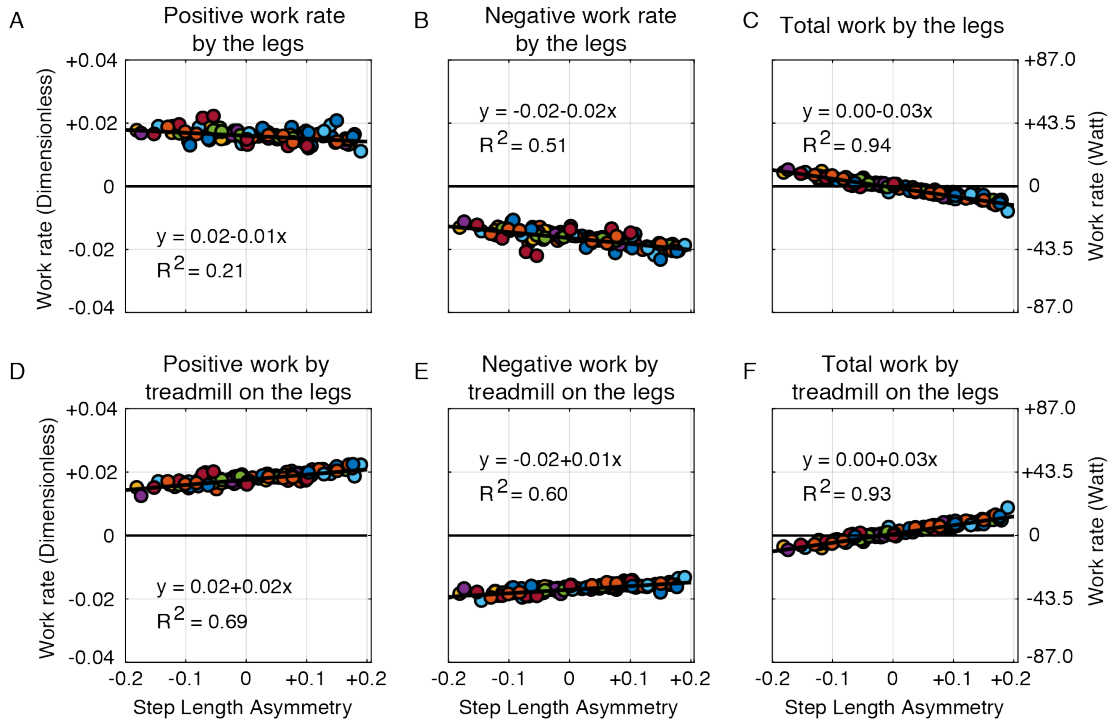

Figure 4.5: Average rate of work performed by the legs and the treadmill belts as a function of step length asymmetry

A) Positive work performed by the legs, **B)** negative work performed by the legs, and **C)** total work performed by the legs. **D)** Positive work performed on the body by the treadmill, **E)** negative work performed on the body by the treadmill, and **F)** total work performed by the treadmill on the body. Work rate is expressed in dimensionless units on the left y-axis and in Watts on the right y-axis. Each data point represents a single trial for an individual participant and each color represents a different participant.

The legs' shift toward performing net negative work at positive step length asymmetries was primarily driven by changes in the fast leg. Across participants, we observed both a ~30 % reduction in positive work (Figure 4.6A, β =0.010, 95% CI [-0.012, 0.008], p=7.34e-17) and a ~36% increase in negative work performed by the fast leg (Figure 4.6C, β = -0.012, 95% CI [-0.014, -0.009], p=7.63e-14) at increasingly positive asymmetries. In contrast, there were no changes in positive work performed by the leg on

the slow belt (Figure 4.6B, p=0.53), but there was a ~21% increase in negative work by the slow leg at positive asymmetries (Figure 4.6D, β = -0.007, 95% CI [-0.010, -0.004], p=4e-5).

As the treadmill performed increasingly more positive work on the body, there was a proportional reduction in positive work performed by the legs (Figure 4.7, β = -0.33, 95% CI [-0.43, -0.23], p=2.8e-9). The slope of this relationship suggests that participants exploited the work performed by the treadmill belts with an effectiveness of approximately 33%. That is, for every 3 Joules of positive work performed by the belts on the person, the person reduced the positive work performed by the legs by about 1 Joule.

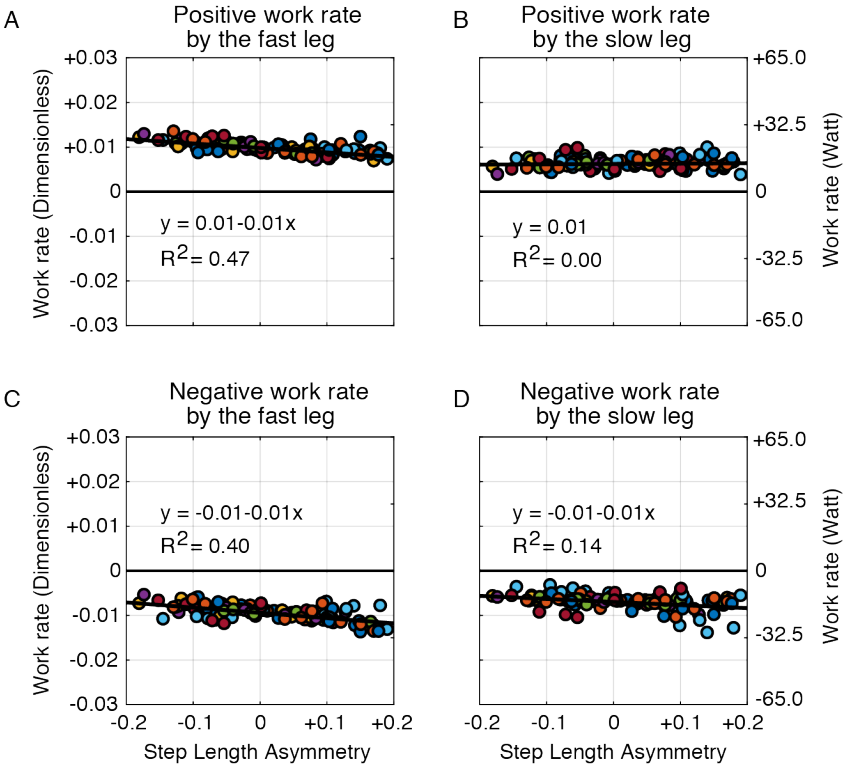

Figure 4.6: Average rate of work performed by the individual legs across levels of step length asymmetry

A) Positive work performed by the fast leg, **B)** positive work performed by the slow leg, **C)** negative work performed by the fast leg, and **D)** negative work performed by the slow leg. Work rate is expressed in dimensionless units on the left y-axis and in Watts on the right y-axis. Each data point represents a single trial for an individual participant and each color represents a different participant.

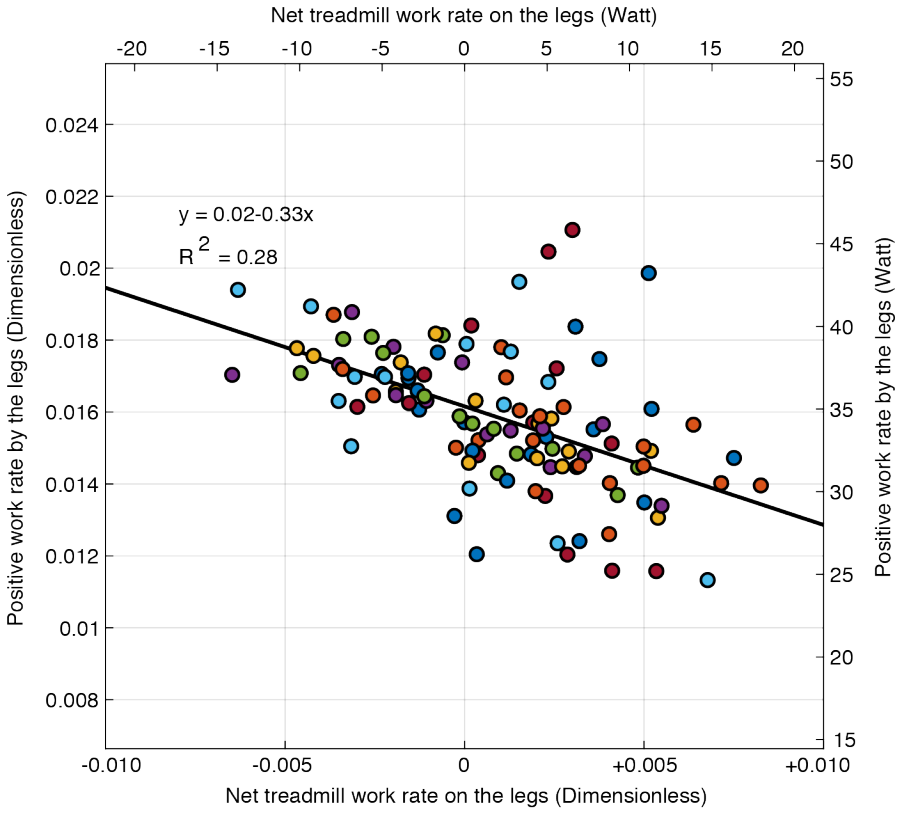

Figure 4.7: Relationship between the average rate of positive work performed by the legs and the average rate of work performed by the treadmill on the body

Work rate is expressed in dimensionless units on the lower x-axis and the left y-axis and in Watts on the upper x-axis and right y-axis. Each data point represents a single trial for an individual participant and each color represents a different participant.

4.4.3. Assistance Provided by the Treadmill Led to a Reduction in Metabolic Cost

The assistance provided by the treadmill at positive step length asymmetries was not only associated with a reduction in positive work performed by the legs but was also associated with a reduction in metabolic cost (Figure 4.8A, β = -1.54, 95% CI [-2.07, -1.02], p=5.34e-8). Since the assistance provided by the treadmill was associated with a reduction in positive work performed by the legs, we also found that metabolic power was strongly correlated with the total positive work performed by the legs (Figure 4.8B, β = 0.105, 95% CI [0.091, -0.119], p=1.89e-27). The slope of this relationship suggests that positive work was performed at an efficiency of about 10%. Overall, by exploiting the assistance provided by the treadmills, participants achieved an approximately 14%

reduction (8 to 18% reduction, 95% CI) in metabolic cost relative to the most costly level of step length asymmetry (Figure 4.8C).

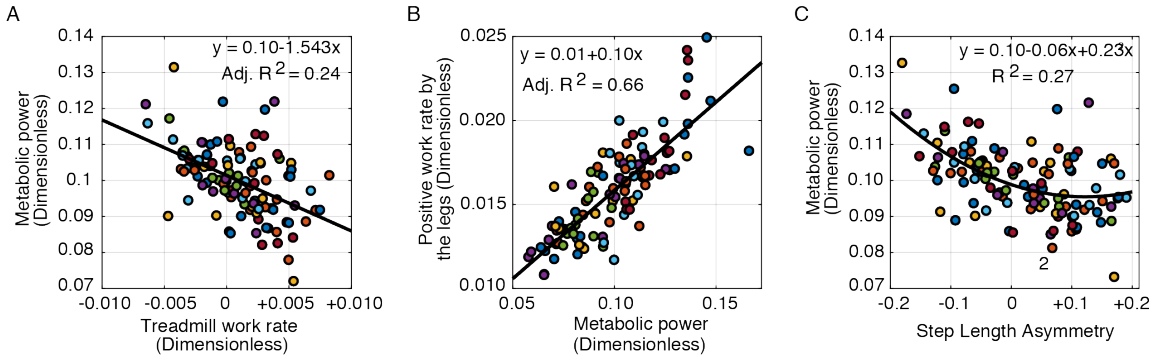

Figure 4.8: Metabolic power, mechanical work, and asymmetry
A) Metabolic power as a function of the rate of work performed by the treadmill on the body. **B)** Positive work rate versus metabolic power. **C)** Metabolic power as a function of step length asymmetry. Each data point represents a single trial for an individual participant.

4.4.4. The Ability to Use Step Length Asymmetry to Exploit Assistance Provided by the Treadmill is Bounded

Although the increase in positive work performed by the treadmill led to a reduction in metabolic cost, we also wanted to determine if this ability to exploit the work performed by the treadmill increased indefinitely or whether there was a specific level of asymmetry that minimized metabolic cost. Our results supported the existence of an energetically optimal level of step length asymmetry as a regression model including both linear and quadratic terms explained the relationship between metabolic cost and step length asymmetry better than a simple linear model (LRStat = 4.83, p=0.028, adjusted R^2 = 0.27, Figure 4.8C). Bootstrap analyses indicated that the asymmetry that minimized metabolic cost had a 95% confidence interval of 0.06 and 0.38, which is consistent with our prediction that positive asymmetries minimize energetic cost.

Although metabolic cost generally decreased with increasingly positive asymmetries as is predicted in our model, experimentally we expected that metabolic cost would increase again at large positive asymmetries given biomechanical constraints associated with walking with extreme positive asymmetries. We confirmed this finding in two participants, who each completed two additional trials where they walked at target levels of 0.20 and 0.25 step length asymmetry. The metabolic cost for three out of four of these trials was 0.027 ± 0.022 greater than the minimum cost predicted from the

regression fit. These increases in metabolic cost at extreme positive asymmetries support the quadratic relationship that we determined in our analysis.

4.4.5. Participants Chose Positive Step Length Asymmetries When Allowed to Freely Adapt

Lastly, we found that participants chose to walk at a level of step length asymmetry near that which minimized metabolic cost when they were allowed to freely select their walking pattern. After experiencing a range of asymmetries during the cost mapping trials, participants tended to plateau at step length asymmetries that were more positive than their natural baseline asymmetry (Figure 4.9, mean: 0.028, 95% CI [0.0018, 0.0434], p=0.010) though they had shorter stride lengths during adaptation (95% CI [929 mm, 999 mm]) than they did when walking at similar levels of asymmetry during the split-belt trials with visual feedback (95% CI [47, 93] mm shorter strides during adaptation, p= 1.03e-05). This positive step length asymmetry markedly differs from the behavior typically observed within a single session of adaptation where participants most often plateau at slightly negative asymmetries (115). In addition, there was no significant difference between the metabolic cost measured at the end of the adaptation trial (0.086, 95% CI [0.074, 0.10]) and the minimum predicted from the regression fit (0.096, p=0.12).

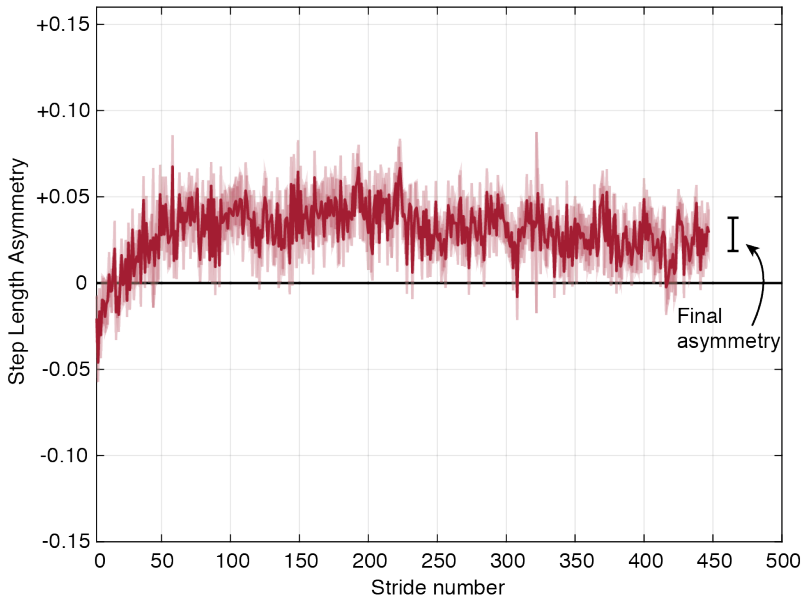

Figure 4.9: Adaptation of step length asymmetry during the adaptation trial in the absence of visual feedback

Participants consistently selected positive asymmetries near those which minimized metabolic cost during the cost mapping trials. The dark blue line represents the average asymmetry as a function

of stride number when averaged across all participants and the light blue area represents the standard deviation about this average. The final error represents the average ± standard deviation level of asymmetry at the end of the split-belt adaptation trial. The step length asymmetry achieved during the last 50 strides was significantly different from their baseline step length asymmetry ($p=0.010$).

4.5. Discussion

Learning to gain assistance from external sources is a general problem for the neuromotor system. We explored this problem using a split-belt treadmill paradigm to determine whether people learn to harness energy from the differences in belt speeds to reduce the metabolic cost of walking. People exploited the assistance provided by the treadmill by changing their step lengths such that the treadmill performed net positive work on the body, thereby allowing the legs to perform net negative work. This shift toward performance of negative work by the legs was associated with a reduction in metabolic cost which likely reflects the energetic benefits of negative work (159). Therefore, the reductions in asymmetry commonly observed during split-belt walking can be interpreted as a strategy generated by the neuromotor system to take advantage of the work performed by the treadmill to reduce energetic cost (82,148).

Similar to using a powered exoskeleton, individuals can learn to coordinate their movement to maximize the assistance from the treadmill's motors. We find that individuals use the assistance from the split-belt treadmill with an effectiveness of 33%, i.e. they reduce their positive work by 1 J for every 3 J of positive work done by the treadmill. While this is not a commonly reported metric in exoskeleton use, Sawicki and Ferris (142) used a similar metric to show that their ankle exoskeletons reduced joint mechanical power by 41% relative to the mechanical power provided by their ankle exoskeleton—similar to our results. We focus on this metric because while the maximum effectiveness possible in powered exoskeletons may be system-dependant and hard to quantify, we can provide a reasoned estimate of the maximum possible effectiveness for split-belt treadmill walking. When the treadmill does positive work on the person, it applies a negative force on the person that has to be cancelled out by an equal positive propulsive force applied by the trailing leg on the treadmill. In applying this propulsive force, the trailing leg has to perform positive work on the treadmill. In fact, the minimum amount of positive work necessary depends on the ratio of the belt speeds. In our experiment, the fast belt moved three times

faster than the slow belt. Since work is the time integral of the dot product of force and velocity, this means that the trailing leg on the slow belt has to at least perform positive work that is roughly one third of the negative work performed by the leading leg on the fast belt. This means that the participants in our study could have at most achieved an effectiveness of ~67%. We only include the fast step in this calculation because any braking force on the slow belt, only further decreases this value.

It is possible that individuals cannot, in practice, exploit the positive work from the treadmill to the degree we have suggested here. One strategy to improve effectiveness in split-belt walking is for individuals to use more positive step length asymmetries. However, the extreme positive asymmetries needed to maximize the positive work performed by the treadmill likely challenge anatomical constraints. In addition, even at less extreme positive asymmetries, an individual might choose to perform more positive work, and consequently also negative work, than necessary simply to feel safe in the new gait (70). We suspect that with practice and appropriate guidance, the effectiveness observed in our study can be improved from that observed here. This is one of the goals of our future research.

The reduction in positive mechanical work we observed was accompanied by a reduction in metabolic cost of 14%. This reduction is comparable to that observed in powered lower-limb exoskeletons that can currently achieve reductions up to 17% (160). Both effectiveness and energetic benefits incurred as a result of learning to walk in lower-limb exoskeletons are similar to that observed in split-belt walking. As described earlier, we suspect that people can be taught to improve their effectiveness and maximize energetic benefits in split-belt walking and when using powered exoskeletons. Because split-belt treadmills are becoming more common in biomechanics labs, split-belt walking could become a model experimental paradigm to understand how the human neuromotor system learns to walk in environments where it is possible to take advantage of external assistance.

Traditionally, studies of split-belt adaptation have shown that after 10-20 minutes of adaptation, individuals converge to step length asymmetries near zero (82,145). This adaptation toward a step length asymmetry of zero is consistent with the hypothesis that step length asymmetry is treated as an error by the nervous system. In this hypothesis, the difference between expected and achieved sensory feedback during movement, known as sensory prediction error, drives motor adaptation (102,156,161). Reductions in

step length asymmetry are also consistent with the hypothesis that individuals converge towards habitual behaviors when exposed to novel environments (162,163). Based on this hypothesis, people adopt steps of equal length because this is the habitual pattern they use regularly. One challenge to both of these notions is that people adopt asymmetric step times in order to take steps of equal length (164) and thus, it is not immediately apparent why the nervous system would choose to reduce errors in step length but not in time. In addition, these asymmetries in step time could lead to sensory prediction errors and are non-habitual behaviors in the time domain. Further evidence that adaptation is not purely driven by sensory prediction errors related to step length asymmetry was provided by a recent study showing that sensory recalibration and motor recalibration have different timescales (115). In this study, the authors postulated that if we recalibrate motor commands in response to sensory prediction errors, then error perception is also updated (18). Therefore, if the same neural processes drive motor and perceptual recalibration during locomotor adaptation, they would change over a similar timescale. However, the authors found that motor and perceptual adaptation to differences in belt speeds occurred over different timescales and are likely independent of each other. The authors also found that after multiple days of adaptation, individuals plateau at positive step length asymmetries. These results, together with our findings that individuals adopt positive asymmetries after being exposed to the cost landscape, refute the idea that split-belt adaptation is explained by the nervous system's desire to minimize perceived errors in step length asymmetry or converge towards habitual behaviors. Instead, energy optimization explains both why people reduce step length asymmetry during single sessions of split-belt adaptation and why they adopt positive asymmetries when provided with more extensive experience.

A logical follow-up question is, if energetic optimization is the goal of split-belt adaptation, why are positive asymmetries that minimize mechanical work and metabolic cost not observed during adaptation? One potential explanation is that the energetic savings for positive asymmetries are minor compared to the cost of symmetry, and this might impede the optimization process. Given that the confidence interval for the step length asymmetry associated with the lowest metabolic cost ranged from 6 to 38%, the energetic gradient might be too shallow for people to obtain meaningful energetic reductions from walking with positive asymmetries. In fact, our results show that the optimal step length asymmetry reduced metabolic cost by only 2% compared to symmetry.

Despite these small savings, after exposure to the step length asymmetry landscape, participants in our study plateaued at positive asymmetries during adaptation. This suggests that people may be willing to adjust how they walk for savings of less than 5% as reported in previous work (75).

Alternatively, positive asymmetries may not have been observed during typical locomotor adaptation studies because energetic optimization occurs over a timescale that is longer than that commonly used in adaptation studies (44,165). To date, most locomotor adaptation studies have been performed using single session paradigms of 10 to 20 minutes in duration (82,145). Thus, short, single bout studies may not provide enough time or experience for individuals to fine tune their steps lengths to achieve the more energetically optimal positive asymmetries. Consistent with the interpretation that energy optimization occurs over a longer timescale, people tend to reach positive asymmetries when allowed to adapt to a split-belt treadmill over multiple days (115). Surprisingly, the visual feedback in our experiment, which exposed participants to positive asymmetries, accelerated the convergence towards positive asymmetries in a single session to that which occurs during multi-day adaptation. The longer timescale for energetic optimization is further supported by work in the upper extremity, which shows that improvements in task performance and fine tuning of upper extremity muscle activation, occurred over a faster timescale than energy minimization (44,165). Overall, we conclude that the symmetric steps commonly observed at the conclusion of previous split-belt adaptation studies and the associated reductions in energetic cost (82,83), may be only a partial picture of a slower energetic optimization process that plateaus at positive asymmetries.

One of the features of our study is that we constrained stride lengths to those measured during baseline with the belts tied at 1.0 m/s. Given this constraint, the metabolic optima that we found in this study is a local minimum for that specific stride length and may not be a global minimum. We imposed this constraint as it would not be practical to characterize the metabolic cost landscape across both the dimensions of step length asymmetry and stride length. Moreover, post-hoc analysis of data from a previous adaptation study (148) showed that there was no change in stride length during split-belt adaptation compared to baseline walking ($p=0.389$). Our constraint on stride length is particularly relevant given the results of the adaptation trial in the current study, where 15/16 participants adapted to the split-belt treadmill using shorter stride lengths. Whether

optimization of stride length can further reduce positive work and metabolic cost during locomotor adaptation remains to be seen.

In conclusion, the process by which people adapt to walking on a split-belt treadmill is just one example of a broad class of tasks in which the neuromotor system learns to exploit external assistance to improve economy. A common feature of these types of tasks is that the process of optimizing the use of assistance may proceed quite gradually in the absence of guided experience. Ultimately, understanding how best to guide people through a range of experiences capable of accelerating the learning and optimization process has important implications for maximizing the utility of assistive devices such as exoskeletons and prostheses.

Chapter 5.

Energetic trade-off between step-to-step transition and limb swing costs explain preferred split belt walking gaits

5.1. Abstract

Split-belt treadmill walking is widely used to understand human gait adaptation. While the adaptation process is traditionally described as the minimization of a sensorimotor prediction error, there is growing evidence that the adaptation is also associated with a reduction in metabolic energetic cost. On a split-belt treadmill, participants can harness energy from the belt speed difference by placing their leading leg ahead on the fast belt, reducing their energetic cost of walking. However, this mechanism predicts that the further ahead the leg placement, the cheaper walking becomes. Contrary to this, the energy minimum in humans occurs at slightly positive asymmetries. Here, we used a computer model to test the hypothesis that this optimality arises due to a trade-off between the step-to-step transition cost and swing cost. We developed an anthropomorphic dynamic walking model that can walk on a dual-belt treadmill optimizing a weighted cost function of transition cost and swing cost. We first identified the weighting for the swing cost c by constraining the walker to match the empirical speed-step length relationship over ground. We then showed that while symmetric gaits are optimal during tied-belt walking, gaits with a small positive step length asymmetry are optimal during split-belt walking. This optimality arises due to the trade-off between transition and swing cost, as the walker reduces its push-off on the fast belt while simultaneously harnessing more energy from the treadmill. A consequence of this trade-off is that the cost of walking with a belt speed difference is always higher than the cost of walking on a tied-belt treadmill at the slow speed. These results are consistent with experimental observations and provide insight into what contributes to the optimal split-belt walking gait.

5.2. Introduction

Split-belt treadmills are widely used to understand fundamentals of human motor adaptation (73,74). Briefly, this involves walking on a treadmill that has two belts side by side, with one foot on each belt. In split-belt walking studies, participants first walk with both belts moving at the same speed and then the belt speeds are split. When this happens, participants need to adjust many aspects of their gait to continue stable walking on the treadmill (147). An often focussed upon aspect of gait in this adaptation process is step lengths. Step length is typically measured as the distance between the malleolus markers placed on each foot, when the leading leg is on the belt being specified. Immediately after the belts are split, participants take a small step on the belt with the faster speed and take a long step on the slow belt. Then, within minutes, participants adapt to execute steps of equal length on both belts (145). This adaptation is explained as the minimization of a sensorimotor prediction error—the nervous system expects its motor commands to produce steps of equal lengths while walking but the difference in belt speeds causes the commands to produce unequal step lengths (32). This is quantified using the metric of *Step Length Asymmetry (SLA)* given by:

$$SLA = \frac{SL_{fast} - SL_{slow}}{SL_{fast} + SL_{slow}} \tag{5.1}$$

where SL_{fast} and SL_{slow} refer to the step lengths on the fast belt and slow belt respectively. SL_{total} is the sum of the two step lengths. A gait with a step length asymmetry of zero is called symmetric and anything else is called asymmetric. While the adaptation process leads to symmetric steps lengths, other aspects of gait such as step times remain asymmetric. It is unclear why the nervous system might only target the sensorimotor prediction error in step lengths. An alternate hypothesis that has developed recently is that the adaptation might be a result of an energy minimization by the nervous system. Here, we use a computer model to understand how and why there might exist an energy optimal step length asymmetry in split-belt walking.

Recent findings suggest that the energy optimal gait lies at a small positive step length asymmetry (84,166,167). These experiments found that if participants are allowed longer-than-traditional durations to walk on the split-belt treadmill, or if they can experience walking with a range of step length asymmetries, they adapt to slightly positive step length

asymmetries rather than symmetry. This adaptation results in a lower metabolic power expenditure than symmetry (84). In a previous study, we used conceptual predictions of the mechanics and energetics of different step lengths to explain this reduction in energetic cost (84). While walking, no net work is required to keep our body moving at a constant speed. However, in each step, when the leading leg contacts the ground, it performs negative work on the body resulting in energy loss. We then need to perform positive work to restore this lost energy. When walking over ground, the ground cannot do work since it is stationary, and hence our legs only do work on our body. However, when walking on a treadmill, the legs do work on the treadmill rather than the body, and the treadmill does an equal and opposite work on the legs, thus keeping the net work of the system still zero. Work is measured as the time integral of the dot product of force and velocity. Therefore, when walking on a split-belt treadmill, the same force can do more work on the fast belt compared to the slow belt. The net force on the body has to be zero since it is moving at a constant velocity. However, a person can achieve this net zero force by applying a large force on the fast belt with the leading leg and an equally large and opposite force with the trailing leg on the slow belt. This allows the person to perform net negative work on the treadmill and causes the treadmill to perform net positive work on the person. The force applied by the legs on the treadmill in this manner is strongly dependent on the step length, with longer step lengths leading to larger force. Thus, with longer step lengths on the fast belt, people can harvest more energy from a split-belt treadmill. While this successfully predicts why participants move away from negative step lengths asymmetries, it also predicts that maximum energy savings can be obtained at an extreme positive asymmetry where the treadmill performs all the work. Metabolic power measurements from participants, on the other hand, suggest that the energetic optimum might lie at slightly positive asymmetries between 0.06 and 0.38 (84). Our simple conceptual model is missing some significant contributors to the energetic cost associated with different step length asymmetries that determine the energetic minimum.

The energetics of over ground walking can be broadly captured using the contribution of two major costs (168). While no net work is performed on the body during constant velocity walking the body does perform positive and negative work within a step, as described earlier. The metabolic energy expenditure associated with this work is termed as the step-to-step transition cost (169). Our conceptual model roughly captured the contribution of this cost. The second cost is the cost of swinging the leg (152). The

forces involved in the swinging of the leg cannot perform any net work on the body since they are forces internal to the body. However, they do perform work on the body and that consumes metabolic energy. There is also some metabolic energy expenditure associated with the rate of production of muscle force. This cost predominantly affects swinging and not the step-to-step transitions since a swinging leg requires a periodic force as determined by the swing frequency. The swing cost is strongly dependent on the step frequency (170). When walking on a split-belt treadmill, the stance foot has to move at the velocity of the belt that it is contacting. This places a constraint on how quickly the swing leg has to move for the leading leg to land at a particular step length. We suspect that the increasing swing cost necessary to step further forward on the fast belt for a given slow belt speed trades off against the increasing benefit of placing the leading leg further forward.

In this study, we use an inverted pendulum-based dynamic walking model to understand the role of transition cost and swing cost in split-belt walking. Inverted pendulum models get their name from their modelling of the stance leg as an inverted pendulum. Such models have been used widely and successfully to capture the fundamental mechanics and energetics of human walking (168,171–174). Here we use a version of such models where the swing leg is modelled as a regular pendulum. A spring connects this leg to the stance leg at the top, representing the torque generated by the muscles that cross the hip in a human. A physiological implementation of the spring might be through bursts of hip torques in opposite directions at the beginning and end of a step. Also in these models, the trailing leg of the inverted pendulum stance leg can apply push-off impulses, representing the propulsion forces generated by humans. The Anthropomorphic Model is the simplest physically realistic inverted pendulum model of human walking (168). It has a point mass representing the torso, legs with distributed mass, and curved massless feet. We use the anthropomorphic model since it allows us to extend the hypothesis from our conceptual model to a physically realistic model with minimal addition of parameters.

We modify the anthropomorphic walker to be able to walk on a treadmill that can have both belts moving at the same or different speeds. We first parameterize the walker by requiring it to reproduce over ground walking gait as obtained from empirical data and reproduced by previous anthropomorphic models. We then use this validated model to solve for walking gaits on a treadmill that has both belts moving at the same constant

speed. Walking over ground and walking on a tied-belt treadmill are mechanically and energetically similar, and only differ in the reference frames used to observe them (175). Therefore, this serves as another check on the model's validity. We calculate the mechanics and energetics for the two conditions and demonstrate their similarity. We then split the belt speeds and solve for the optimal gait. We hypothesize that an anthropomorphic model that minimizes a combined cost of the step-to-step transition and leg swing finds that the optimal step length asymmetry is positive and comparable to the adaptation observed in humans.

5.3. Dynamic walking model

We adapted the over ground anthropomorphic walker to walk on a treadmill while keeping the original parameters. Our walker exists only in the sagittal plane and consists of a point mass *m0* attached to the top of the stance leg with a weld joint that represents the torso and pelvis (Figure 5.1). The walker has two legs with distributed mass *I1, I2,* distributed mass *m1, m2*, and radius of gyration r_{gyr}. Each leg has a massless curved foot with radius *r*. The parameter values for these are kept constant and listed in Table 5.1. The walker also consists of a spring with a tunable stiffness *Khip* between the swing leg and the stance leg. All quantities are expressed in dimensionless units using total mass *M=m0+m1+m2*, leg length *L=l1=l2*, and time *t=sqrt(L/g)* where *g* is the constant for acceleration due to gravity.

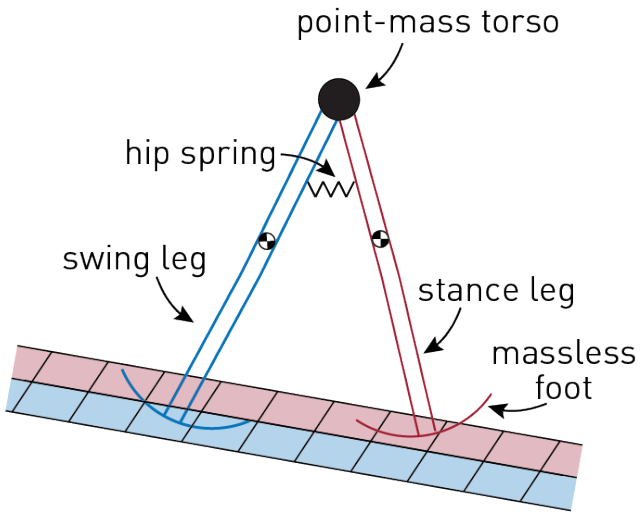

Figure 5.1: Anthropomorphic split-belt walker
The anthropomorphic split-belt walker uses a hip spring and impulsive push-off from the trailing leg to move on a treadmill whose belts may be stationary, moving at equal speeds or at different speeds.

Table 5.1:Fixed parameter values for the split belt walker

Fixed parameters	Values (non-dimensionalized)
m0	0.68
m1	0.16
m2	0.16
I1	1
I2	1
l_c	0.645
r_{gyr}	$\sqrt{\frac{1}{12}}$
r	0.3

We use projected Newton-Euler equations to derive the equations for the system. Only one leg can contact the treadmill at any given time, eliminating double support. The stance leg can apply a push-off impulse immediately before the foot of the swing leg contacts the treadmill. When the foot of the swing leg, that is now the leading leg, contacts the treadmill, the trailing leg has already broken contact. The leading leg is then constrained to move at the velocity of the treadmill belt it contacted. This may be zero (over ground), same for both belts (tied-belt) or different for each belt (split-belt). We calculate the collision impulse to satisfy this constraint and recalculate the equations of motion with the leading leg as the stance leg.

A gait cycle consists of two consecutive steps, known as a stride. We use ODE45 in MATLAB 2019a (Mathworks, NA,USA) to simulate a step using 8 initial conditions: horizontal and vertical positions of the end point of the stance leg, stance leg angle measured from the vertical, swing leg angle measured from the stance leg, linear velocity of the end point of the stance leg in the horizontal and vertical directions, angular velocity of the stance leg, and angular velocity of the swing leg. We used the optimization algorithm to find the initial stance leg angle and position, as described later in the chapter. The swing leg angle and angular velocity is determined by the stance leg position and angle. Rather than use event detection algorithms to determine the foot contact with the belt, we set step time to be the simulation time for the integration. We solve for the step time by enforcing non-linear constraints, which is described in the next paragraph. At the end of a step, we calculate the push-off and collision dynamics, re-set the stance leg to be the leading leg and the swing leg to be the trailing leg, and run ODE45 again to simulate the next step.

To be considered a successful stride, all simulations of a stride were subject to four non-linear constraints. The first constraint is to ensure a gait cycle—the angle and angular velocity of the stance and the swing legs at the end of a stride had to equal that at the beginning of the stride. The second constraint is dependent on the walking condition. When walking over ground—treadmill belt velocity set to zero—the average velocity of the point mass torso over a step had to match the desired walking speed. When walking on a treadmill, there was no constraint on the velocity of the point mass torso but the horizontal position of the foot of the leading leg at the end of the stride had to be the same as it was at the beginning of the stride. This ensured that the model remained at the same spot on the treadmill over a complete stride, which we refer to as station keeping. The third constraint was that the vertical position of the foot of the swing leg should be

zero—the feet should be on the ground—at the end of each step in the stride. This constraint serves the purpose of event detection by ensuring that the length of a simulation, which is our step time, is exactly until the foot of the leading leg contacts the ground. The fourth and final constraint is that the direction of the collision impulse should be positive—the ground cannot pull on the model. These constraints ensure that a gait cycle is representative of a human walking gait. However, multiple gaits can satisfy these constraints.

We search for the gait cycle that meets the above constraints and minimizes energetic cost. As described earlier, we are interested in the contribution of two costs to split-belt treadmill walking: step-to-step transition cost and swing cost. We estimate step-to-step transition cost as the rate of positive mechanical work done by the walker in a stride. We calculate positive work as the difference in the walker's total energy before and after push-off. We divide the work by step time to obtain positive work rate. For this calculation, we measure energy of the walker from the reference frame of the belt that is in contact with the foot. This may be stationary during over ground, moving at the same velocity for both steps during tied-belt, or moving at different velocities for each step during split-belt walking. To convert work to energetic cost, we multiply positive work rate by a factor of four which approximates metabolic power if muscles were operating at 25% efficiency (176). We calculate swing cost as the time rate of change of force generated by the spring in each step given as:

$$Swing\ cost = \frac{Khip \cdot peak\ swing\ angle}{t_{step}} \tag{5.2}$$

We multiplied this value with a constant *c* to obtain a metabolic power equivalent. We sum these values for the two steps in a stride and obtain an objective function for each stride. The final objective function minimized by the optimization is given as:

$$Cost = 4 \cdot Positive\ work\ rate + c \cdot Swing\ cost \tag{5.3}$$

We used MATLAB's fmincon function to solve for the optimal gait cycle that satisfied our constraints. We had 9 input parameters to the solver. The initial angle, horizontal and vertical position of the stance leg were used to find the initial conditions for the integration. The step times for the two steps in a stride served as the simulation time for each step. Finally, the push-off for each step and the spring stiffness for each step

were required to determine the kinematics of a step. This algorithm allowed us to set up all our constraints as non-linear and swap between optimizing an objective function or only solving for gaits that satisfied our constraints. The latter was useful to identify reasonable initial conditions for the optimizer, which is described later in the chapter. The details of the optimizer are provided in Table 5.2.

Table 5.2: Properties of the optimizer used with the split-belt treadmill walker

Optimizer properties	Values
Algorithms	sqp
Tolerance function	1e-9
Constraint tolerance	1e-8
Step tolerance	1e-10

We used data from literature to determine the weighting *c* on the rate of swing cost. Kuo 2001 determines that the relationship between walking speeds and preferred step lengths, that are also the energy optimal step lengths, is given by: step length = speed$^{0.42}$. We then searched through a range of values for *c* to determine which value, when our objective function is minimized, gives a gait that matches this speed-step length relationship, a process also used by Kuo to determine a similar weighting on swing cost for their Anthropomorphic model (Figure 5.2). We determined *c* to be 0.4326. This means that when walking at a given steady speed, the transition cost contributes about 10 times more than the swing cost to the total energetic cost of taking a step.

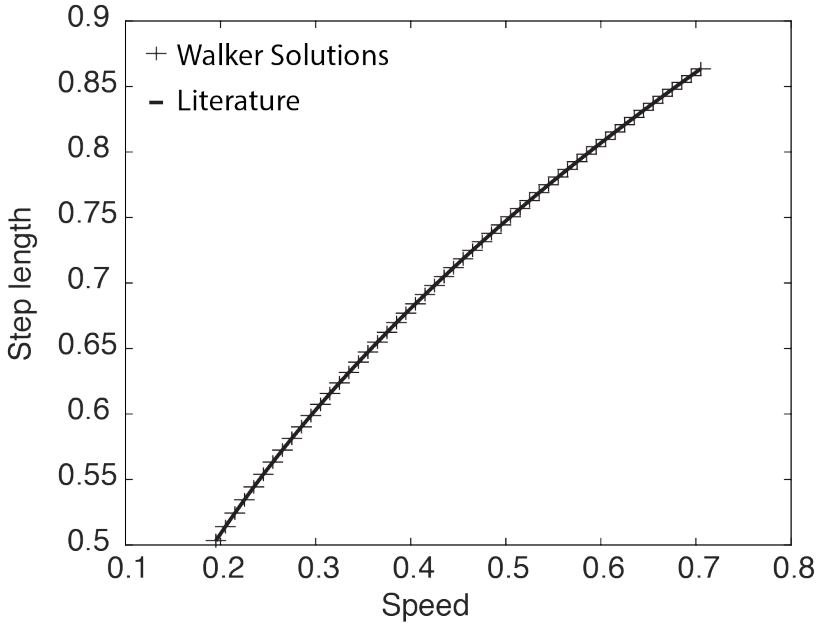

Figure 5.2: Speed - step length relationship for over ground walking
We allowed the split-belt walker to find the energy optimal gait over ground when walking at a range of speeds. Black cross hairs show the results found by the walker. Black line shows the empirical relationship from literature, which was also found by the over ground anthropomorphic walker developed in Kuo 2001.

We characterize a gait based on how a stride is powered, the step lengths, and energy required for the stride. A stride is powered from the push-off impulse and hip spring stiffness. Note that a spring is a conservative system and thus cannot do net work on the walker typically. However, since we allow the spring stiffness to change between steps here, the spring can do net work on the walker between the two steps. We report the push-off impulse and spring stiffness for each step. We also report step length, and step length asymmetry to compare with the step length asymmetry measures observed in participants. Symmetry is defined as a gait where the step lengths of two consecutive steps are equal, same as in humans. We measure Step Length Asymmetry as given in Equation 5.1. We report energetics to compare the energetics of walking on a tied-belt and split-belt treadmill.

5.4. Tied-belt walking

We validate the walker by comparing the over ground gait with the tied-belt treadmill gait. The energy optimal over ground walking gait is well established and should be equivalent to the energy optimal gait on a tied-belt treadmill. Therefore, we first verify that the addition of a treadmill belt produces accurate gait before splitting the belt speeds to study split-belt walking. To obtain initial conditions for the optimizer, we first solved for an over ground gait at each speed while constraining the step time to match the speed-step length relationship from Kuo 2001. This required no objective function since a gait is fully constrained for a step time at a given speed. Figure 5.3 shows the solutions that the walker discovered for each speed. We then used these solutions as initial conditions to optimize for tied-belt gaits.

We first compared the symmetric gaits in the over ground and treadmill conditions. The over ground walking gait for the anthropomorphic walker could only produce symmetric gait because it used a step as a gait cycle, rather than a stride as our walker here does. Therefore, we enforced symmetry in our walker. We constrained the step time, push-off impulse, and spring stiffness for the two steps within a stride be equal. Here, both belts moved backward at the same speed as the corresponding forward speed of the point mass in the over ground condition. We found that the symmetric tied-belt treadmill gaits are identical to the over ground gaits and consume the same energy (Figure 5.3). Similar to human walking, the increase in speed is due to an increase in step length and a decrease in step time. This is reflected in both push-off and spring stiffness increasing with increasing speed. Consequently, the cost also goes up steeply with walking speed. Note that this is cost per unit time, representative of metabolic power.

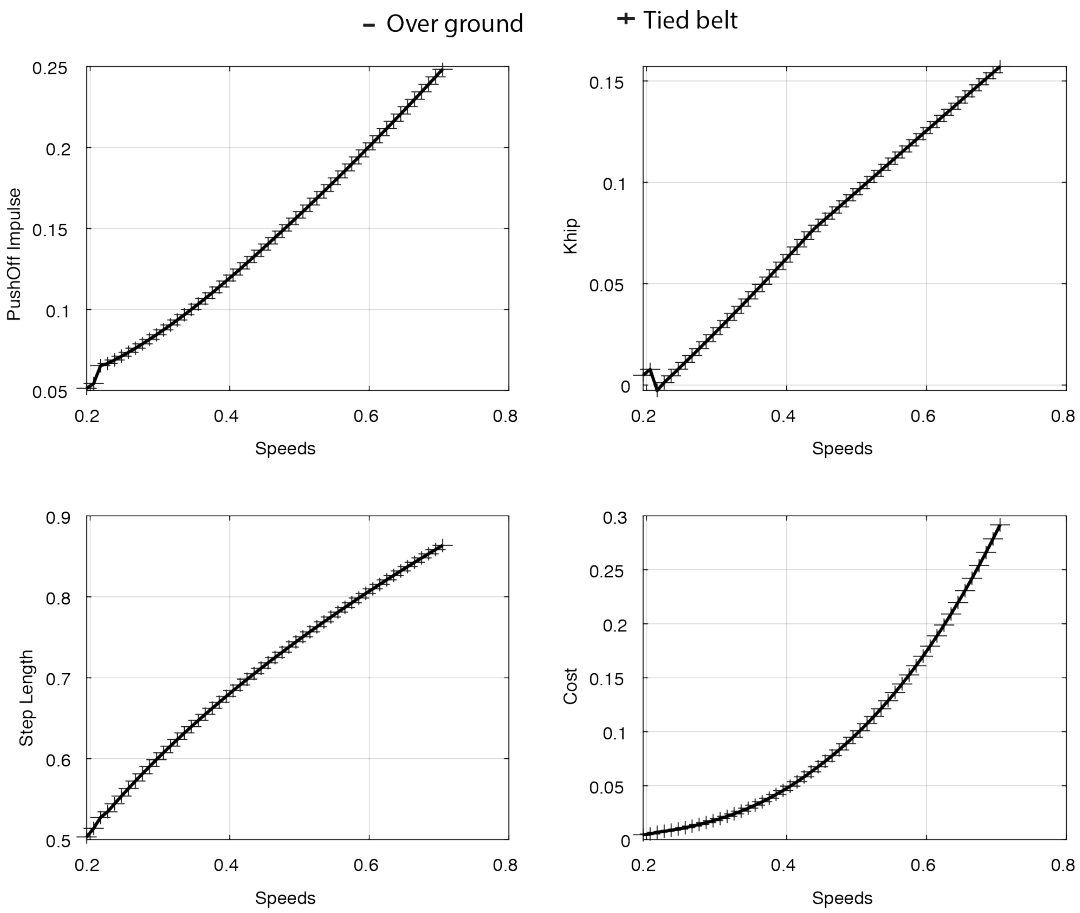

Figure 5.3: Gait parameters of symmetry-enforced energy optimal gait during over ground and tied-belt walking

The push-off (top left), spring stiffness (top right), step length (bottom left), and cost (bottom right) for the energy optimal gait when symmetry was enforced during tied-belt walking was identical to those of over ground walking at corresponding speeds.

We then removed the symmetry constraint to test whether symmetric gaits are energetically optimal. We allowed the step time, push-off impulse and spring stiffness for the two steps within a stride to be different. We started from the same initial conditions as we did when searching for symmetric gaits and searched for solutions. The solutions are nearly identical to the symmetric gait solutions (Figure 5.4). We suspect that the slight asymmetry found at some speeds is reflective of the optimizer's tolerances since the asymmetry leads to very slight variations in energetic cost.

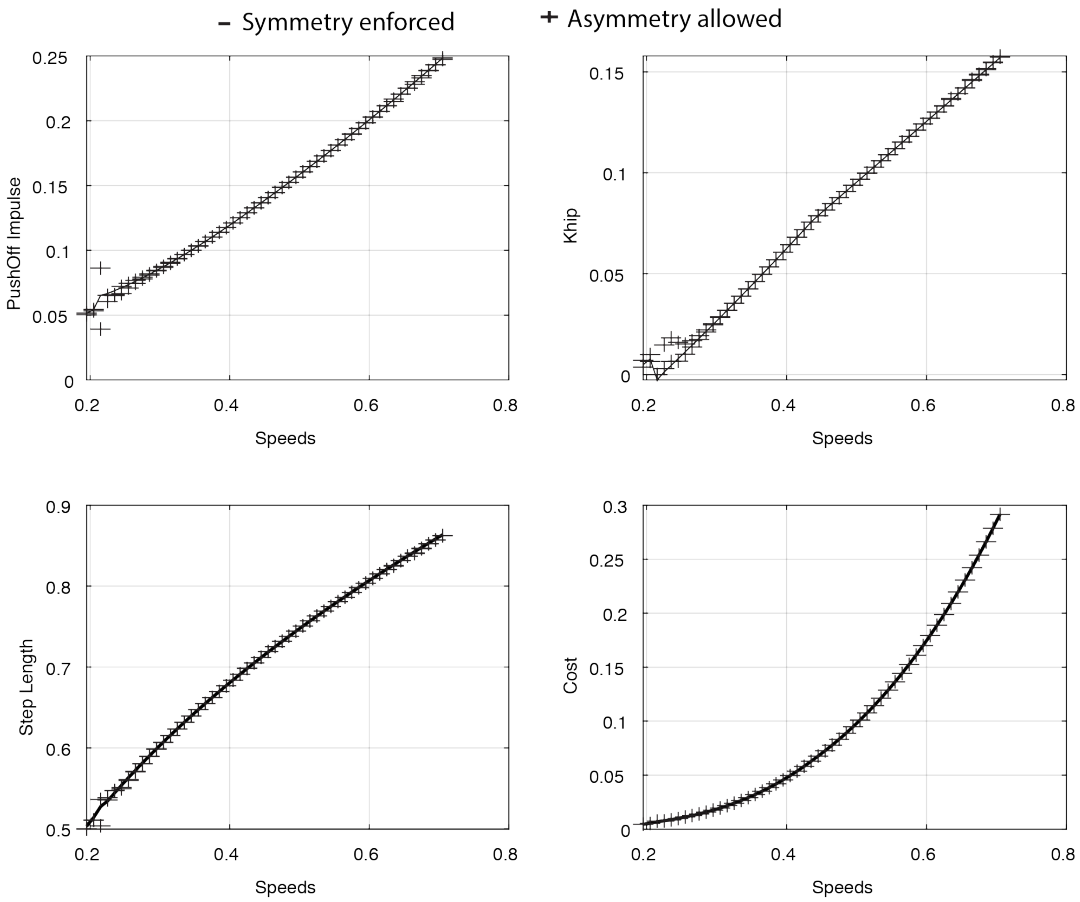

Figure 5.4: Gait parameters of energy optimal tied-belt walking when asymmetry is allowed

When allowed to choose asymmetrical gaits during tied belt walking, the walker found that the symmetrical gaits were energy optimal. The push-off (top left), spring stiffness (top right), step length (bottom left), and cost (bottom right) for the energy optimal gait when asymmetry was allowed during tied-belt walking was identical to those when asymmetry was not allowed.

5.5. Split-belt walking

We solved for the optimal split-belt walking gait. We selected a slow belt speed of 0.3 and initial conditions that matched the symmetric gait at that speed. We did not enforce symmetry—the solver was free to choose a different push-off force and hip spring stiffness for each step within the stride. We increased the belt speed difference by 0.01 up to 0.4. Note that the slow belt speed was always 0.3 and the fast belt speed increased to provide

the increased belt speed difference. We used the solution to one belt speed difference as the initial condition for the next.

The optimal split-belt walking gait was one with a small positive step length asymmetry (Figure 5.5). As the belt speed difference increased, the required asymmetry became more positive. In our previous study, we measured that the average metabolic optimum of our participants had a 95% confidence interval of 0.06 and 0.38 (84). They were walking with a non-dimensional belt speed difference of 0.32. Our walker here predicts an energy optimal step length asymmetry for that belt speed difference to be 0.2, supporting our observations from participants.

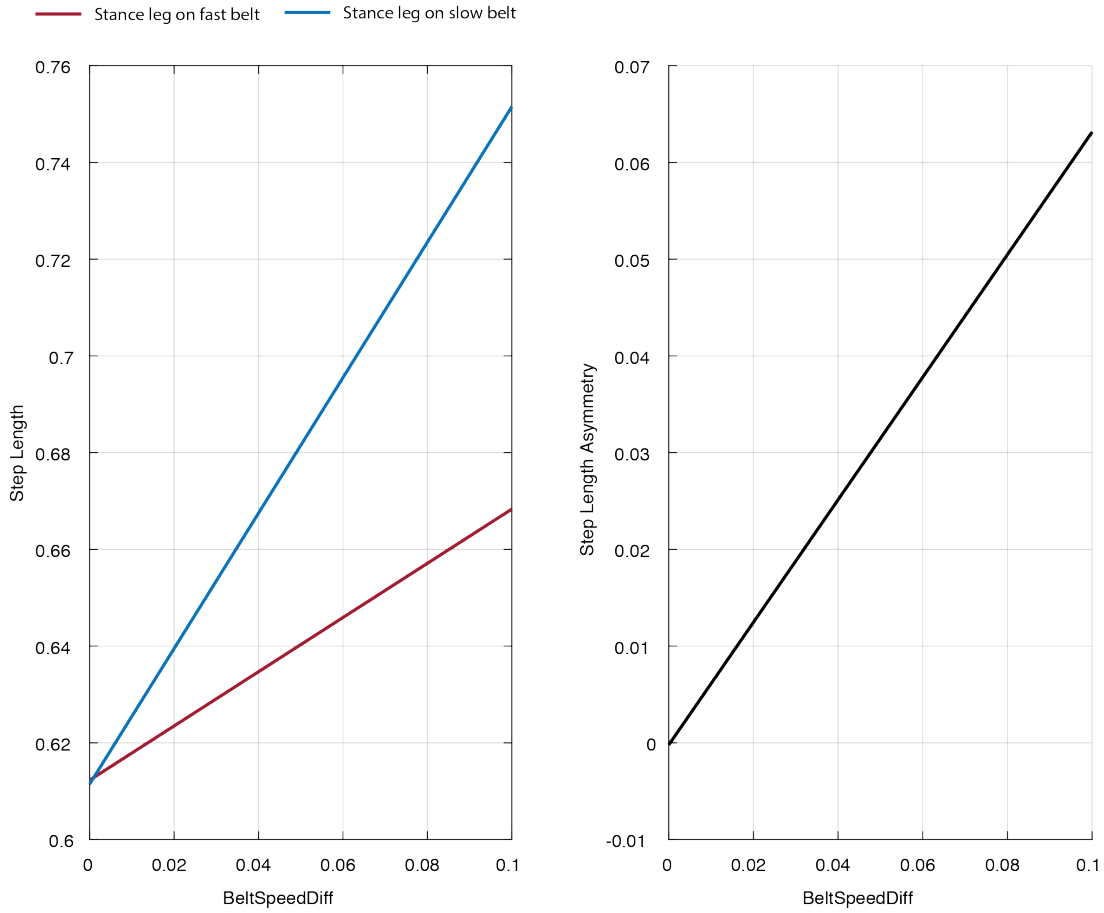

Figure 5.5: Effect of belt speed difference on step length and Step Length Asymmetry
As the belt speed difference increases, the walker takes longer steps when the stance leg is on the slow belt leading (shown right) leading to more positive step length asymmetries (shown right).

The gait is symmetrically powered at the tied-belt speed and the asymmetry steadily increases with increase in belt speed difference (Figure 5.6). The push-off impulse by both feet go up with increasing belt speed difference but the push-off impulse on the fast leg increases more slowly. This is consistent with our hypothesis. As the fast belt speed increases, as it does with increase in belt speed difference, push-off on the fast belt leads to a larger power and hence larger mechanical work by the leg. Therefore, it is beneficial to reduce push-off on the fast belt. We also find that with increasing belt speed difference, the spring stiffness goes down when the stance leg is on the slow belt allowing the swing leg to reach further forward on to the fast belt to harness energy.

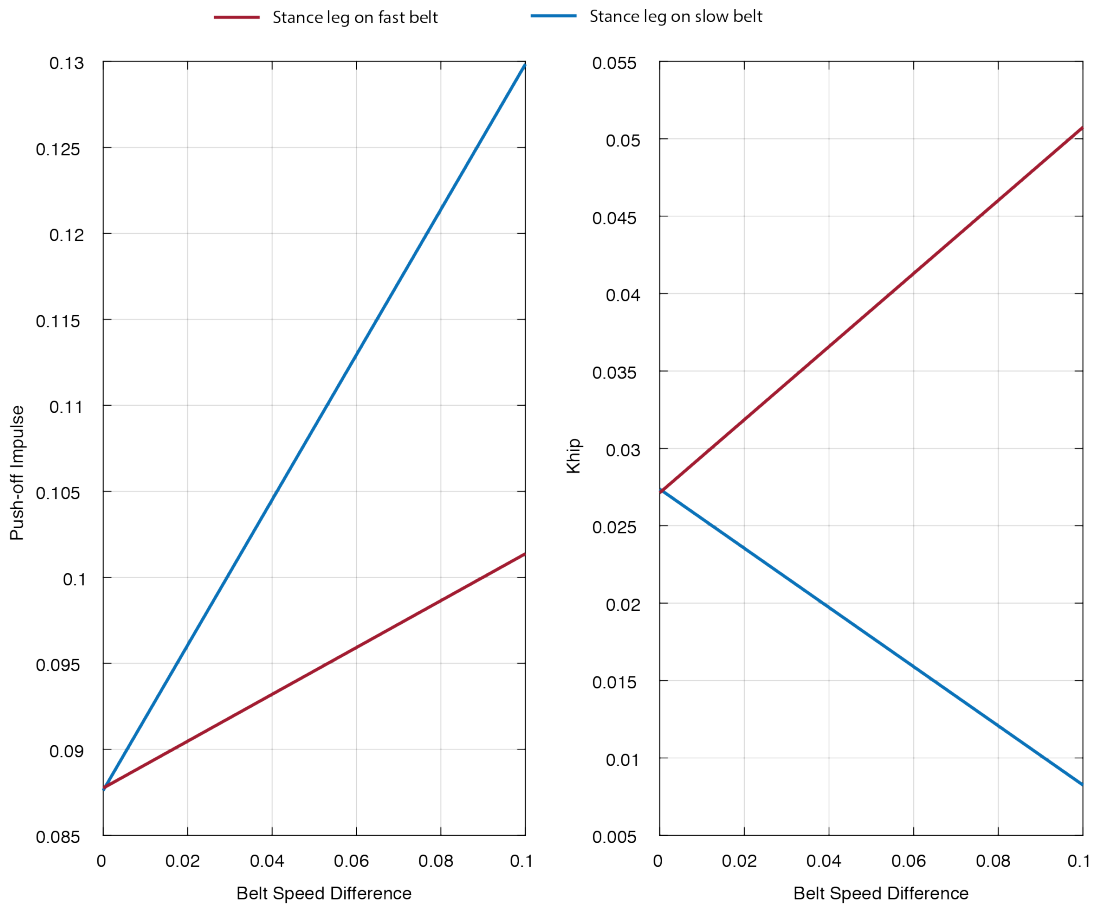

Figure 5.6: Effect of belt speed difference on push-off impulse and spring stiffness With increase in belt speed difference, the walker pushes off less on the fast belt (right, red) allowing it to perform less push-off work. The walker simultaneously reduces the spring stiffness when the stance leg is on the slow belt (right, blue) allowing it to place the swing leg further forward on the fast belt and harness more energy.

The cost of the optimal gait increased with increasing belt speed difference (Figure 5.7). Since the belt speed difference of zero is a condition where the belts are tied-at the slow belt speed, this means that walking on a split belt treadmill is always more expensive than walking on a treadmill tied at the slow belt speed. However, the cost at every belt speed difference was less than the cost of walking if both belts were tied at the corresponding fast belt speed. These results are consistent with experimental observations.

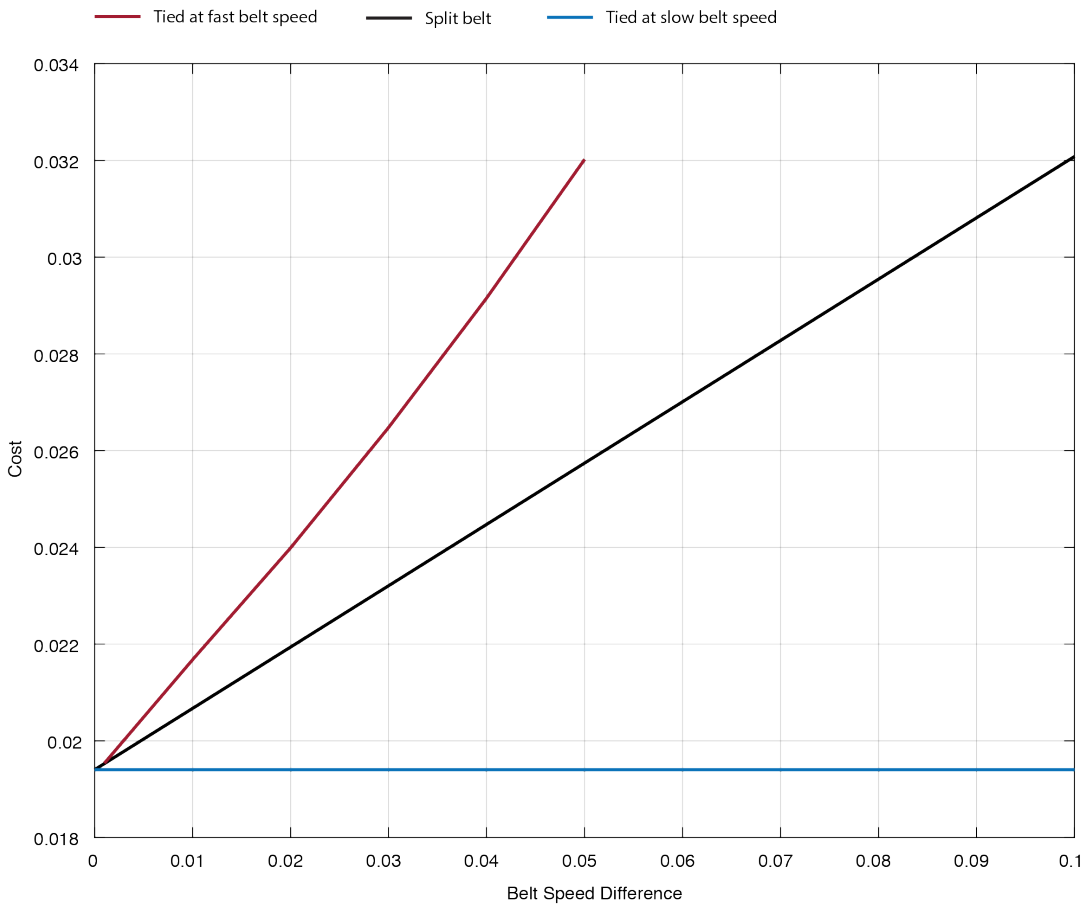

Figure 5.7: Effect of belt speed difference on walking cost
The cost of walking on a split-belt treadmill (black) is always higher that the cost of walking at only the slow belt speed (blue) but lower than the cost of walking only at the fast belt speed (red).

5.6. Discussion

We developed a computer model of an anthropomorphic walker on a split-belt treadmill. It consists of a point-mass torso, two legs with distributed mass, and a curved massless foot at the end of each leg. It is powered by an impulsive push-off by the trailing leg and can vary its hip spring stiffness between two consecutive steps. These sources of power contribute to the energetic cost of walking as transition cost and swing cost, similar to over ground walking. The walker searched for gaits that minimized an objective function that was a weighted sum of the transition cost and swing cost. In agreement with empirical data and literature, the walker found that symmetrical gaits are the cheapest when walking on a treadmill where both belts are moving at the same speed. However, when the belt speeds were split such that one belt was faster than the other, the walker found that the optimal way to walk was to take a slightly longer step on the fast belt. This is a gait with a slightly positive step length asymmetry which is consistent with our observations from a previous study where we measured the metabolic power of walking at different step length asymmetries in participants (84). This step length asymmetry is obtained by both changing the push-off impulses to reduce work by the walker and changing the spring stiffness to increase work by the treadmill on the walker. The optimality is predicted by a trade-off between transition cost and swing cost, similar to over ground walking. Due to this trade-off the cost of walking on a split-belt treadmill is always higher than the cost of walking on a treadmill that is tied at the slow belt speed.

The anthropomorphic split-belt walker can only make broad predictions about the energy optimal gait. Two features particularly could improve the applicability of our modelling results to human split-belt adaptation. Unlike humans, our model does not have a double support period. A double support period allows for the push-off to be spread out and therefore affects the push-off impulse required before heel-strike. This may have implications for the metabolic energetic cost (168,171). Such implications could be exaggerated in split-belt treadmill walking since work by the push-off force can be divided between two belts that have different velocities. This extra level of control may allow a walking person to find cheaper gaits for the same step length asymmetry. Second, the addition of a torso in over ground walking models has little effect on the overall gait. However, in split-belt walking larger step length asymmetries can lead to larger asymmetries in the lateral forces, causing the body to experience a torque about the

vertical axis. A torso may aid in countering this torque and the resulting metabolic cost may act as another trade-off in our objective function.

The minimization of sensorimotor prediction error observed in split-belt walking studies may be a result of an energy optimization process. The hypothesis of sensory prediction error fits within the framework of an optimization process, as observed in upper limb adaptation experiments (40). Our walker here has no prediction of a normal walking gait in any of the conditions. However, when placed in a split-belt condition, it selects a step length asymmetry that is close to zero. Combined with recent results from our group that participants can overshoot symmetry with more experience walking on a split-belt treadmill, this suggests that the observed preferences to step length symmetry may be the result of a slow or incomplete energy optimization process. A recent study by Carly et al. found that people trade-off minimizing step length asymmetry when the push-off required to maintain a steady gait is altered using inclines and declines (177). This finding is consistent with the results of our walker and suggests that the energy optimization process may be speeded up by increasing the energetic penalty for not optimizing. The trade-off between transition cost and swing cost identified here can also inform our understanding of experimental results in split-belt walking. Adaptations to split-belt treadmill walking exhibit a differential learning for spatial and temporal parameters (164). Transition cost and swing cost contribute differentially to how far one can step and how quickly one can step (168,174). Extensions of our split-belt dynamic walker presented here can help us understand the cause of such differences. Our results here add support to the growing argument that the observed minimization of prediction error of step lengths, and other kinematic adaptations to walking on a split-belt treadmill may be a part of an energy minimization process by the nervous system.

Chapter 6.

Discussion

6.1. Summary

In this thesis, I used two distinct walking tasks to understand the principles of energy optimization underlying human walking gait adaptations. I built a mechatronic system that can manipulate the metabolic energetic cost associated with different walking gaits from -50% to over +250% relative to the user's normal cost of walking. Participants adapt their gait toward new energetic optima when walking in this system. I used this system to study adaptation to cost landscapes of varying steepness. I found that a steeper cost gradient in a novel situation is not sufficient for the nervous system to initiate adaptation. I also probed the role of metabolic energetic cost in split-belt gait adaptation. I showed through analysis of experimental data that the gait participants adapt to is characterized by a lower energetic cost because it allows participants to harness energy from the belt speed difference. I then used computer modelling to demonstrate that transition cost and swing cost trade-off in split-belt walking to give rise to the energy optimal walking gait.

To understand how the nervous system adapts movement, we need to understand what objective, algorithms, and physical machinery drive the adaptation. In this thesis, I show that metabolic energetic cost serves as a significant objective in novel walking situations where it was not previously known to play a significant role. I then identify previously unknown principles governing the algorithms of energy optimization in these situations. In two separate walking tasks, participants and a computer model adapted their preferred walking gait to one that reduced energetic cost. I designed the first task to selectively manipulate the energetic cost associated with different walking gaits and found that participants adapted their gait to reduce their energetic cost of walking. In the second task, I evaluated the energetic cost associated with different walking gaits in the well-established task of split-belt walking to show that participants adapt their gait to reduce their energetic cost of walking. In both these tasks, I identified significant principles of the energy optimization process. With the mechatronic system, I showed that in tasks where initiation of adaptation is not spontaneous, only increasing the cost gradient is insufficient

to initiate the adaptation process. On the other hand, in split-belt walking, participants always spontaneously initiate adaptation on exposure to a split-belt treadmill, do not adapt to the minimum in traditional experiments but can do so with more experience walking on the split-belt treadmill. Therefore, it is unclear how different features of a novel situation drive energy optimization. Towards understanding this process, I identified that two costs—transition cost and swing cost—primarily contribute to the energy minimal split-belt walking gait.

6.2. General implications

While the focus of in this thesis has been on energy optimization in walking, the results are broadly applicable. The mechatronic force control system can apply accurate and precise forces quickly. These forces may be constant or applied as a function of walking gait. Both these methods are being tested and used in improving mobility of patients (86,87,178). Small modifications to the system can allow the forces to be targeted to different regions of the body where such assistance may be required (87). The system can also be used to apply forces as a function of a different movement parameters, though modifications to sensors maybe necessary for detecting movement other than gait. Finally, the mechatronic system can also act to perturb movement. The control system affords easy access to changing proportional-integral-derivate gains. Thus, the system can quickly change from perturbing to rewarding, allowing researchers to study their trade-offs when learning to move in novel situations.

Identifying features of a novel situation that allow spontaneous initiation of adaptation is relevant across motor tasks and objectives. Our nervous systems do not always initiate adaptation in novel situations. This is observed in a range of tasks such as walking with exoskeletons, split-belt treadmill walking with gradually changing speeds, and adaptations to force-fields and visuomotor rotations with interference (9,12,117–119,121). However, some changes to the same tasks allow the nervous system to initiate adaptation (9,24,74,75,120). This is a phenomenon observed beyond a laboratory setting, though harder to discern. A famous example is the Fosbury Flop where it was not evident that an improvement to the human high jump technique was possible, but when certain environmental changes made it evident, people quickly adapted their technique (179). The

hypothesis I tested was the role of cost gradient in initiating adaptation. In tasks where adaptation is initiated, a larger movement variability has been associated with faster learning (131). Variability is typically thought to be used by the nervous system to learn about the cost landscape and the cost gradient. A recent study directly tested this by providing participants with reward feedback that had different probabilities, in a reaching task, and found that steeper gradients led to faster learning (180). Thus, we have evidence across tasks that the cost gradient is used in adaptation but is insufficient to initiate adaptation.

Principles of adaptation identified using split-belt walking have been successful in informing us about general motor adaptation. Split-belt treadmill walking has uncovered principles underlying the effect of conscious learning, effect of the interaction between information about the body and the environment, generalization of walking gait adaptations from treadmill to over ground, and the neural mechanisms of motor adaptation (73,74,121). These adaptations are generally thought to be the result of a minimization of a sensorimotor prediction error. This is supported by findings that damage to the cerebellum disrupts split-belt adaptation while damage to the other brain regions do not have a similar effect (73). In this thesis, I demonstrate that the split-belt walking gait is characterized by a reduction in metabolic energetic cost and identify a particular mechanism that participants can adopt to acquire energy from the treadmill belt speed difference. Participants can further use different strategies to use this energy and reduce their energetic cost of walking. I present evidence that participants also use such strategies and consequently reduce their energetic cost of split-belt treadmill walking—a result that corroborates observations in previous literature (47,85,181). My computer model supports the existence of an energy optimal gait similar to what participants find after sufficient experience with walking on the treadmill, by trading off energetic costs associated with swing and push-off. This gait is different from that traditionally observed in split-belt walking and that which has informed the previously mentioned impacts to general motor adaptation. Importantly, these results of energy minimization do not negate existing understanding of split-belt gait adaptations but rather place them in a larger, more unifying framework for understanding the different aspects of the adaptation.

6.3. Future Directions

The results presented here definitely provide more questions than answers, as is the result of any scientific endeavour. This is highlighted by negative and positive results alike in this thesis. Both the evidence against the role of cost gradient in the initiation of adaptation and the evidence for energy minimization in split-belt walking open the floor for further research.

The mechatronic force control system can be used to probe how metabolic energy affects human walking. The system is presently designed to apply forces to the user's hip less than 120ms after toe-off. This limits the control available to the nervous system to manipulate its gait for the next step at which point, the force, and thus energetic cost, is manipulated again. We do not think this is a serious limitation for the projects presented here because the nervous system still has control over a step and through the duration of the experiments to adapt, and we do observe such an adaptation. Importantly, we were only interested in the high-level adaptation of step frequency to probe the process of energy optimization. However, localized forces to the feet, hip and legs have been shown to result in kinematic adaptations that differ at pre-swing and during swing (71,72). Understanding the effects of modulating when the force is applied in our system is an avenue worth investigating. Another aspect of the system design that can be examined is how quickly forces are applied as a function of gait. Physiological sensors that can rapidly detect energetic cost would benefit from rapid energetic cost changes to determine how to adapt and may find it difficult to attribute an energetic cost change to a gait parameter if the changes are slow or averaged over many steps. On the other hand, slower sensors may filter out rapid changes in energetic cost and find it harder to adapt to them. The mechatronic force control system can apply a force that changes step-to-step, is averaged across two or more steps, or is constant throughout. Experiments designed around this may shed light on the mechanism used by the nervous system to sense and process energetic cost during energy optimization of walking gait.

The fundamental concept behind identifying cues used by the nervous system in the initiation of energy optimization is salient cost savings. The associated hypothesis is that the nervous system will initiate adaptation when it 1) senses that changing its movement can be beneficial, and 2) senses how it needs to change its movement to gain that benefit. Therefore, the lack of initiation of adaptation to steeper cost gradients can

mean two things: salient cost savings do not cue the nervous system to initiate adaptation in novel situations or the nervous system was unable to sense salient cost savings using the cost gradient. In the framework of optimization, the role of variability in adapting to novel motor tasks strongly suggest that the nervous system may use salient cost savings (16,46). A potential finding counter to this hypothesis may be that the nervous system does not adapt towards a salient cost saving if the nervous system's previous experience suggests that the required adaptation is "too risky" (99,182). A study that can directly differentiate between the detection and use of such saliency would be quite beneficial to the field. One application of this would be in understanding whether the movement preferences of older adults is due to the inability of their nervous systems to detect salient cost savings or because equally salient cost savings are weighted less.

An inability of the nervous system to sense salient cost savings using the cost gradient suggests two possibilities. First is that the nervous system was unable to sense that cost savings were available at all. Second is that the nervous system was unable to sense how to adapt to obtain the cost savings. Both these hypotheses are described in Section 3.5. With regards to the first hypothesis, whether the nervous system is able to sense the energetic cost savings provided by the force changes depends on the nervous system's mechanism of sensing energetic cost. Identifying the physiological sensors involved in sensing metabolic energetic cost would be a valuable discovery here. In the meantime, experiments aimed to determine the time required by the nervous system to sense a metabolic energetic cost change during a motor task would be valuable. Regarding the second hypothesis, I manipulated energetic cost as a function of only one gait parameter in the experiments presented in this thesis. Perhaps, an even more targeted manipulation such as manipulating energetic cost at the level of joint angles might aid in understanding how the nervous system senses how to adapt. An area where this could be tested would be in the use of exoskeletons—they can modulate control and provide context to the nervous system at the level of joints, while still manipulating energetic cost as a function of a high-level gait parameter. Even as more exoskeletons are being designed and manufactured, the mechanisms of human interaction with the devices is poorly understood. Identifying key principles of energy optimization during walking using exoskeletons can advance both fundamental and applied science.

Understanding human motor adaptation is incomplete without understanding the environment of the adaptation. A split-belt treadmill where the belts are moving at different

speeds does not only place different velocity constraints on the feet but can also transfer energy to the walking person. Therefore, identifying mechanisms of harnessing this energy from the split-belt treadmill is beneficial to understanding split-belt gait adaptations. One approach to this is to understand observed adaptations in the context of this available energy. Another approach is to identify how best to harness this energy from the split-belt treadmill during walking. This latter approach is similar to learning how to use assistive devices and has several potential benefits. In chapter 4, we identify one mechanism to harness energy, that is to place the leading leg further ahead on the fast belt. Using such a gait, participants may theoretically be able to reduce 1 J of positive work they need to perform during walking for every 1.5 J of energy provided by the treadmill, when the two belt speeds are 1.5 ms^{-1} and 0.5 ms^{-1}. There are likely many limitations to achieving this level of benefit in practice, one of which is addressed in Chapter 5. It may be valuable to identify such limitations and subsequently, strategies to overcome some of them.

Energy optimization may be an objective in split-belt gait adaptations. Step-to-step transition cost and swing cost can explain energy-optimal and preferred gaits in steady-state over ground walking (168). Their ability to also explain walking in a novel situation suggests that energy optimization may affect split-belt walking gait adaptations. The dynamic walking model presented in this thesis can perhaps be modified to include knees, a torso, and a double support period which may provide more realistic predictions of human behaviour. The model can be used to identify how these energetic costs contribute to split-belt walking gaits under different constraints such as belt speed differences, fixed foot placement, and fixed stance time (81). The dynamic walking model can only predict preferences, and not the adaptation process. An insightful next step for the model would be to embed it within a learning model—perhaps based on reinforcement learning—to identify mechanisms of the energy optimization process in split-belt gait adaptations. Finally, split-belt walking models and experiments can serve as a paradigm to study the earlier mentioned principles of sensing metabolic energetic cost, cost saliency, and the initiation of energy optimization in walking.

6.4. Conclusion

The work in this thesis advances our knowledge of how we learn to walk in changing situations. I show that our walking gait is strongly affected by energy minimization using two different novel tasks. I develop a new system and a new approach to understand principles of energy optimization during walking gait adaptations. With the new system, I show that a steeper cost gradient may not be a sufficient cue for the nervous system to initiate optimization. With the new approach, I show that we should consider the split-belt treadmill's ability to provide energy to walking users, which may explain the gait adaptations as an optimization of energetic cost. Both the force control system and the approach for identifying how one can harness energy from a split-belt treadmill, are applicable to studies beyond this thesis. At an applied level, understanding adaptation to the force control system and to a split-belt treadmill, and the systems themselves, can be useful in rehabilitation programs and gait training.

References

1. Kandel ER, Schwartz JH, Jessell TM, Siegelbaum S, Hudspeth AJ. Principles of neural science. Vol. 4. McGraw-hill New York; 2000.

2. McMahon TA. Muscles, reflexes, and locomotion. Princeton University Press; 1984.

3. Huxley H, Hanson J. Changes in the cross-striations of muscle during contraction and stretch and their structural interpretation. Nature. 1954 May;173(4412):973–6.

4. McGeer T. Passive Dynamic Walking. The international journal of robotics research. 1990;9(2):62–82.

5. Brown IE, Loeb GE. A reductionist approach to creating and using neuromusculoskeletal models. InBiomechanics and neural control of posture and movement. New York, NY.: Springer; 2000. 48–163 p.

6. Sherrington CS. On the proprio-ceptive system, especially in its reflex aspect. Brain. 1907;29(4):467–82.

7. Sherrington CS. Flexion-relex of the limb, crossed extension-reflex, and reflex stepping and standing. The Journal of physiology. 1910; 40(1-2),28.

8. Shadmehr R, Krakauer JW. A computational neuroanatomy for motor control. Experimental brain research. 2008;185:359–381.

9. Krakauer JW, Hadjiosif AM, Xu J, Wong AL, Haith AM. Motor Learning. Comprehensive Physiology. 2019 Apr;9:613–63.

10. Adrian MH, John WK. Theoretical models of motor control and motor learning. In: Routledge Handbook of Motor Control and Motor Learning [Internet]. Routledge; 2012. Available from: https://www.taylorfrancis.com/books/9780203132746

11. Davidson PR, Wolpert DM. Motor learning and prediction in a variable environment. Current Opinion in neurobiology. 2003;13:1–6.

12. Wolpert DM, Diedrichsen J, Randall Flanagan J. Principles of sensorimotor learning. Nature Reviews Neuroscience. 2011;12:739–751.

13. Krakauer JW, Pine ZM, Ghilardi M-F, Ghez C. Learning of visuomotor transformations for vectorial planning of reaching trajectories. Journal of Neuroscience. 2000;20:8916–8924.

14. Shadmehr R, Mussa-Lvaldi FA. Adaptive representation of dynamics during learning of a motor task. Journal of Neuroscience [Internet]. 1994;74(5). Available from: http://www.jneurosci.org/content/jneuro/14/5/3208.full.pdf

15. Emken JL, Benitez R, Sideris A, Bobrow JE, Reinkensmeyer DJ. Motor adaptation as a greedy optimization of error and effort. Journal of neurophysiology. 2007;97(6):3997–4006.

16. Wu HG, Miyamoto YR, Gonzalez Castro LN, Olveczky BP, Smith MA. Temporal structure of motor variability is dynamically regulated and predicts motor learning ability. Nature neuroscience. 2014;17(2):312.

17. Diedrichsen J, White O, Newman D, Lally N. Use-dependent and error-based learning of motor behaviors. Journal of Neuroscience. 2010;30(15):5159–5166.

18. Izawa J, Rane T, Donchin O, Shadmehr R. Motor adaptation as a process of reoptimization. Journal of Neuroscience. 2008;28(11):2883–91.

19. Izawa J, Shadmehr R. Learning from sensory and reward prediction errors during motor adaptation. PLoS Comput Biol [Internet]. 2011;7(3). Available from: http://e.guigon.free.fr/data/masterMSR/IzawaShadmehr11.pdf

20. Todorov E. Optimality principles in sensorimotor control. Nature neuroscience. 2004;7(9):907–15.

21. Maynard Smith J. Optimization theory in evolution. Annual review of ecology and systematics. 1978;9(May):31–56.

22. Alexander RM. Optima for animals. Princeton University Press; 1996.

23. FitzHugh R. A model of optimal voluntary muscular control. Journal of mathematical biology. 1977;4(3):203–36.

24. Wolpert DM, Flanagan JR. Computations underlying sensorimotor learning. Current opinion in neurobiology. 2016 Apr;37:7–11.

25. Franklin DW, Wolpert DM. Computational mechanisms of sensorimotor control. Neuron. 2011; 72(3):425–442.

26. Sutton RS, Barto AG, Williams RJ. Reinforcement learning is direct adaptive optimal control. IEEE Control Systems Magazine. 1992; 12(2):19-22. Available from: https://pdfs.semanticscholar.org/6bf0/853b3c385b8ef10a8ae2365ef435c979ec47.pdf

27. Franklin DW, Burdet E, Tee KP, Osu R, Chew C-M, Milner TE & Kawato M. CNS learns stable, accurate, and efficient movements using a simple algorithm. Journal of neuroscience. 2008;28(44):11165–11173.

28. Sutton RS, Barto AG. Reinforcement learning: An introduction [Internet]. 2012. Available from: https://pdfs.semanticscholar.org/83c8/b4938ce24eb84f8388faa36810c5432dfa2e.pdf

29. Haith AM, Krakauer JW. Model-based and model-free mechanisms of human motor learning. InProgress in motor control. 2013. p. 1–21. Springer, New York, NY. Available from: http://link.springer.com/10.1007/978-1-4614-5465-6_1

30. Martin TA, Keating JG, Goodkin HP, Bastian AJ, Thach WT. Throwing while looking through prisms I. Focal olivocerebellar lesions impair adaptation. Brain. 1996;119:1183–1198.

31. Criscimagna-Hemminger SE, Bastian AJ, Shadmehr R. Size of error affects cerebellar contributions to motor learning. Journal of neurophysiology. 2010 Apr;103(4):2275–84.

32. Morton SM, Bastian AJ. Cerebellar contributions to locomotor adaptations during splitbelt treadmill walking. Journal of Neuroscience. 2006;26(36):9107–9116.

33. Schlerf J, Ivry RB, Diedrichsen J. Encoding of sensory prediction errors in the human cerebellum. Journal of Neuroscience. 2012 Apr 4;32(14):4913–22.

34. Seidler RD, Kwak Y, Fling BW, Bernard JA. Neurocognitive mechanisms of error-based motor learning. InProgress in Motor Control. 2013. p. 39–60. Springer New York, NY; Available from: http://link.springer.com/10.1007/978-1-4614-5465-6_3

35. Krakauer JW, Mazzoni P. Human sensorimotor learning: adaptation, skill, and beyond. Current opinion in neurobiology. 2011;21(4):636-44.

36. Thorndike E. Animal intelligence : Experimental studies. Transaction Publishers; 1970

37. Schultz W. Neuronal reward and decision signals: from theories to data. Physiological reviews. 2015;95(3):853–951.

38. Sutton RS, Barto AG. Reinforcement learning: An introduction. 2017. Available from: http://incompleteideas.net/book/bookdraft2017nov5.pdf

39. Gutierrez-Garralda JM, Moreno-Briseño P, Boll M-C, Morgado-Valle C, Campos-Romo A, Diaz R, et al. The effect of Parkinson's disease and Huntington's disease on human visuomotor learning. European journal of neuroscience. 2013;38(6):2933–40.

40. Izawa J, Rane T, Donchin O, Shadmehr R. Motor adaptation as a process of reoptimization. Journal of Neuroscience. 2008 Mar 12;28(11):2883–91.

41. Domínguez-Zamora FJ, Gunn SM, Marigold DS. Adaptive gaze strategies to reduce environmental uncertainty during a sequential visuomotor behaviour. Scientific Reports. 2018 Dec;8(1):1-13.

42. McNeill Alexander R. Energetics and optimization of human walking and running: the 2000 Raymond Pearl memorial lecture. American journal of human biology. 2002;14(5):641–648.

43. Sparrow WA, Newell KM. Metabolic energy expenditure and the regulation of movement economy. Psychonomic Bulletin & Review. 1998;5(2):173–196.

44. Huang HJ, Kram R, Ahmed AA. Reduction of metabolic cost during motor learning of arm reaching dynamics. Journal of Neuroscience. 2012;32(6):2182–90.

45. Selinger JC, Wong JD, Simha SN, Donelan JM. How humans initiate energy optimization and converge on their optimal gaits. Journal of Experimental Biology. 2019; 222(19), jeb198234

46. Herzfeld DJ, Shadmehr R. Motor variability is not noise, but grist for the learning mill. nature neuroscience. 2014;17(2):149.

47. Finley JM, Bastian AJ, Gottschall JS. Learning to be economical: the energy cost of walking tracks motor adaptation. The Journal of physiology. 2013 Feb;591(4):1081–1095.

48. Shadmehr R, Huang HJ, Ahmed AA. A representation of effort in decision-making and motor control. Current biology. 2016;26:1929–1934.

49. Whipp BJ, Ward SA. Determinants and control of breathing during muscular exercise. British journal of sports medicine. 1998 Sep 1;32(3):199.

50. Davis JA, Whipp BJ, Wasserman K. The relation of ventilation to metabolic rate during moderate exercise in man. European Journal of Applied Physiology and Occupational Physiology. 1980 Aug;44(2):97–108.

51. Miller MJ, Tenney SM. Hypoxia-induced tachypnea in carotid-deafferented cats. Respiration physiology. 1975;23(1):31–9.

52. Heymans JF, Heymans C. Sur les modifications directes et sur la régulation réflexe de l'activité du centre respiratoire de la tête isolée du chien. Arch Int Pharmacodyn Ther. 1927;33:273–372.

53. Wong JD, O 'connor SM, Selinger JC, Donelan JM. Contribution of blood oxygen and carbon dioxide sensing to the energetic optimization of human walking. Journal of Neurophysiology. 2017;118:1425–1433.

54. Amann M, Blain GM, Proctor LT, Sebranek JJ, Pegelow DF, Dempsey JA. Implications of group III and IV muscle afferents for high-intensity endurance exercise performance in humans. The Journal of physiology. 2011;589(21):5299–309.

55. Coote JH, Hilton SM, Perez-Gonzalez JF. The reflex nature of the pressor response to muscular exercise. The Journal of physiology. 1971;215(3):789–804.

56. Pearson KG. Proprioceptive regulation of locomotion. Current opinion in neurobiology. 1995;5(6):786–91.

57. Dean JC. Proprioceptive Feedback and Preferred Patterns of Human Movement. Exercise and sport sciences reviews. 2013 Jan;41(1):36. Available from: https://www.ncbi.nlm.nih.gov/pmc/articles/PMC5997460/pdf/nihms972700.pdf

58. Wise RA. Brain reward circuitry: insights from unsensed incentives. Neuron. 2002;36(2):229–40.

59. Wong JD, Maxwell Donelan J. Principles of Energetics and Stability in Legged Locomotion. In: Humanoid Robotics: A Reference. Dordrecht: Springer Netherlands; 2017. p. 1–28. Available from: http://link.springer.com/10.1007/978-94-007-7194-9_67-1

60. Donelan JM, Kram R, Kuo AD. Mechanical and metabolic determinants of the preferred step width in human walking. Proceedings of the Royal Society of London. Series B: Biological Sciences. 2001 Oct 7;268(1480):1985-92. Available from: https://www.ncbi.nlm.nih.gov/pmc/articles/PMC1088839/pdf/PB011985.pdf

61. Waters RL, Mulroy S. The energy expenditure of normal and pathologic gait. Gait and Posture. 1999;9:207–231.

62. Molen NH, Rozendal R.H. Energy expenditure in normal test subjects walking on a motor driven treadmill. Proceedings of the Koninklijke Nederlandse Akademie van Wetenschappen Series C Biological and medical sciences. 1967;70(2):192–200.

63. Elftman H. Studies of gait. 1966 p. 363–377. Available from: www.jbjs.org

64. Ralston HJ. Energy-speed relation and optimal speed during level walking. Internationale Zeitschrift für Angewandte Physiologie Einschliesslich Arbeitsphysiologie. 1958;17:277–283.

65. Minetti AE, Ardigo LP, Saibene F. The transition between walking and running in humans: metabolic and mechanical aspects at different gradients. Acta physiologica scandinavica. 1994;150(3):315–323.

66. Bertram JE, Ruina A. Multiple walking speed-frequency relations are predicted by constrained optimization. Journal of theoretical Biology. 2001;209(4):445–53.

67. Cavagna GA, Franzetti P. The determinants of the step frequency in walking humans. The Journal of physiology. 1986;373:235–242.

68. Srinivasan M, Seethapathi N. The metabolic cost of changing walking speeds is significant, implies lower optimal speeds for shorter distances, and increases daily energy estimates. Available from: http://dx.doi.org/10.1098/rsbl.2015.0486orviahttp://rsbl.royalsocietypublishing.org.Biomechanics

69. Yandell MB, Zelik KE. Preferred Barefoot Step Frequency is Influenced by Factors Beyond Minimizing Metabolic Rate. Scientific reports. 2016;6:23243.

70. Hunter LC, Hendrix EC, Dean JC. The cost of walking downhill: Is the preferred gait energetically optimal? Journal of biomechanics. 2010;43(10):1910–5.

71. Lam T, Anderschitz M, Dietz V. Contribution of feedback and feedforward strategies to locomotor adaptations. Journal of neurophysiology. 2006;95:766–73.

72. Fortin K, Blanchette A, McFadyen BJ, Bouyer LJ. Effects of walking in a force field for varying durations on aftereffects and on next day performance. Experimental brain research. 2009;199(2):145–155.

73. Bastian AJ. Understanding sensorimotor adaptation and learning for rehabilitation: current opinion in neurology. 2008 Dec;21(6):628–33.

74. Torres-Oviedo G, Vasudevan E, Malone L, Bastian AJ. Locomotor adaptation. InProgress in Brain Research. Elsevier; 2011. p. 65–74. Available from: https://linkinghub.elsevier.com/retrieve/pii/B9780444537522000138

75. Selinger JC, O'Connor SM, Wong JD, Donelan JM. Humans can continuously optimize energetic cost during walking. Current biology. 2015;25(18):2452–2456.

76. Abram SJ, Selinger JC, Donelan JM. Energy optimization is a major objective in the real-time control of step width in human walking. Journal of biomechanics. 2019;91:85–91.

77. Hollerbach JM, Mills R, Tristano D, Christensen RR, Thompson WB, Xu Y. Torso force feedback realistically simulates slope on treadmill-style locomotion interfaces. 2001 p. 939–952. Report No.: 12.

78. Hayward RC, Hollerbach JM. Implementing virtual stairs on treadmills using torso force feedback nProceedings 2002 IEEE International Conference on Robotics and Automation (Cat. No. 02CH37292) 2002 May 11 (Vol. 1, pp. 586-591). IEEE.

79. Parker CR, Carrier DR, Hollerbach JM. Validation of torso force feedback slope simulation through an energy cost comparison. Eurohaptics Conference, 2005 and Symposium on Haptic Interfaces for Virtual Environment and Teleoperator Systems, 2005 World Haptics 2005 First Joint. 2005;446–451.

80. Dewolf AH, Ivanenko YP, Mesquita RM, Lacquaniti F, Willems PA. Neuromechanical adjustments when walking with an aiding or hindering horizontal force. European journal of applied physiology. 2020 Jan;120(1):91–106.

81. Gonzalez-Rubio M, Velasquez NF, Torres-Oviedo G. Explicit control of step timing during split-belt walking reveals interdependent recalibration of movements in space and time. Frontiers in human neuroscience. 2019;13:207.

82. Finley JM, Bastian AJ, Gottschall JS. Learning to be economical: the energy cost of walking tracks motor adaptation. The Journal of physiology. 2013 Feb;591(4):1081–95.

83. Selgrade BP, Thajchayapong M, Lee GE, Toney ME, Chang Y-H. Changes in mechanical work during neural adaptation to asymmetric locomotion. The Journal of Experimental Biology. 2017 Aug 15;220(16):2993-3000.

84. Sánchez N, Simha SN, Donelan JM, Finley JM. Taking advantage of external mechanical work to reduce metabolic cost: the mechanics and energetics of split-belt treadmill walking. The Journal of physiology. 2019 Aug;597(15):4053-68.

85. Selgrade BP, Toney ME, Chang Y-H. Two biomechanical strategies for locomotor adaptation to split-belt treadmill walking in subjects with and without transtibial amputation. Journal of biomechanics. 2017 Feb;53:136–43.

86. Gonabadi AM, Antonellis P, Malcolm P. A system for simple robotic walking assistance with linear impulses at the center of mass. IEEE Transactions on Neural Systems and Rehabilitation Engineering. 2020 Jun;28(6):1353–62.

87. Penke K, Scott K, Sinskey Y, Lewek M. Propulsive forces applied to the body's center of mass affect metabolic energetics post-stroke. Archives of Physical Medicine and Rehabilitation. 2019 Jun 1;100(6):1068-75; Available from: https://linkinghub.elsevier.com/retrieve/pii/S000399931831445X

88. Wolpert DM. Computational approaches to motor control. Trends in cognitive sciences. 1997;6:209–216.

89. Todorov E, Jordan MI. Optimal feedback control as a theory of motor coordination. Nature neuroscience. 2002;5(11):1226–35.

90. Scott SH, Norman KE. Computational approaches to motor control and their potential role for interpreting motor dysfunction. Current opinion in neurology. 2003 Dec 1;16(6):693-8.

91. Flash T, Hogan N. The coordination of arm movements: an experimentally confirmed mathematical model. Journal of neuroscience. 1985;5(7):1688–1703.

92. Kuo AD, Donelan JM. Dynamic principles of gait and their clinical implications. Physical therapy. 2010;90(2):157–174.

93. Srinivasan M, Ruina A. Computer optimization of a minimal biped model discovers walking and running. Nature. 2006;439(7072):72–75.

94. Kording KP, Tenenbaum JB, Shadmehr R. The dynamics of memory as a consequence of optimal adaptation to a changing body. Nature neuroscience. 2007;10(6):779.

95. Zarrugh MY, Radcliffe CW. Predicting metabolic cost of level walking. European journal of applied physiology and occupational physiology. 1978;38(3):215–223.

96. Umberger BR, Martin PE. Mechanical power and efficiency of level walking with different stride rates. Journal of Experimental Biology. 2007;210(18):3255–65.

97. Minetti AE, Capelli C, Zamparo P, Di Prampero PE, Saibene F. Effects of stride frequency on mechanical power and energy expenditure of walking. Medicine and Science in Sports and Exercise. 1995;27(8):1194–1202.

98. Tumer EC, Brainard MS. Performance variability enables adaptive plasticity of “crystallized” adult birdsong. Nature. 2007;450:1240–1245.

99. O’Brien MK, Ahmed AA. Rationality in human movement. Exercise and Sport Sciences Reviews. 2016;44(1):20–28.

100. Galea JM, Mallia E, Rothwell J, Diedrichsen J. The dissociable effects of punishment and reward on motor learning. Nature neuroscience. 2015;18(4):597–602.

101. Wolpert DM, Flanagan JR. Motor prediction. Current biology. 2001;11(18):R729–R732.

102. Shadmehr R, Smith MA, Krakauer JW. Error correction, sensory prediction, and adaptation in motor control. Annual review of neuroscience. 2010;33:89–108.

103. Gottschall JS, Kram R. Energy cost and muscular activity required for propulsion during walking. Journal of Applied Physiology. 2003;94(5):1766–1772.

104. Pratt GA, Williamson MM. Series elastic actuators. Intelligent Robots and Systems 95’Human Robot Interaction and Cooperative Robots’, Proceedings 1995 IEEE/RSJ International Conference on 1995 Aug 5. 1995;1:399–406.

105. Molen NH, Rozendal RH, Boon W. Fundamental characteristics of human gait in relation to sex and location. Proceedings of the Koninklijke Nederlandse Akademie van Wetenschappen Series C Biological and medical sciences. 1972;45(3):215–223.

106. Snaterse M, Ton R, Kuo AD, Donelan JM. Distinct fast and slow processes contribute to the selection of preferred step frequency during human walking. Journal of Applied Physiology (Bethesda, Md : 1985). 2011;110(6):1682–1690.

107. Pagliara R, Snaterse M, Donelan JM. Fast and slow processes underlie the selection of both step frequency and walking speed. Journal of Experimental Biology. 2014;(217):2939–2946.

108. Lamarra N, Whipp BJ, Ward SA, Wasserman K. Effect of interbreath fluctuations on characterizing exercise gas exchange kinetics. Journal of Applied Physiology. 1987;62(5):2003–2012.

109. Brockway JM. Derivation of formulae used to calculate energy expenditure in man. Human nutrition. Clinical nutrition. 1987;41(6):463–471.

110. Selinger JC, Donelan JM. Estimating instantaneous energetic cost during non-steady-state gait. Journal of Applied Physiology. 2014;117(11):1406–15.

111. Ortega JD, Farley CT. Effects of aging on mechanical efficiency and muscle activation during level and uphill walking. J ournal of Electromyography and Kinesiology. 2015 Feb 1;25(1):193-8.

112. McLean RA, Sanders WL, Stroup WW. A unified approach to mixed linear models. The american statistician. 1991;45(1):54–64.

113. Körding KP, Wolpert DM. Bayesian decision theory in sensorimotor control. Trends in cognitive sciences. 2006;10(7):319–326.

114. Donelan JM. Motor control: no constant but change. Current biology. 2016;26(20):R915–R918.

115. Leech KA, Roemmich RT, Day KA, Bastian AJ. Movement and perception recalibrate differently across multiple days of locomotor learning. Journal of neurophysiology. 2018;114(1):608–23.

116. Caputo JM, Collins SH. An experimental robotic testbed for accelerated development of ankle prostheses. In Robotics and automation (ICRA), 2013 IEEE international conference on 2013 May 6. 2013;2645–2650.

117. Gupta R, Ashe J. Motor Force Field Learning Influences Visual Processing of Target Motion. Journal of neurophysiology. 2007;97(37):738–45.

118. Jackson RW, Collins SH. An experimental comparison of the relative benefits of work and torque assistance in ankle exoskeletons. Journal of Applied Physiology. 2015;541–557.

119. Wong JD, Selinger JC, Donelan JM. Is natural variability in gait sufficient to initiate spontaneous energy optimization in human walking? Journal of neurophysiology. 2019;121:1848–1855.

120. Zhang J, Fiers P, Witte KA, Jackson RW, Poggensee KL, Atkeson CG, & COllins SH. Human-in-the-loop optimization of exoskeleton assistance during walking. Science. 2017;356(6344):1280-4.

121. Roemmich RT, Bastian AJ. Two ways to save a newly learned motor pattern. Journal of neurophysiology. 2015 Jun;113(10):3519–30.

122. Simha SN, Wong JD, Selinger JC, Donelan JM. A mechatronic system for studying energy optimization during walking. IEEE Transactions on Neural Systems and Rehabilitation Engineering. 2019;27(7):1416–1425.

123. Kidd C, Piantadosi ST, Aslin RN. The goldilocks effect: human infants allocate attention to visual sequences that are neither too simple nor too complex. PLoS One. 2012 May 23;7(5). Available from: https://www.ncbi.nlm.nih.gov/pmc/articles/PMC3359326/

124. Adamczyk PG, Collins SH, Kuo AD. The advantages of a rolling foot in human walking. Journal of Experimental Biology. 2006 Oct 15;209(20):3953–63.

125. Weir JB de V. New methods for calculating metabolic rate with special reference to protein metabolism. The Journal of physiology. 1949;109(1–2):1–9.

126. Iwamoto GA, Waldrop TG, Kaufman MP, Botterman BR, Rybicki KJ, Mitchell JH. Pressor reflex evoked by muscular contraction: contributions by neuraxis levels. Journal of Applied Physiology. 1985 Aug 1;59(2):459–67.

127. Mitchell JH, Kaufman MP, Iwamoto GA. The exercise pressor reflex: its cardiovascular effects, afferent mechanisms, and central pathways. Annual Review of Physiology. 1983;45(1):229–42.

128. Guerguiev J, Kording KP, Richards BA. Spike-based causal inference for weight alignment. arXiv:191001689. 2020 Feb 1; Available from: http://arxiv.org/abs/1910.01689

129. Howard IS, Wolpert DM, Franklin DW. The value of the follow-through derives from motor learning depending on future actions. Current biology. 2015 Feb;25(3):397–401.

130. Howard IS, Wolpert DM, Franklin DW. The effect of contextual cues on the encoding of motor memories. Journal of neurophysiology. 2013 May 15;109(10):2632–44.

131. Miyamoto YR, Wang S, Smith MA. Implicit adaptation compensates for erratic explicit strategy in human motor learning. Nature Neuroscience. 2020 Mar;23(3):443-55. Available from: http://www.nature.com/articles/s41593-020-0600-3

132. Van de Putte M, Hagemeister N, St-Onge N, Parent G, de Guise J a. Habituation to treadmill walking. Bio-medical materials and engineering. 2006;16(1):43–52.

133. Wall JC, Charteris J. A kinematic study of long-term habituation to treadmill walking. Ergonomics. 1981;24(7):531–42.

134. Mochon S, McMahon TA. Ballistic walking: an improved model. Mathematical Biosciences. 1980;52(3–4):241–60.

135. Herr H. Exoskeletons and orthoses: Classification, design challenges and future directions. Journal of NeuroEngineering and Rehabilitation. 2009;6(1):1–9.

136. Ferris DP. The exoskeletons are here. Journal of NeuroEngineering and Rehabilitation. 2009;6(1):1–3.

137. Ferris DP, Sawicki GS, Daley MA. A Physiologist's Perspective on Robotic Exoskeletons for Human Locomotion. International Journal of Humanoid Robotics. 2007;04(03):507–28.

138. Gordon KE, Ferris DP. Learning to walk with a robotic ankle exoskeleton. Journal of Biomechanics. 2007;40(12):2636–44.

139. Gordon KE, Kinnaird CR, Ferris DP. Locomotor adaptation to a soleus EMG-controlled antagonistic exoskeleton. Journal of neurophysiology. 2013;109(January):1804–14.

140. Koller JR, Jacobs DA, Ferris DP, Remy CD. Learning to walk with an adaptive gain proportional myoelectric controller for a robotic ankle exoskeleton. Journal of NeuroEngineering and Rehabilitation. 2015;12(1):1–14.

141. Selinger JC, Donelan JM. Myoelectric Control for Adaptable Biomechanical Energy Harvesting. IEEE Transactions on Neural Systems and Rehabilitation Engineering. 2016;24(3):364–73.

142. Sawicki GS, Ferris DP. Mechanics and energetics of level walking with powered ankle exoskeletons. Journal of Experimental Biology. 2008;211(9):1402–13.

143. Malcolm P, Derave W, Galle S, De Clercq D. A Simple Exoskeleton That Assists Plantarflexion Can Reduce the Metabolic Cost of Human Walking. PLoS One. 2013;8(2):1–7.

144. Galle S, Malcolm P, Collins SH, De Clercq D. Reducing the metabolic cost of walking with an ankle exoskeleton: interaction between actuation timing and power. Journal of NeuroEngineering and Rehabilitation. 2017;14(1):1–16.

145. Reisman DS, Block HJ, Bastian AJ. Interlimb coordination during locomotion: what can be adapted and stored? Journal of neurophysiology. 2005;94(4):2403–15.

146. Dietz V, Zijlstra W, Duysens J. Human neuronal interlimb coordination during split-belt locomotion. Experimental Brain Research. 1994;101(3):513–20.

147. Prokop T, Berger W, Zijlstra W, Dietz V. Adaptational and learning processes during human split-belt locomotion: interaction between central mechanisms and afferent input. Experimental Brain Research. 1995;106(3):449–56.

148. Sánchez N, Park S, Finley JM. Evidence of energetic optimization during adaptation differs for metabolic, mechanical, and perceptual estimates of energetic cost. Scientific Reports. 2017;7(1).

149. Burdett RG, Skrinar GS, Simon SR. Comparison of mechanical work and metabolic energy consumption during normal gait. Journal of orthopaedic research : official publication of the Orthopaedic Research Society. 1983;1(1):63–72.

150. Umberger BR, Gerritsen KGM, Martin PE. A Model of Human Muscle Energy Expenditure. Computer methods in biomechanics and biomedical engineering. 2003 May 1;6(2):99-111.

151. Ellis RG, Howard KC, Kram R. The metabolic and mechanical costs of step time asymmetry in walking. Proceedings Biological Sciences / The Royal Society. 2013;280(1756):20122784.

152. Doke J, Donelan JM, Kuo AD. Mechanics and energetics of swinging the human leg. The Journal of experimental biology. 2005;208(Pt 3):439–45.

153. Zeni JA, Richards JG, Higginson JS. Two simple methods for determining gait events during treadmill and overground walking using kinematic data. Gait and Posture. 2008 May;27(4):710–4.

154. Roemmich RT, Long AW, Bastian AJ. Seeing the errors you feel enhances locomotor performance but not learning. Current biology. 2016;26(20):2707–16.

155. Leech KA, Roemmich RT. Independent voluntary correction and savings in locomotor learning. The Journal of Experimental Biology. 2018;(June):jeb.181826.

156. Roemmich RT, Long AW, Bastian AJ. Seeing the errors you feel enhances locomotor performance but not learning. Current biology. 2016;26(20):2707–16.

157. Donelan JM, Kram R, Kuo AD. Simultaneous positive and negative external mechanical work in human walking. Journal of Biomechanics. 2001;35(1):117–24.

158. Nakagawa S, Schielzeth H. A general and simple method for obtaining R2 from generalized linear mixed-effects models. Methods in Ecology and Evolution. 2013;4(2):133–42.

159. Herzog W. The mysteries of eccentric muscle action. Journal of Sport and Health Science. 2018;00:5–6.

160. Ding Y, Kim M, Kuindersma S, Walsh CJ. Human-in-the-loop optimization of hip assistance with a soft exosuit during walking. Science Robotics. 2018;3(15):eaar5438.

161. Vazquez A, Statton MA, Busgang SA, Bastian AJ. Split-belt walking adaptation recalibrates sensorimotor estimates of leg speed but not position or force. Journal of neurophysiology. 2015;114(6):3255–67.

162. de Rugy a., Loeb GE, Carroll TJ. Muscle coordination is habitual rather than optimal. Journal of Neuroscience. 2012;32(21):7384–91.

163. Loeb GE. Optimal isn't good enough. Biological Cybernetics. 2012;106(11–12):757–65.

164. Finley JM, Long A, Bastian AJ, Torres-Oviedo G. Spatial and temporal control contribute to step length asymmetry during split-belt adaptation and hemiparetic gait. Neurorehabilitation and neural repair. 2015 Sep;29(8):786-95.

165. Balasubramanian R, Howe RD, Member S. Task Performance is Prioritized Over Energy Reduction. IEEE transactions on bio-medical engineering. 2009;56(5):1–9.

166. Sánchez N, Simha S, Donelan JM, Finley J. Using asymmetry to your advantage: learning to acquire and accept external assistance during prolonged split-belt walking. bioRxiv. 2020;

167. Seethapathi N. Transients, variability, stability and energy in human locomotion. The Ohio State University; 2018.

168. Kuo AD. A simple model of bipedal walking predicts the preferred speed-step length relationship. Journal of biomechanical engineering. 2001;123(3):264–269.

169. Kuo AD, Donelan JM, Ruina A. Energetic consequences of walking like an inverted pendulum: step-to-step transitions. Exercise and sport sciences reviews. 2005 May;33(2):88–97.

170. Doke J, Kuo AD. Energetic cost of producing cyclic muscle force, rather than work, to swing the human leg. Journal of Experimental Biology. 2007;210:2390–2398.

171. McGeer T. Passive Dynamic Walking. The International Journal of Robotics Research. 1990;9(2):62–82.

172. McGeer T. Principles of walking and running. Advances in comparative and environmental physiology. 1992;11:113-39.

173. Garcia M, Chatterjee A, Ruina A, Coleman M. The Simplest Walking Model: Stability, Complexity, and Scaling [Internet]. 1998. Available from: http://www.asme.org/terms/Terms_Use.cfm

174. Kuo AD. Energetics of Actively Powered Locomotion Using the Simplest Walking Model. J. Biomech. Eng. 2002 Feb 1;124(1):113-20.

175. van Ingen Schenau GJ. Some fundamental aspects of the biomechanics of overground versus treadmill locomotion. Medicine and Science in Sports and Exercise. 1980;12(4):257–61.

176. Margaria R. Positive and negative work performances and their efficiencies in human locomotion. Int Z Angew Physiol Einschl Arbeitsphysiol. 1968;25(4):339–51.

177. Sombric CJ, Torres-Oviedo G. Augmenting propulsion demands during split-belt walking increases locomotor adaptation of asymmetric step lengths. Journal of NeuroEngineering and Rehabilitation. 2020 Dec;17(1):1-5.

178. Heitkamp LN, Stimpson KH, Dean JC. Application of a novel force-field to manipulate the relationship between pelvis motion and step width in human walking. IEEE Transactions on Neural Systems and Rehabilitation Engineering. 2019 Oct;27(10):2051–8.

179. Goldenberg J, Lowengart O, Oreg S, Bar-Eli M. How do revolutions emerge?: lessons from the fosbury flop. International Studies of Management & Organization. 2010 Jul;40(2):30–51.

180. Cashabackid JGA, Lao CK, Palidis DJ, Coltmanid SK, Mcgregor HR, Gribbleid PL. The gradient of the reinforcement landscape influences sensorimotor learning. PLOS computational biology. 2019 Mar 4;15(3):e1006839. 2019; Available from: https://doi.org/10.1371/journal.pcbi.1006839

181. Selgrade BP, Thajchayapong M, Lee GE, Toney ME, Chang Y-H. Changes in mechanical work during neural adaptation to asymmetric locomotion. The Journal of Experimental Biology. 2017;220(16):2993–3000.

182. O'Brien MK, Ahmed AA. Asymmetric valuation of gains and losses in effort-based decision making. Daunizeau J, editor. PLoS ONE. 2019 Oct 15;14(10):e0223268.